

PROSTHETIC FOOT DESIGN WITH BIOMIMETIC ANKLE MECHANISM

A Thesis

presented to

the Faculty of the Graduate School

at the University of Missouri-Columbia

In Partial Fulfillment

Of the Requirements for the Degree

Master of Science

by

COLIN GRACE

Dr. Josiah Bryan, Thesis Supervisor

MAY 2021

APPROVAL

The undersigned, appointed by the dean of the Graduate School, have examined the thesis entitled

PROSTHETIC FOOT DESIGN WITH
BIOMIMETIC ANKLE MECHANISM

presented by Colin Grace,

a candidate for the degree of Master of Science,

and hereby certify that, in their opinion, it is worthy of acceptance.

Dr. Josiah Bryan

Dr. Yuyi Lin

Dr. Ferris Pfeiffer

ACKNOWLEDGEMENTS

I would like to thank Dr. Josiah Bryan for his guidance and his willingness to help make my project my own. It has been a fantastic learning opportunity to learn and grow.

I would like to thank Tracy Ell and Andrew Dotzler for their insights into prosthetic production and always being available for my many questions.

I would also like to thank my parents and sisters for their endless support and for always believing in me.

I would also like to thank my partner Jasmine for the kick in the pants I needed to join this program, and for always (lovingly) pushing me to be my best self.

Lastly, I wish to thank Charlie and Maeve for their sage wisdom and great conversation.

TABLE OF CONTENTS

| | |
|----------------------------------------------|----|
| ACKNOWLEDGEMENTS | ii |
| LIST OF FIGURES | v |
| LIST OF TABLES | x |
| 1. ABSTRACT | 1 |
| 2. INTRODUCTION | 2 |
| 2.1. Amputee Statistics | 2 |
| 2.2. Foot Biomechanics and the Gait Cycle | 6 |
| 2.3. Contemporary Prosthetic Devices | 14 |
| 3. PROSTHETIC DESIGN | 20 |
| 3.1. Design Parameters | 20 |
| 3.2. Current Design | 26 |
| 3.3. Design Features | 33 |
| 3.3.1. Foot Plates | 33 |
| 3.3.2. Fox Float DPS | 39 |
| 3.3.3. Ball Joint Stud Attachment Bracket | 43 |
| 3.3.4. QA1 Ball Joint | 46 |
| 3.3.5. Ball Joint Housing Attachment Bracket | 49 |
| 3.4. Design Cost | 51 |
| 4. Simulations | 57 |
| 4.1. Foot Plates | 58 |
| 4.2. Ball Joint Stud Attachment Bracket | 75 |

| | |
|--------------------------------------------|-----|
| 4.3. Ball Joint Housing Attachment Bracket | 91 |
| 5. Conclusion | 100 |
| 5.1. Discussion | 100 |
| 5.2. Limitations | 101 |
| 5.3. Future Work | 103 |
| 5.4. Conclusion | 105 |
| Appendix A: Component Gallery | 106 |
| REFERENCES | 113 |

LIST OF FIGURES

| | |
|--------------------------------------------------------------------------------------------------------------------------|----|
| Fig. 1 – Anatomy of the Human Foot | 7 |
| Fig. 2 – Arches of the Foot | 7 |
| Fig. 3 – Cardinal Planes of the Human Body | 9 |
| Fig. 4 – Foot Movements in the Cardinal Planes | 10 |
| Fig. 5 – Phases of Walking and Running Cycles | 12 |
| Fig. 6 – Dynamic Response and Microprocessor-Controlled Prosthetic Feet | 16 |
| Fig. 7 – Gallery of Influential Prosthetic Designs | 24 |
| Fig. 8 – Isometric View of Prosthetic Design | 26 |
| Fig. 9 – Alternate Isometric View of Prosthetic Design | 29 |
| Fig. 10 – Top View of Prosthetic Design | 30 |
| Fig. 11 – Profile View of Prosthetic Design | 31 |
| Fig. 12 – Rear View of Prosthetic Design | 32 |
| Fig. 13 – Isometric View of Foot Plates | 33 |
| Fig. 14 - Detail of Threaded Standoffs in Upper- and Lower-Foot Plates | 35 |
| Fig. 15 – Profile View of Foot Plates | 36 |
| Fig. 16 – Top and Bottom Views of Foot Plates | 37 |
| Fig. 17 – Detail of Spherical Bearing Recess and Axle Pass-through | 37 |
| Fig. 18 – a) Foot Dowel Pin inserted in Spherical Bearings. b) Full front assembly with Fox Float Shock and Mount Kit | 38 |
| Fig. 19 – Profile Comparison of Prosthetic and Natural Foot | 38 |
| Fig. 20 – Fox Float DPS Piston | 39 |

| | |
|-----------------------------------------------------------------------------------------|----|
| Fig. 21 – (left to right) Fox Float 3-Position Lever, Open Mode Adjust, and Rebound | |
| Adjustment | 41 |
| Fig. 22 – Detail View of Fox Float DPS Shock Connection Points | 42 |
| Fig. 23 – Alternate Detail View of Fox Float DPS Shock Connection Points | 42 |
| Fig. 24 – Ball Joint Stud Attachment Bracket | 43 |
| Fig. 25 – a) Section View of Ball Joint Stud Attachment Bracket, b) PTM-WH Pyramid | |
| Connector | 45 |
| Fig. 26 – QA1 1210-105 Upper Ball Joint | 46 |
| Fig. 27 – Exploded View of QA1 Ball Joint | 48 |
| Fig. 28 – Ball Joint Housing Attachment Bracket | 49 |
| Fig. 29 – a) Ball Joint Housing Attachment Bracket Section View, b) Ball Joint Assembly | |
| Section View | 50 |
| Fig. 30 – Exploded View of Prosthetic Assembly | 55 |
| Fig. 31 – Lower Foot Plate Forward Toe Shear von Mises Stress (psi) | 60 |
| Fig. 32 – Lower Foot Plate Forward Toe Shear Displacement (mm) | 60 |
| Fig. 33 – Lower Foot Plate Forward Toe Shear Factor of Safety | 61 |
| Fig. 34 – Lower Foot Plate Rearward Toe Shear von Mises Stress (psi) | 61 |
| Fig. 35 – Lower Foot Plate Rearward Toe Shear Displacement (mm) | 62 |
| Fig. 36 – Lower Foot Plate Rearward Toe Shear Factor of Safety | 62 |
| Fig. 37 – Lower Foot Plate Upward Toe Shear von Mises Stress (psi) | 63 |
| Fig. 38 – Lower Foot Plate Upward Toe Shear Displacement (in) | 64 |
| Fig. 39 – Lower Foot Plate Upward Toe Shear Factor of Safety | 64 |
| Fig. 40 – Lower Foot Plate Downward Toe Shear von Mises Stress (psi) | 65 |

| | |
|----------------------------------------------------------------------------------|----|
| Fig. 41 – Lower Foot Plate Downward Toe Shear Displacement (in) | 65 |
| Fig. 42 – Lower Foot Plate Downward Toe Shear Factor of Safety | 66 |
| Fig. 43 – Lower Foot Plate Left Toe Shear von Mises Stress (psi) | 67 |
| Fig. 44 – Lower Foot Plate Left Toe Shear Displacement (mm) | 67 |
| Fig. 45 – Lower Foot Plate Left Toe Shear Factor of Safety | 68 |
| Fig. 46 – Lower Foot Plate Right Toe Shear von Mises Stress (psi) | 68 |
| Fig. 47 – Lower Foot Plate Right Toe Shear Displacement (in) | 69 |
| Fig. 48 – Lower Foot Plate Right Toe Shear Factor of Safety | 69 |
| Fig. 49 – Lower Foot Plate Bending Force von Mises Stress (psi) | 70 |
| Fig. 50 – Lower Foot Plate Bending Force Displacement (mm) | 71 |
| Fig. 51 – Lower Foot Plate Bending Force Factor of Safety | 71 |
| Fig. 52 – Lower Foot Plate Bending Force Factor of Safety Detail | 72 |
| Fig. 53 – Upper Foot Plate Bending Force von Mises Stress (psi) | 73 |
| Fig. 54 – Upper Foot Plate Bending Force Displacement (mm) | 74 |
| Fig. 55 – Upper Foot Plate Bending Force Factor of Safety | 74 |
| Fig. 56 – Stud Attachment Bracket Forward Shearing Force von Mises Stress (psi) | 76 |
| Fig. 57 – Stud Attachment Bracket Forward Shearing Force Displacement (mm) | 77 |
| Fig. 58 – Stud Attachment Bracket Forward Shearing Force Factor of Safety | 77 |
| Fig. 59 – Stud Attachment Bracket Rearward Shearing Force von Mises Stress (psi) | 78 |
| Fig. 60 – Stud Attachment Bracket Rearward Shearing Force Displacement (mm) | 78 |
| Fig. 61 – Stud Attachment Bracket Rearward Shearing Force Factor of Safety | 79 |
| Fig. 62 – Stud Attachment Bracket Upward Shearing Force von Mises Stress (psi) | 80 |
| Fig. 63 – Stud Attachment Bracket Upward Shearing Force Displacement (mm) | 80 |

| | |
|-----------------------------------------------------------------------------------------|----|
| Fig. 64 – Stud Attachment Bracket Upward Shearing Force Factor of Safety | 81 |
| Fig. 65 – Stud Attachment Bracket Downward Shearing Force von Mises Stress (psi) | 81 |
| Fig. 66 – Stud Attachment Bracket Downward Shearing Force Displacement (mm) | 82 |
| Fig. 67 – Stud Attachment Bracket Downward Shearing Force Factor of Safety | 82 |
| Fig. 68 – Stud Attachment Bracket Normal Force Arm von Mises Stress (psi) | 84 |
| Fig. 69 – Stud Attachment Bracket Normal Force Arm Displacement (mm) | 84 |
| Fig. 70 – Stud Attachment Bracket Normal Force Arm Factor of Safety | 85 |
| Fig. 71 – Stud Attachment Bracket Pyramid Connector von Mises Stress (psi) | 86 |
| Fig. 72 – Stud Attachment Bracket Pyramid Connector Displacement (mm) | 87 |
| Fig. 73 – Stud Attachment Bracket Pyramid Connector Factor of Safety | 87 |
| Fig. 74 – Stud Attachment Bracket Pyramid Connector Factor of Safety Detail | 88 |
| Fig. 75 – Stud Attachment Bracket Ball Joint Area von Mises Stress (psi) | 89 |
| Fig. 76 – Stud Attachment Bracket Ball Joint Area Displacement (mm) | 90 |
| Fig. 77 – Stud Attachment Bracket Ball Joint Area Factor of Safety | 90 |
| Fig. 78 – Housing Attachment Bracket Opening Normal Simulation von Mises Stress (psi) | 92 |
| Fig. 79 – Housing Attachment Bracket Opening Normal Simulation Displacement (mm) | 92 |
| Fig. 80 – Housing Attachment Bracket Opening Normal Simulation Factor of Safety | 93 |
| Fig. 81 – Housing Attachment Bracket Opening Shearing von Mises Stress (psi) | 94 |
| Fig. 82 – Housing Attachment Bracket Opening Shearing Displacement (mm) | 94 |
| Fig. 83 – Housing Attachment Bracket Opening Shearing Factor of Safety | 95 |
| Fig. 84 – Housing Attachment Bracket Bolt Hole Normal Simulation von Mises Stress (psi) | 96 |
| Fig. 85 – Housing Attachment Bracket Bolt Hole Normal Simulation Displacement (mm) | 96 |
| Fig. 86 – Housing Attachment Bracket Bolt Hole Normal Simulation Factor of Safety | 97 |

| | |
|--------------------------------------------------------------------------------------|-----|
| Fig. 87 – Housing Attachment Bracket Bolt Hole Total Shearing von Mises Stress (psi) | 98 |
| Fig. 88 – Housing Attachment Bracket Bolt Hole Total Shearing Displacement (mm) | 98 |
| Fig. 89 – Housing Attachment Bracket Bolt Hole Total Shearing Factor of Safety | 99 |
| Fig. 90 – Ball Joint Stud Attachment Bracket Drawing | 106 |
| Fig. 91 – Ball Joint Housing Attachment Bracket Drawing | 107 |
| Fig. 92 – Lower Foot Plate Isometric View | 108 |
| Fig. 93 – Lower Foot Plate Top View | 109 |
| Fig. 94 – Lower Foot Plate Profile View | 109 |
| Fig. 95 – Lower Foot Plate Toe Area Detail | 110 |
| Fig. 96 – Upper Foot Plate Isometric View | 111 |
| Fig. 97 – Upper Foot Plate Profile View | 111 |
| Fig. 98 – Upper Foot Plate Top View from Housing Attachment Bracket Connection | 112 |
| Fig. 99 – Upper Foot Plate Top View from Lower Foot Plate Connection | 112 |

LIST OF TABLES

| | |
|----------------------------------------------------------------------------------------|----|
| Table 1 – Prosthetic Design Comparison | 25 |
| Table 2 – Zoltek PX35 Material Properties | 34 |
| Table 3 – Price Comparison of Ball Joint Attachment Bracket Manufacturing Methods | 53 |
| Table 4 – Prosthetic Component Costs and Manufacturers | 56 |
| Table 5 – Lower Foot Plate 1 st and 2 nd Toe Shear Simulations | 59 |
| Table 6 – Lower Foot Plate 3 rd and 4 th Toe Shear Simulations | 64 |
| Table 7 – Lower Foot Plate 5 th and 6 th Toe Shear Simulations | 66 |
| Table 8 – Lower Foot Plate Bending Force Simulation | 71 |
| Table 9 – Upper Foot Plate Bending Force Simulation | 73 |
| Table 10 – Stud Attachment Bracket Arm 1 st and 2 nd Simulations | 76 |
| Table 11 – Stud Attachment Bracket Arm 3 rd and 4 th Simulations | 79 |
| Table 12 – Stud Attachment Bracket Arm 5 th Simulation | 83 |
| Table 13 – Stud Attachment Bracket Pyramid Connector Simulation | 86 |
| Table 14 – Stud Attachment Bracket Ball Joint Area simulation | 89 |
| Table 15 – Housing Attachment Bracket Upper Opening Normal Simulation | 92 |
| Table 16 – Housing Attachment Bracket Upper Opening Shearing Simulation | 93 |
| Table 17 – Housing Attachment Bracket Bolt Holes Normal Simulation | 96 |
| Table 18 – Housing Attachment Bracket Bolt Holes Shearing Simulation | 97 |

1. ABSTRACT

This thesis proposes a novel lower-limb prosthetic device. Current prosthetics either have overly simplistic designs with inaccurate biomechanics or use delicate microprocessors that are easily damaged in harsh environments. This thesis aims to address these concerns by creating a novel device that combines a pneumatic damping system with a ball joint, resulting in a robust design with improved biomechanics. This prosthetic offers an affordable alternative that can be completely rebuilt while providing added comfort through improved biomechanics. Overall, this thesis contributes to the literature by proposing and discussing an innovative design for an affordable, comfortable, biomechanically sound alternative for lower limb prostheses.

2. INTRODUCTION

2.1. Amputee Statistics

Nearly 2 million people are living with limb loss in the United States alone, with an estimated 185,000 amputations occurring annually [1–3]. Lower limb amputations are the most common type of amputation by far, accounting for 90.3% of total amputations in the United States [4]. Limb loss occurs for many reasons and can vary by population. Data collected by Ziegler-Graham et al. found the majority of amputations are caused by vascular disease, including diabetes and arterial diseases (54%), followed by trauma (45%), and cancer (<2%) [1]. Survey data collected by the Amputee Coalition show traumatic incidents as a primary cause of lower limb amputations (47.7%), followed by non-diabetes related infections (12.8%), and cancer (12.5%) [4]. The different sources indicate that traumatic injuries are predominant among adolescents and adults under the age of 45, while vascular disease becomes the predominant cause among adults 65 and older. Lower limb amputations are a life changing events that can radically affect an amputee’s physical, psychological, and social well-being. The most obvious effect of lower limb amputation is the loss of mobility. Amputees are unable to walk without some form of assistance, making them more susceptible to falls and collisions. Daily tasks that were previously taken for granted become significantly more difficult or outright impossible to perform following an amputation. For example, preparing food, getting dressed, and housework may all require more time and exertion, leaving the amputee fatigued. Amputees must also regularly perform stretching exercises for muscle contractures or risk being unable to use their prosthetic limb. Many amputees suffer residual limb pain or phantom limb pain, the latter of

which affects up to 80% of amputees. In addition, poor lower limb circulation makes amputees more prone to infections and deep vein thrombosis.

While physical adjustments are stressful for amputees, emotional and psychological changes can also be significant for the amputee and people close to them as well. Adapting to life without a limb's sensory feedback, as well as suffering chronic aches and pains can be mentally taxing. Amputees may be prone to body image issues surrounding their injured limb, such as anxiety and sexual impairment and/or dysfunction. If the amputation is a result of a traumatic incident, the amputee may experience post-traumatic stress disorder (PTSD) or similar psychological conditions. Amputations can also affect a person's ability to partake in social activities and hobbies they previously enjoyed. The amputee may be physically incapable of participating in previous activities, or pain may prevent them from doing so [5]. As a result, it is unsurprising that depression is common among amputees during early loss and in subsequent adjustment periods [5]. Due to physical impairment, social adjustment, and psychological stress, amputees may socially withdraw or feel isolated, resulting in irritability. While irritability is a common symptom of depression and anxiety, this symptom may add additional relationship strains if amputees lash out at sources of social support, such as caretakers. Fortunately, there are many resources available for amputees and family members to develop coping strategies necessary to regain a positive and healthy outlook. It is important to consider the diverse physical and psychological challenges amputees encounter to fully consider the importance of robust and accessible prosthetics.

When designing prosthetic devices, it is important to first understand which elements are most important to amputees. A clear understanding of the most important properties to amputees will guide the design process towards an effective end product. Generally, information about

prosthetic devices is obtained through patient surveys. The Amputee Coalition surveyed 1,200 amputees to gain insight into their relationship with prosthetic devices. This survey found that the majority of amputees own a prosthetic device (94.8%), with 89.2% of respondents regularly wearing their devices [4]. However, not all amputees reported consistently wearing their devices. Amputees attributed inconsistent use to three main reasons: ease of performing daily tasks without their prosthetic (76.5%), discomfort (35.3%), and a dislike of the device's appearance (35.3%) [4]. This survey suggests that prosthetic designs that can comfortably and easily assist with daily tasks are necessary improvements for amputees. And while a prosthetic's appearance is important, this variable is individually subjective and variable. As a result, prosthetic designs that allow for a customizable appearance and that can suit a person's unique tastes and preferences is necessary.

Determining reasons amputees choose not to use prosthetic devices is another important consideration. The survey performed by the Amputee Coalition reports that 5.2% of amputees do not own any kind of prosthetic device [4]. Reasons for not owning one fell into four general categories: not wanting a device (39.6%), being satisfied with other types of assisted devices (33.3%), the prosthetic device not being covered by their insurance (14.6%), and unaffordability of the prosthetic device (12.5%) [4]. While limited data exists on why an amputee would choose to forego a prosthetic device, a few reasons could be surmised. Some people may meet their movement needs using non-prosthetic devices such as crutches or a wheelchair. Others may have received improper training on how to use their device effectively, resulting in uncomfortable or awkward device operation. Others still may have been fit with a prosthesis that was inappropriate for their functional needs or goals. Both improper training and fit could result in discomfort or frustration for the user, leading to an abandonment of the device. Affordability is another

important aspect to consider when examining reasons why amputees forego prostheses. Of course, a more affordable prosthetic would be easier for an amputee to obtain and is more likely to be covered by health insurance. The financial burden of obtaining an appropriate prosthetic is considerable. Depending on their features, prosthetic devices can cost anywhere between \$5,000 to \$70,000, with insurance covering 10-50% of the total cost on average [6]. Despite the expense, amputees still seek prosthetics for the mobility they provide. Anything that can be done to make prosthetics more affordable and thereby accessible, helps the amputee increase their overall health and mobility. If a prosthetic can demonstrate effectiveness and affordability, obtaining a prosthetic device could be more accessible and potentially replace other assistive devices.

In a collaborative survey performed by researchers at John Hopkins University and the Amputee Coalition of America, amputees were polled to rate their overall satisfaction with their prosthetic device, as well as other factors related to their experiences as amputees. This survey found that 83.7% of amputees who owned a prosthetic device wore it 7 days a week, with an average daily use of around 12 hours [5]. While the majority of those surveyed reported satisfaction with their prosthetic device, there are still areas for improvement. 91% of surveyed participants reported experiencing some type of pain, with 83% experiencing pain in two or more body areas [5]. The reported types of pain stem from residual limb pain (70%), phantom pain (80%), non-amputated limb pain (49%), and back pain (62%) [5]. The added pain from prosthetic use creates additional mobility limitations for amputees, thereby hindering their ability to participate in various activities. For example, amputees who are not active enough are more likely to develop chronic health problems that can result in invasive medical interventions, such as surgery. While much of a prosthetic's comfort comes from the interface between the

prosthetic socket and residual limb, the prosthetic itself can improve comfort by moving more like a natural limb. Overcompensations made by other parts of the body will be reduced by more natural limb motion, which will reduce back and non-amputated limb pain. Therefore, it is critically important to develop a comfortable prosthetic device to improve comfort and reduce future disease development and burden.

2.2. Foot Biomechanics and the Gait Cycle

The foot is an intricate limb capable of adapting to a wide variety of uneven surfaces. Not only does the foot provide cushioning to the body, the foot also provides traction for movement, awareness of joint and body positions for balance, and leverage for propulsion [7]. The foot is composed of 26 bones in three sections, with four additional bones between the ankle and hip to form the lower extremity, as seen in Figure 1. The hindfoot is composed of the heel bone (calcaneus) and ankle bone (talus), which contribute to the complex motion of pronation and supination [7]. The midfoot includes the navicular, cuboid, and cuneiform bones, also known as the lesser tarsus [7]. These midfoot joints are largely fixed, partly forming the medial longitudinal arch and lateral longitudinal arch. The forefoot is composed of the five metatarsals as well as the phalanges [7]. The first and fifth metatarsals are able to move up and down to adapt to uneven surfaces. In addition, the combination of fixed midfoot and flexible forefoot creates the lever that makes propulsion possible during the gait cycle. The bones of the foot are held in place by ligaments that transmit the body's weight to the calcaneus and the metatarsal heads [7]. The foot bones, combined with ligamentous and muscular support, form two longitudinal arches and a transverse arch that protect the foot by redistributing pressure to create

a foot that is both rigid and mobile, as seen in Figure 2 [7]. Unsurprisingly, foot movement is almost as complex as the structure that composes it.

<https://www.webmd.com/pain-management/picture-of-the-feet>

Figure 1 - Anatomy of the Human Foot [8]

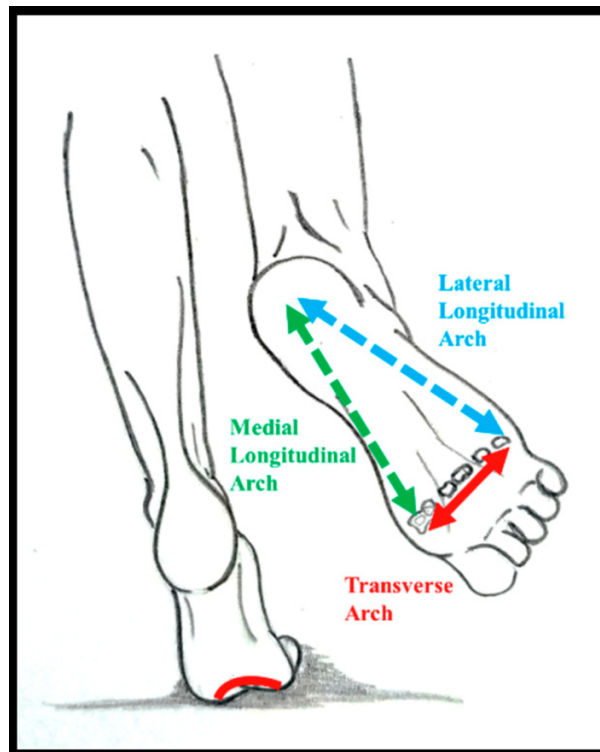


Figure 2 - Arches of the Foot [9]

Foot movements have special definitions in the cardinal planes (Figure 3Figure 4)[10]. Motions within the sagittal plane are dorsiflexion (upward) and plantar flexion (downward). The frontal plane is responsible for inversion and eversion, while the horizontal plane results in adduction, or internal rotation. Internal rotation refers to the distal portion of the foot moving toward the midline of the body on its vertical axis. The horizontal plane is also responsible for

abduction, or external rotation, of the foot when the end of the foot moves away from the midline of the body [7].

Because the mechanical axes of the foot are not perpendicular to any cardinal planes, almost all motions of the foot are triplanar, except in some cases of uniaxial motion [7]. The foot shifts throughout the gait cycle from an “unlocked” state, able to adapt to varied terrain, to a “locked” rigid lever which propels the leg forward with body weight [7]. This shift in states occurs at the subtalar joint, itself a combination of the calcaneocuboid and talonavicular synovial gliding joints. When the subtalar joint pronates, the axes of both joints become parallel, allowing a flexible foot with increased motion [7]. During supination of the subtalar joint, the axes move out of alignment and “lock”, making the foot rigid [7]. The ability of this joint to lock and unlock results from internal and external rotation of the entire lower limb [7]. Although this may be beyond the scope of this project, an ideal prosthetic device will also be able to transition between a locked and unlocked state. This will more closely mirror the natural foot/ankle mechanism and allow the prosthetic foot to both adapt to uneven terrain and propel the body forward during locomotion.

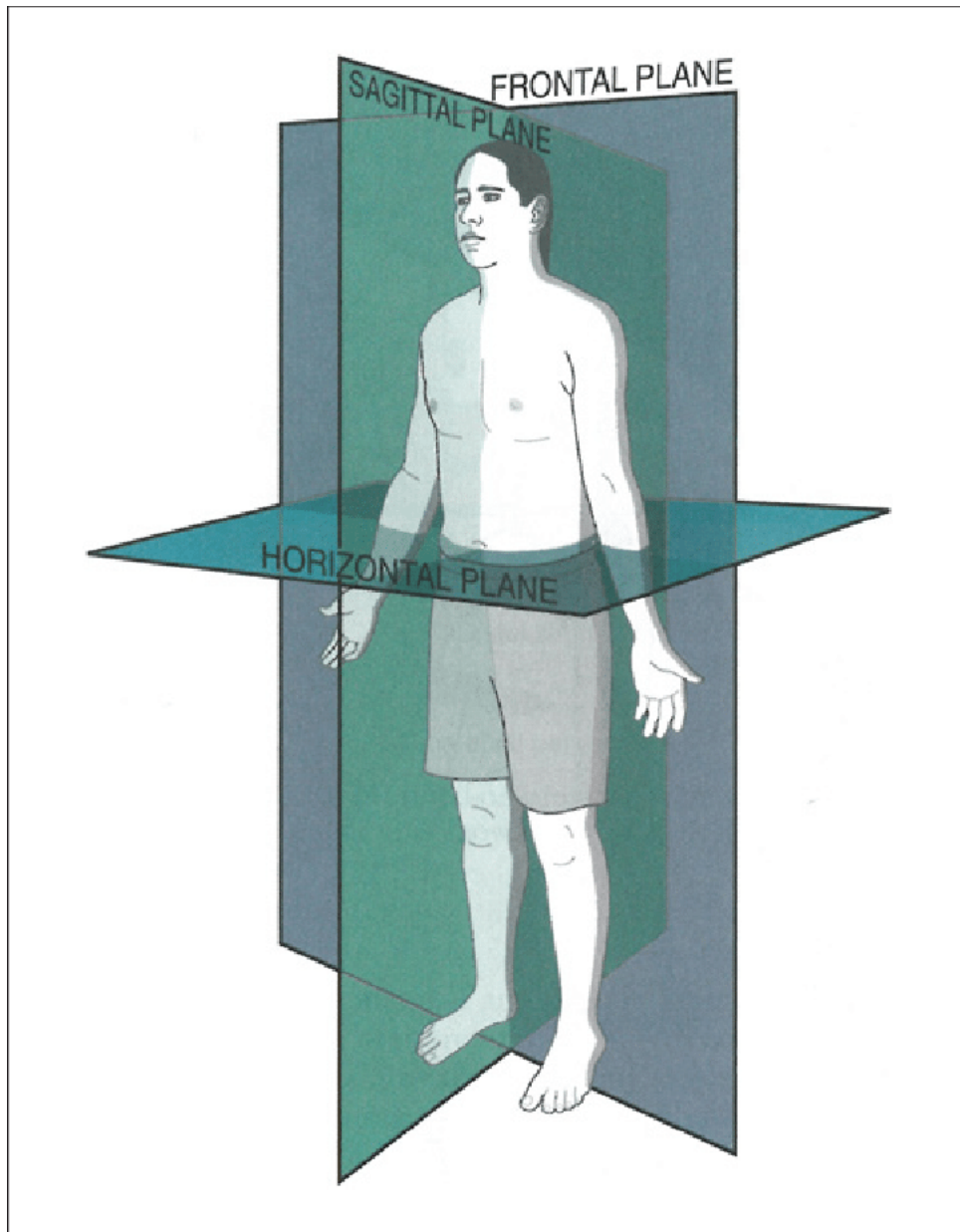


Figure 3 Cardinal Planes of the Human Body [11]

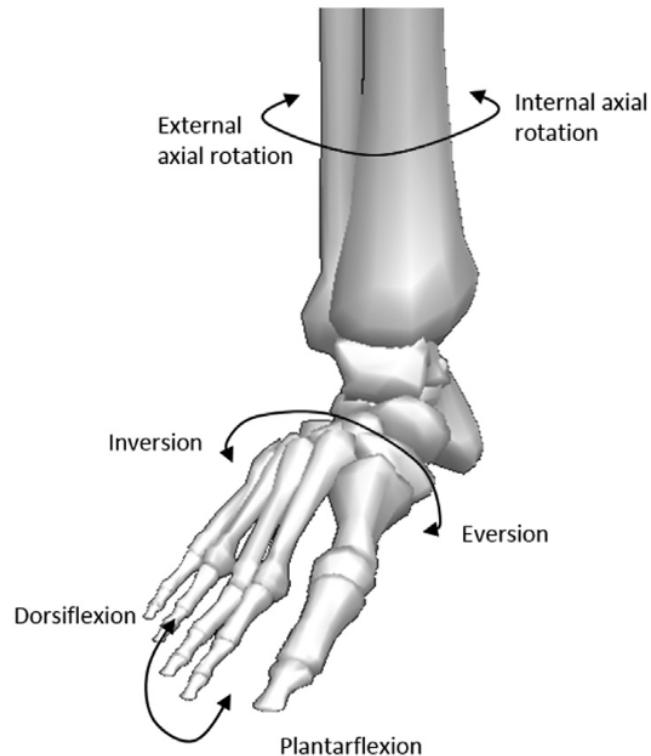


Figure 4 - Foot Movements in the Cardinal Planes [10]

There are two main phases of the gait cycle when walking: the stance phase and the swing phase (Figure 5). Walking at speeds between 1-1.25 m/s (2.2-2.8 mph), a person averages approximately 60 cycles/min and spends 60% of each cycle in the stance phase and 40% in the swing phase [7]. The gait cycle begins with the heel strike period of one leg and ends with the next heel strike of the same leg. Within the stance phase, the heel strike makes up the first 0-15% of the phase, followed by midstance from 15-30%, push off from 30-45%, and leg acceleration of the swinging leg from 45-60% [7]. The last 40% of the gait cycle is subdivided between swing-through of the leg and deceleration of the swinging leg [7]. There is a short period of double limb support for approximately 11% of the gait cycle when walking. Double limb support

occurs when both legs are in contact with the ground, with one leg ending its stance phase as the other leg begins its stance phase.

The running gait cycle differs substantially from the walking gait cycle (Figure 5). Gait speed can be classified as either jogging (3.31 m/s; 8 min/mile), running (4.77 m/s; 6 min/mile), or sprinting (10.8 m/s; 2.47 min/mile) [7]. As gait speed increases, the amount of time spent in the stance phase shifts to around 40%, while 60% is spent in the swing phase. Stride length and stride rate increase with gait speed, and double limb support ceases. Increasing gait speed also introduces a new phase within the swing phase: the float phase. During the float phase, the body is unsupported and “floats” above the ground momentarily before the opposite limb touches ground. The float phase occurs for 30% of the running gait cycle, with 15% occurring before the swing phase and 15% after the swing phase [7]. In addition, the vertical oscillation of the body’s center of gravity decreases with increased speed and the body maintains a forward lean during the running cycle. At a running pace, contact usually occurs in the posterior third of the foot (rearfoot or heel strikers) [7]. Most of the forward force generated during running is provided by the swinging arm and leg rather than the stance limb. Despite an understanding of running characteristics, there have been no definitive studies to determine the most efficient running style, or even what constitutes an efficient running style [7]. Different runners show no correlation between stride rate and stride length; some increase their stride rate while decreasing stride rate, while others do the opposite. Prosthetic feet should therefore be designed to accommodate a variety of gait patterns. They must be able to easily transition between walking and running modalities and be durable enough to withstand the large forces encountered while walking and running.

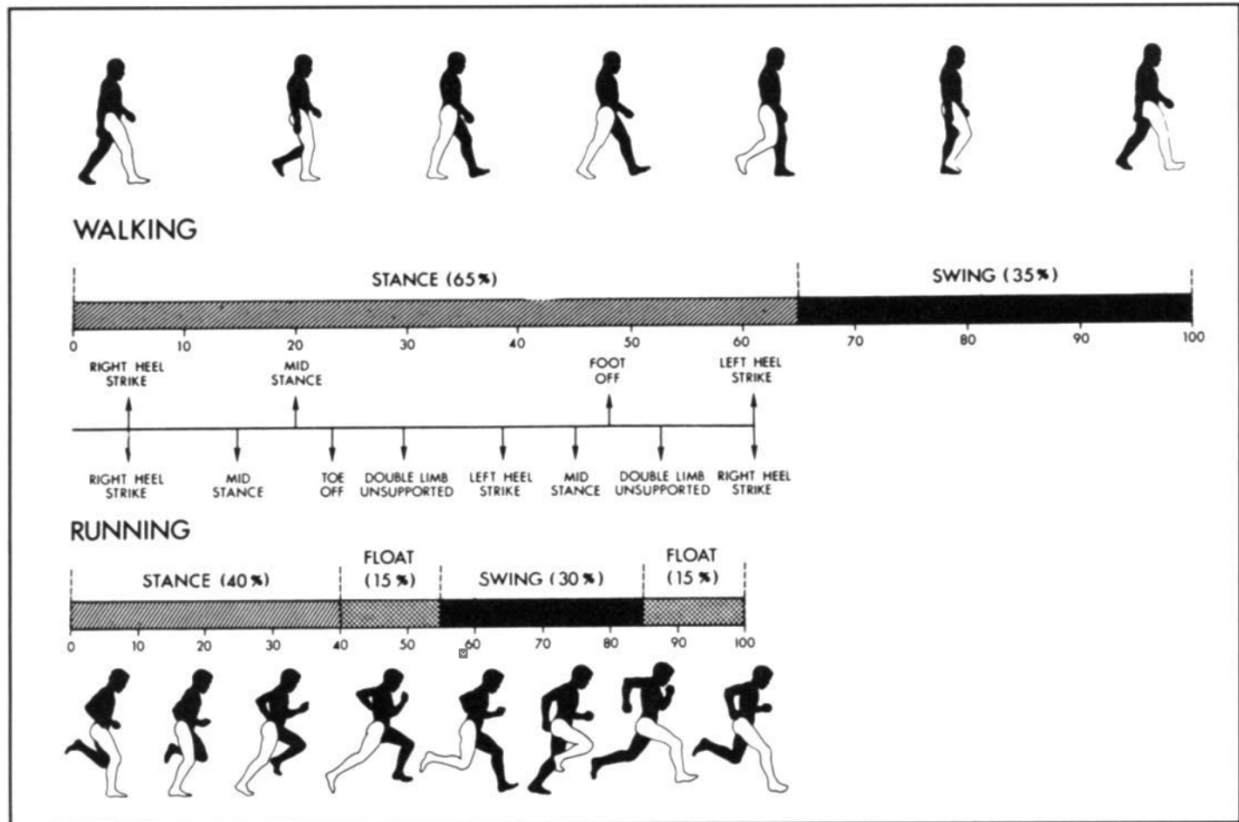


Figure 5 - Phases of Walking and Running Cycles [7]

A unique feature of the human foot is its adaptability to changes in locomotion requirements [12]. Parallel anatomical structures in the foot, the plantar intrinsic foot muscles and the plantar aponeurosis ligaments, work together to provide passive and active structures in the foot. Plantar intrinsic foot muscles, located within the longitudinal arch (LA), are composed of short muscles fibers attached to long tendons. This shape allows the largest of these muscles, the flexor digitorum brevis (FDB) and abductor hallucis (AH), to store and return significant amounts of energy during a stretch-shorten cycle. The central nervous system (CNS) uses these passive and active structures to modulate the energetic functions of the foot. The foot is able to increase energy absorption with muscle activation as well as increase power generated via tendon recoil rather than muscle. During low loading force tasks, such as walking or standing,

the foot effectively acts like a passive spring-like structure [12]. As the loading force requirements of the foot increase, intrinsic foot muscles such as the FDB muscles activate to increase the foot's capacity to absorb or generate energy. Stored energy can provide a burst of energy as the longitudinal arch recoils to aid in forward propulsion. In addition, actively controlling the energetic function of the human foot allows the foot to transform between an energy conserving structure and an energy damper as locomotion requirements change [12]. This ability to store, release, and dissipate energy is an important feature to emulate when designing lower limb prosthetic devices. Many prosthetic feet are capable of energy storage and return, yet cannot change their resistance. A tunable spring damper system could provide a simplified approximation and allow the prosthetic foot to adapt to various locomotion requirements.

The ankle complex bears a range of forces ranging from five times a person's bodyweight while walking, up to thirteen times bodyweight running or other intense activities [10]. A 250 lb person (113.4 kg) will experience forces of 5.56 kN while walking and up to 14.46 kN while running. Studies have shown that roughly 83% of the loads are transmitted through the tibiotalar joint, with the remaining 17% transmitted through the fibula. Of the load carried across the tibiotalar joint, 77-90% is applied to the talar dome, and the remaining load transmitted across the medial and lateral surfaces [10]. Despite these high loads, the ankle's large surface area spreads the loads over a wider area, resulting in lower stresses than at the knee and hip. Consequently, any mechanism used to simulate an ankle must also be able to withstand the large loads encountered while still providing the necessary range of mobility across the three cardinal planes.

A thorough understanding of lower limb biomechanics and the gait cycle when walking and running reveals the most important characteristics when designing a prosthetic lower limb.

The prosthetic must move in the three cardinal planes and help return energy during locomotion. It must be able to withstand the forces encountered during running, walking, jumping, and other high impact activities. Additionally, the prosthetic's fit must remain comfortable for extended periods of time. This project's proposed design aims to create a rugged prosthetic with a natural gait pattern by enabling ankle motion in the three cardinal planes.

2.3. Contemporary Prosthetic Devices

Over the past few decades, research and improved technology have vastly improved the functionality of lower limb prosthetics. Devices are made from materials such as carbon fiber, aluminum, and titanium to be strong and lightweight. Modern prosthetics are capable of mimicking some natural foot movements, such as inversion/eversion and plantar- and dorsiflexion. Many devices have multi-axial rotation and shock absorption like natural feet, and are capable of storing and returning some of the energy generated during walking [13].

Prosthetic feet can be categorized by the anticipated activity level of the user as well as by the structure of the prosthetic itself [13]. Activity levels are ranked on a scale from K1 to K4, with K4 being the highest activity level. Feet in the K1-K2 range favor user stability and comfort and are designed for simple ambulation with minimal environmental barriers. K3-K4 level feet are robustly designed to withstand the high activity levels of their users and allow more mobility and dynamic energy return than lower-level prostheses. Prosthetics rarely fall into one particular activity level, but instead work within a range of activity levels. This allows flexibility for amputees, as they can use fewer prosthetic devices for a wider range of activities.

Lower limb prosthetics follow two structural forms: non-articulating and articulating. Non-articulating feet are used by people with reduced mobility ranges, while articulating feet are

used by those with higher activity levels. The different types of structural forms are described below to better understand the variations among prosthetic devices.

Two types of non-articulating feet exist: solid ankle cushioned heel (SACH) and elastic keel feet. These feet are used primarily by K1-K2 level amputees who have low mobility and who do a limited amount of walking. Non-articulating feet are rigidly attached to the prosthetic shank and use compressible heels to provide stability and cushioning. Non-articulating designs are beneficial for their durability, affordability, and are virtually maintenance free [13].

The simplest articulating foot designs are single-axis feet and multi-axial feet. Single axis feet have an ankle joint allowing the foot to move up and down to enhance knee stability, and multi-axis feet can also move side to side at the ankle for better stability on uneven surfaces [13]. While allowing more mobility than non-articulating feet, articulating devices still favor stability over mobility and are used by amputees in the K2-K3 activity range.

Dynamic response feet are another type of articulating prosthetic (Figure 6). These feet store energy during the roll-over portion of the gait cycle to release it during push off. They also contribute to a more natural gait style and an increased range of motion. Some dynamic response feet feature a split-toe design to simulate inversion and eversion and provide stability on uneven surfaces. This prosthetic style is used by people with more active lifestyles or those wishing to move to a higher activity level [13].

<https://www.proteorusa.com/rush-foot-collection>

<https://www.ossur.com/en-us/prosthetics/feet/proprio-foot>

Figure 6 – The dynamic response Rush Foot by Ability Dynamics (left) and the microprocessor-controlled Proprio Foot by Össur

While dynamic energy response feet function much better than their predecessors, there are still areas for improvement. Dynamic response limbs have one stiffness profile meant to accommodate the widest expected range of activities. By contrast, the natural limb automatically varies its stiffness depending on the activity. As a result, amputees are often in situations where their device is either too stiff or not stiff enough. Many dynamic-response prosthetics work like simple springs, so that flexure of the limb provides both shock absorption and energy storage/release as the foot flexes. Because the prosthetic works like a simple spring, the energy stored by the foot is released almost immediately as the prosthetic returns to its upright neutral position. This can become unsafe when traversing sloped or uneven terrain, since the release of energy cannot be controlled. The prosthetic does not work with, but against the amputee as the device forces itself to its neutral position. Furthermore, dynamic response prosthetics can only approximate the foot's natural range of motion, making positions like crouching or leaning more difficult. The prosthetic is unable to rest flat on the ground like a natural foot, which can make sitting for extended periods of time uncomfortable. Due to these limitations, amputees are often forced to make compensatory movements when walking and running, causing them to move at a slower pace than non-amputees while simultaneously exerting greater amounts of energy [14–17]. Moreover, movement compensations cause accelerated stress and wear on the remaining natural limbs, leading to further surgical interventions. A review of current prosthetic foot designs suggests there is room for improvement and innovation in dynamic energy response. An improved dynamic response system would have variable stiffness profiles and would be able to delay energy return when moving. This would result in anatomically accurate foot motion that is more comfortable for the user.

The most complex type of articulating prosthetic is the microprocessor (MP) foot (Figure 6). MP feet use a web of sensors to dynamically adjust the foot/ankle components based on inputs from the limb and the environment [13]. The microprocessors determine ankle position and damping resistance based upon input signals to improve balance and mobility [13]. As a result, MP feet are able to quickly adapt to sloped surfaces and other uneven terrain, as well as provide powered propulsion to improve walking capabilities in real time [13]. The microprocessors in these prosthetics are capable of customizing various features based on activity for a more individualized and natural feel. Powered MP feet may enable subjects to increase their self-selected walking speed to that of able-bodied individuals, and can reduce sound knee loading by 15-20% at higher walking speeds [13]. Overall, the benefits of MP feet include their adaptability, customizability, and improved comfort over other types of prosthetic devices.

As with any design, MP feet also have their disadvantages. Firstly, MP feet require batteries to power the processors, which require regular recharging simply to use the prosthetic. The delicate electronics used in MP feet prohibit their use in wet or dusty environments [13]. Batteries and electronics are also negatively affected by cold weather, artificially limiting their use unless well shielded from the elements. MP feet generally fall into the K2-K3 activity levels and cannot be used by higher activity level amputees. These feet can be heavier and noisier than other prosthetic feet, and their added complexity makes them significantly more expensive than other options [13]. The complexity, delicacy, and expense represent key limitations for MP feet, ultimately making them useful for a small group of amputees.

Lower limb prosthetics vary widely in their prices. While many components can be mass produced, ultimately each prosthetic needs to be customized to fit the amputee using the device.

SACH and elastic keel feet will cost between \$5,000-\$7,000, while articulating feet will cost between \$10,000-\$15,000 as designs become more complex [6]. Dynamic response feet prices start at around \$12,000 and increase with complexity and added features. Hydraulic and other advanced mechanical systems usually cost upwards of \$15,000 [6]. MP foot costs start at \$20,000-\$30,000. Prices are dependent on various factors, such as health insurance coverage, government reimbursements, and production quantities made for different prosthetics [6]. Any reductions that can be made in producing a reliable prosthetic device will benefit the amputee and reduce the already significant burden caused by amputation.

The following chapters will describe this project's design in greater detail. Chapter 3 describes existing prosthetics that were influential to this design, and also provides detailed descriptions of the design components and their costs. Chapter 4 details various component simulations that test the components' ability to withstand expected forces. Finally, Chapter 5 provides a discussion of the prosthetic design, and lists limitations and areas of future work.

3. PROSTHETIC DESIGN

3.1. Design Parameters

The design parameters for this project were determined in two steps, with the goal of improving previous prosthetic foot designs. The first step in the design process involved reviewing patient and design engineer surveys to ascertain how current prosthetics can be improved to satisfy users' needs. Patients' firsthand experience using prosthetics provided invaluable feedback necessary to improve designs, while professional input described observations or trends reported by their patients and provided design feedback. The review of patient and developer responses revealed that improved comfort is the most important characteristic to consider in a prosthetic design [4,5,18,19]. In one survey, 35.3% of amputees reported discomfort as their main reason for not wearing a prosthesis [5]. Although the comfort of amputees is largely improved at the interface between the prosthetic socket and residual limb, prosthetic feet are also capable of improving the amputee's comfort. A prosthetic foot can increase comfort by tailoring its motion characteristics to the user's preferences. A prosthetic that functions more like a natural foot should prove to be more comfortable, while reducing the stresses placed upon the residual limb and other limbs. While not a direct improvement, a prosthetic foot that can be tuned to each user and that can move naturally will help reduce fatigue and indirectly improve the user's comfort during its use.

The second most important design characteristic identified by prosthetic users was increased mobility [4,5,19]. A prosthetic with increased mobility will be able to automatically adapt to uneven terrain, such as stairs or hills, across different axes. An improved prosthetic would also enable users to kneel, enter and exit cars, or don footwear more easily than current

prosthetics allow. A prosthetic with improved mobility could also alternate between different resistance modalities depending on the activity. This would enable amputees to engage in a wider range of activities, such as running, swimming, or cycling, which would benefit both their mental and physical well-being. And because the prosthetic functions more like a natural foot, the user will be able to walk at a faster self-selected speed while expending less energy. Reduced energy expenditure would also reduce the amount of stress placed upon the residual limb and other limbs, reducing pain. The result would be a comfortable prosthetic offering greater mobility while requiring less energy and fewer compensatory movement patterns.

Another important design characteristic identified when designing a prosthetic device is its appearance. This not only refers to its cosmetic appearance, but to the form of the device as well. A foot prosthetic should strive to mimic the natural foot's shape; doing so serves several purposes. An anatomically correct foot shape will feel more natural to the user, requiring less time to adapt to the prosthesis. Designing a shape that resembles a natural foot also enables the user to wear a wider variety of footwear. Cosmetic covers that make the foot appear more natural also encourage use of the prosthetic device. Surveys performed by the Amputee Coalition have shown that of the 10.8% of amputees that do not regularly wear their device, 35.3% reported their device's appearance as the reason [4]. Many commercially available prosthetics come with cosmetic covers in a range of skin tones. These help the prosthetic to fit in shoes better as well as provide traction while barefoot. An attractive prosthetic design will make amputees feel more comfortable wearing their device and will encourage them to wear their device more often.

The second step was to compare and contrast the various commercially available prosthetic designs available to amputees. These designs were evaluated based upon the feedback provided by patients and design engineers, which were then tabulated to clearly show common

features, as well as highlight areas in which further improvements could be made. Table 1 lists a selection of the tabulated prosthetic feet and describes features and unique design aspects. The listed prosthetics were chosen based on their influence on this project's design.

As more prosthetic feet were added to the full table, it became clear that hydraulic or pneumatic pistons were the best choice for this design. Ottobock's Meridium, Blatchford's Echelon line, Össur's Pro-Flex line, and the VF2 by BioDapt all use hydraulic or pneumatic pistons (Table 1). Both hydraulic and pneumatic pistons use fluid to control and transmit power: hydraulics use incompressible liquids such as oil, while pneumatics use compressible gasses such as air. The benefits that hydraulics/pneumatics provide to prosthetic devices lie in their ability to conform to slopes and uneven terrain. Hydraulics/pneumatics allow the leg to self-align on slopes and enable the user to easily rotate the leg over the foot when walking up and down uneven terrain. By contrast, dynamic response prosthetics simply propel the foot forward, which can be dangerous on uneven terrain and forces the user to make compensatory movements (Figure 6). Hydraulics/pneumatics reduce pressure in the residual socket and are less tiring for the user since they do not have to fight against their prosthetic. These features increase the user's comfort and energy efficiency. Pneumatics in particular use compressible gasses, which provides some amount of shock resistance. The VF2 by BioDapt uses a Fox Float DPS shock that can be tuned by the user. This tunable shock can be used as a variable damping system, providing varying resistance based on locomotion requirements. The user's ability to tune the shock as needed, as well as the shock's ready availability, are why it was chosen in this project's design too.

Another feature commonly found in prosthetic feet was a "split toe" foot plate, where the bottom plate of the prosthetic is split down part of its length rather than the plate being one solid

piece. This feature is apparent in the differences in shape between BioDapt's VF2 and Blatchford's Echelon VT in Figure 7. Splitting the foot plate improves the prosthetic's mobility by enabling some inversion and eversion. A split toe was included in this project's design to improve the prosthetic's mobility and facilitate adaptability to various terrain.

This project also focused on prosthetic designs that sought to improve ankle mobility. However, few designs reviewed for this project and included in Table 1 placed a large emphasis on ankle mobility improvement. Only designs such as the Triton Side Flex by Ottobock and the Pro-Flex Pivot by Össur sought to improve foot inversion/eversion or plantarflexion/dorsiflexion, respectively (Figure 7). According to amputees, a prosthetic's degree of mobility is the next most important characteristic behind comfort [4,5,19]. The lack of prosthetics seeking to improve mobility reveals a market shortcoming, as well as an area of improvement. This project's design significantly improves ankle mobility by using a ball joint to provide plantarflexion, dorsiflexion, inversion, eversion, adduction, and abduction.

<https://www.biodaptinc.com/products/vf2.html>

<https://www.ottobockus.com/products/triton-prosthetics-feet/>

<https://www.blatchfordus.com/products/echelonvt/>

<https://www.ottobockus.com/products/meridium/>

<https://www.ossur.com/en-us/prosthetics/feet/pro-flex-pivot>

Figure 7 - Clockwise from top left: VF2 by BioDapt, Triton Side Flex by Ottobock, Echelon VT by Blatchford, Meridium by Ottobock, and Pro-Flex Pivot by Össur

An outline for a prosthetic design began to take shape once these parameters had been determined. The main foci for this design were improved mobility as well as energy storage and

return as the means to improve comfort. The expectation is that through improving mobility, the prosthetic device will be able to move more like a natural foot and will therefore feel more comfortable for the user. Likewise, by developing a foot with good energy storage and return properties, the prosthetic foot will reduce user fatigue and improve overall comfort when moving about. The means with which this device attempts to improve mobility, energy storage/return, and ultimately user comfort, is through the use of a ball joint ankle and pneumatic piston, respectively.

| Model/ Brand | Weight | Type | Activity Level | Features |
|----------------------------------|---------------------|-------------|-----------------------|-------------------------------------------------------------------------------------------------------------------------------------------------------------------------------------------------------------------------------------------------------------------------------------------------------------------------------------------------|
| Echelon VT/ Blatchford | 1.88 lb (855 g) | Mechanical | K3 | <ul style="list-style-type: none"> - Hydraulic control of plantar- and dorsiflexion - Dorsiflexed toes increase ground clearance - Vertical shock absorption reduces shear forces - Split toe design for ground compliance |
| Echelon VAC/ Blatchford | 1.56 lb (700 g) | Mechanical | K3 | <ul style="list-style-type: none"> - Hydraulic control of plantar- and dorsiflexion - Integrated vacuum system generated through walking motion - Vacuum system does not require power - Split toe design for ground compliance |
| Meridium/ Ottobock | 3.31 lb (1500 g) | MP | K2 | <ul style="list-style-type: none"> - Toe plate with split toe achieves considerable ground contact - Microprocessor controls plantar- and dorsiflexion with adjustable hydraulics - 4 axis kinematics allow adaptations to natural movement patterns - Prosthetic lowers itself to floor when sitting |
| Triton Side Flex/ Ottobock | 1.62 lb (737 g) | Mechanical | K3-K4 | <ul style="list-style-type: none"> - Integrated torsion bar allows full-ground contact on uneven surfaces, even whilst walking - Customizable shock-absorbing heel wedge - Polymer base spring connects forefoot and heel spring - Split toe design for ground compliance |
| Pro-Flex LP Torsion/ Össur | 2.11 lb (960 g) | Mechanical | K2-K4 | <ul style="list-style-type: none"> - Torsion module added for rotational and vertical shock absorption - Full length toe and ‘reverse tapered’ technology allow greater dorsiflexion - Split toe design for ground compliance |
| Pro-flex Pivot/ Össur | 2.02 lb (920 g) | Mechanical | K2-K3 | <ul style="list-style-type: none"> - Pivot mechanism provides 27° of ankle motion - Biomimetic movement provides 13% load reduction of contralateral limb - Split toe design for ground compliance |
| VF2/ BioDapt | 2.63 lb (1190 g) | Mechanical | K3-K4 | <ul style="list-style-type: none"> - Pneumatic control of plantar- and dorsiflexion - 28° of ankle dorsiflexion - Carbon sole plate with interchangeable soles for various activities |

Table 1 Prosthetic Design Comparison

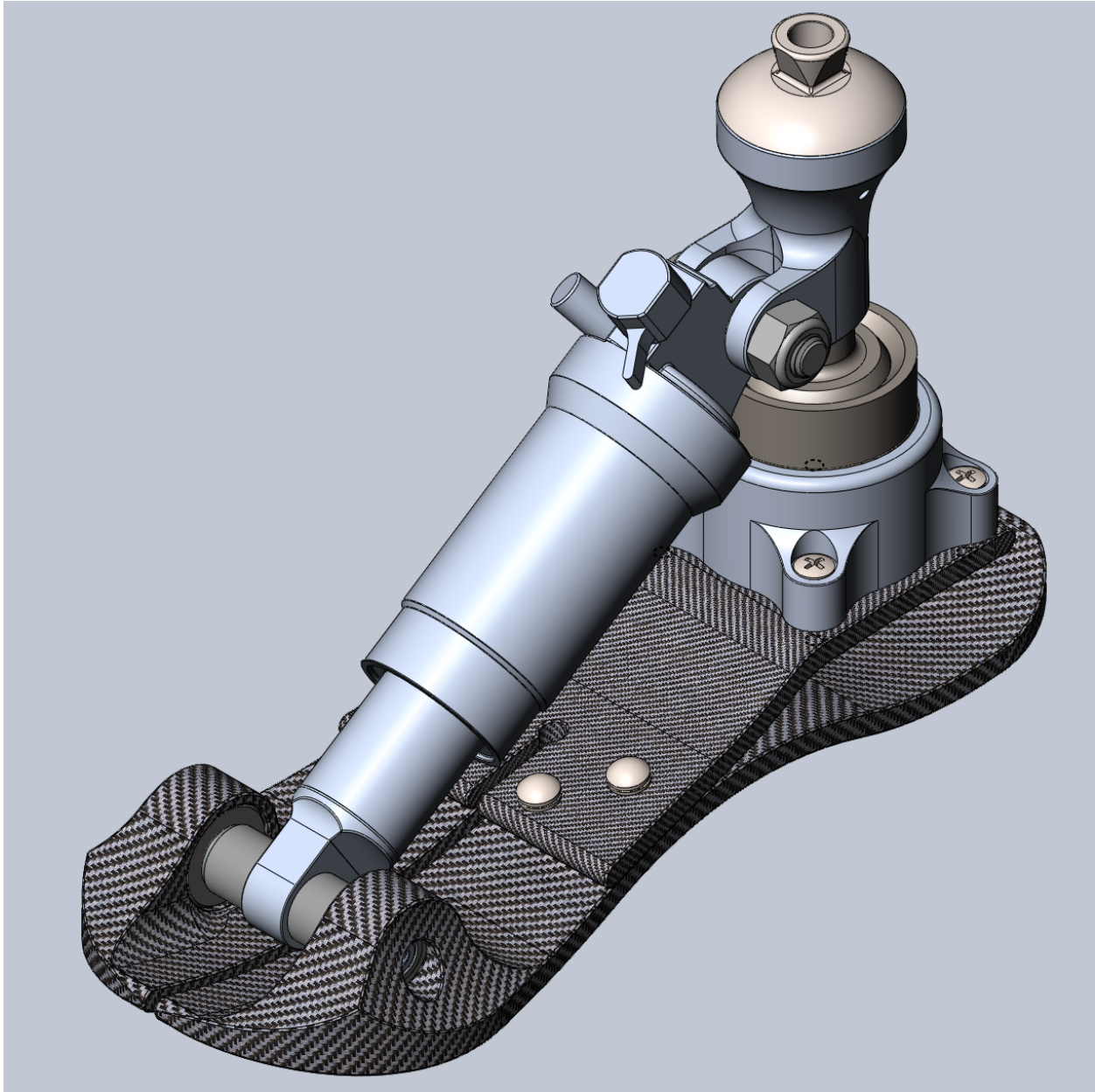


Figure 8 - Isometric View of Prosthetic Design

3.2. Current Design

This project proposes an articulated prosthetic foot design that more closely mirrors natural foot motion than other currently available devices. This prosthetic uses a tunable

pneumatic piston to damp and redistribute forces generated from walking. Using a pneumatic piston works more effectively than simple leaf spring designs commonly found in most articulated prosthetics, as pneumatic pistons do not release energy immediately after storing it. This allows for a more natural gait pattern rather than the unnatural gait pattern caused by accommodating a traditional spring. As an added benefit, the pneumatic pistons provide better force damping than leaf springs from vertical shock and other forces generated during walking and running. Pneumatic pistons can be adjusted to fine tune their damping performance when walking, and their performance can be adjusted as needed for different foot functionality, such as higher resistance for running or athletic activities. Overall, the addition of a pneumatic piston vastly improves the functionality, comfort, and lifespan of the prosthetic foot.

Although several commercially available prosthetic designs have successfully used hydraulic and pneumatic pistons, their range of ankle mobility is still limited. To improve the ankle mobility found in prosthetic feet, this design used a ball joint as an ankle mechanism. The inclusion of a ball joint is an important design innovation, as ball joints allow movement across all three cardinal planes, making them ideal ankle analogues. The joint is capable of 360° of motion in the horizontal plane and is also able to pivot about the sagittal and coronal planes. This range of movement will allow a prosthetic to pronate, supinate, invert, evert, and pivot similar to a natural ankle. This design's particular ball joint is normally found in automobile suspension systems, but can work for prosthetics as well (Figure 27) [20]. The rugged design of the proposed prosthetic allows it to operate in a wide range of harsh environments. This ball joint is completely rebuildable for easy repair or replacement. The ball joint can also be pre-loaded with a torque nut to fine-tune the movement resistance within the housing. These features make the ball joint's foot motion highly customizable and affordable. The addition of a ball joint to a

dynamic response foot further increases the foot's functionality by increasing the prosthetic's ankle mobility and resulting in more natural foot motion.

This project aimed to use standardized and off-the-shelf components whenever possible to reduce costs and facilitate maintenance. Lower limb prosthetics use standardized hardware to connect the foot and prosthetic socket together. Using standardized parts allows the amputee to use this device without buying additional special equipment, while continuing to use any other devices they already own. Other components in the device use standardized hardware that is easy to source. Easily sourced hardware enables easier construction by the manufacturer and easier repairs by the prosthetist. Off-the-shelf components are more cost effective since they do not require specialized manufacturing to produce. Using these parts results in a prosthetic device that is faster and easier to construct, with hardware that can be replaced quickly and easily, and makes the device cheaper for both the user and manufacturer.

This prosthetic design will use carbon fiber for the foot plates' material. Carbon fiber is a strong material that can be molded into a variety of forms. The foot plates are composed of two separate carbon fiber pieces bolted together. The lower foot plate is curved to provide passive suspension and allow the foot to store and release some energy encountered while moving. The front of the lower plate has recesses in the top of the foot plate to hold swivel joints in place (Figure 9), as well as a split toe design (Figure 10). The split toe works in conjunction with the ball joint to allow inversion and eversion of the foot, creating natural foot motion. Inversion and eversion of the split toe also allow the front axle of the hydraulic piston to pivot, enabling greater adduction and abduction at the ankle. The upper foot plate is cantilevered off the lower foot plate to provide further passive suspension for the prosthetic foot. The ball joint attaches to the upper foot plate and allows the ball joint to be located in the same relative position as a natural ankle

joint. Carbon fiber has been used successfully in many commercially available prosthetics and is an ideal material for the foot plates because of its high strength, low weight, and ability to be formed into complex shapes.

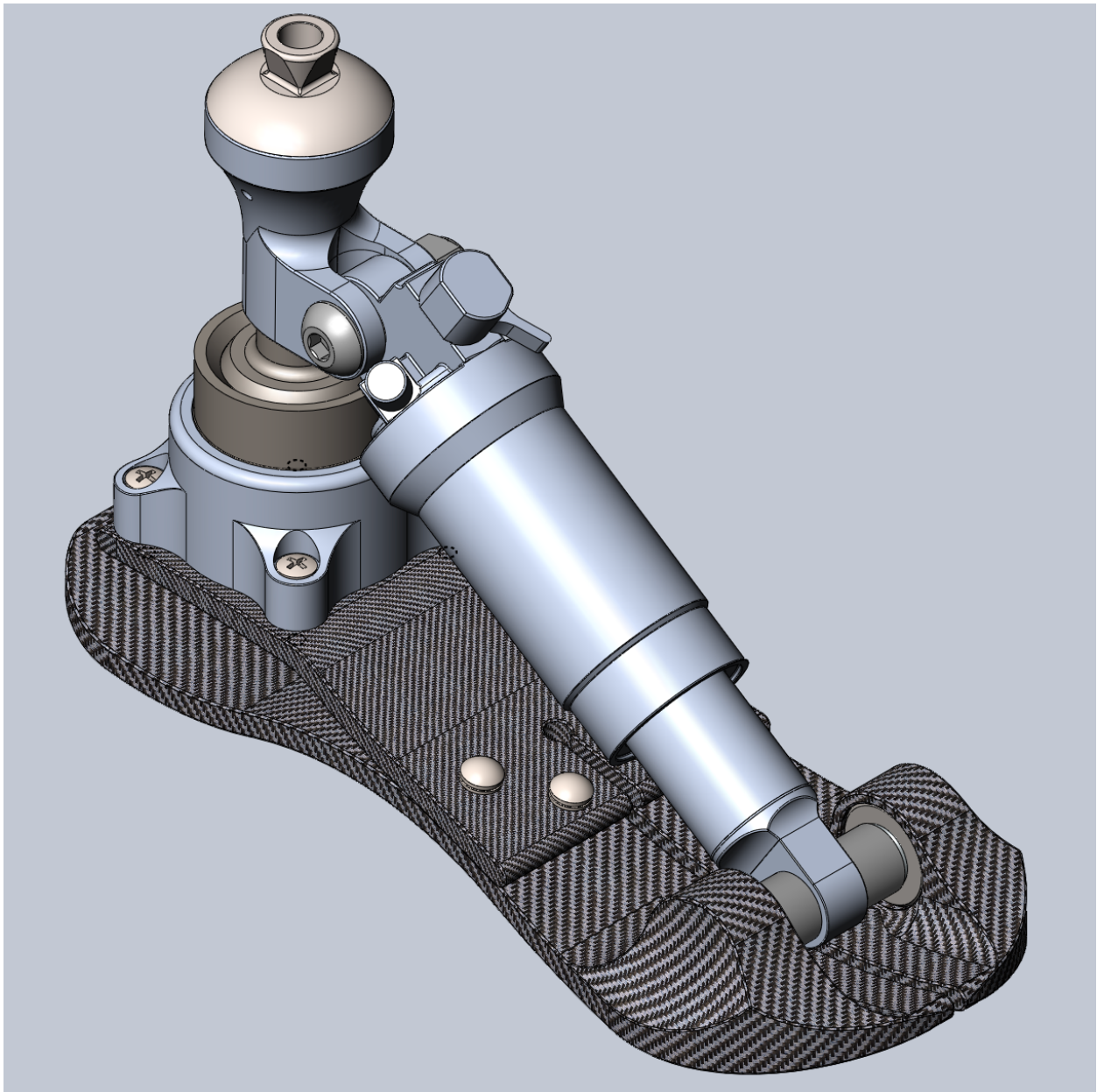


Figure 9 - Alternate Isometric View of Prosthetic Design

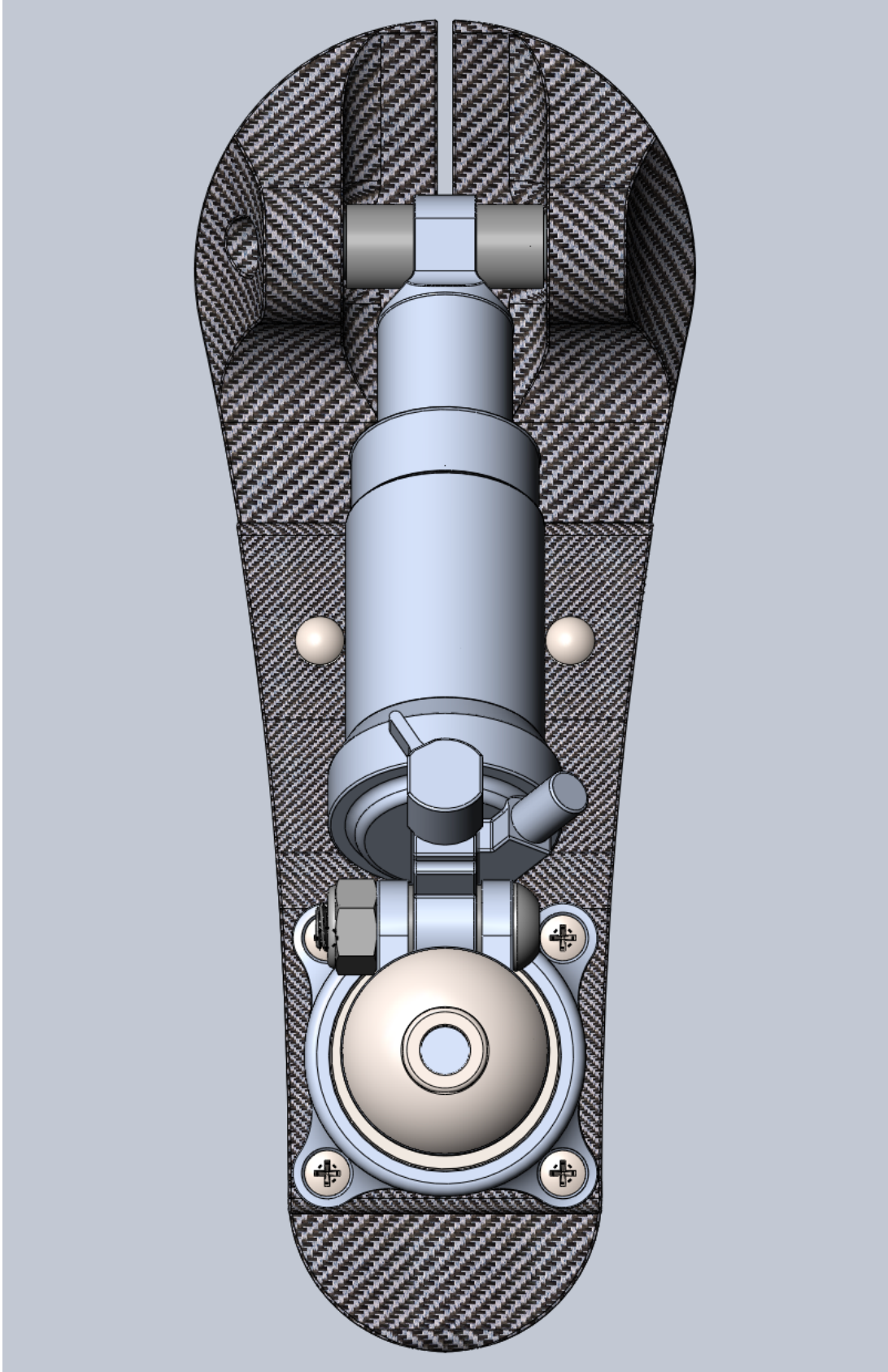


Figure 10 - Top View of Prosthetic Design

In summary, the primary features of the proposed design include the ball joint, the pneumatic shock, and use of standardized components. The ball joint ankle provides a larger range of motion in the foot, enabling the user to move across a wide variety of terrain more confidently. The pneumatic piston functions similarly to the muscles and tendons of natural feet by improving the prosthetic's ability to conform to uneven terrain. In addition, the piston absorbs shock forces generated during movement. The stiffness provided by the carbon fiber foot plates aid in passive shock absorption, as well as aid in inversion and eversion of the prosthetic foot. Standardized components help the prosthetic to remain affordable and work reliably with other prosthetic components an amputee may already use. In addition, standardized components allow parts of the prosthetic to be repaired or replaced as needed, increasing the prosthetic's usable lifespan. Because this design does not use microprocessors or other electronics, it can be used in a wide variety of environments without fear of contamination or failure. Combined, these features result in a robust prosthetic foot that is affordable for the user and more closely mimics natural foot movement.

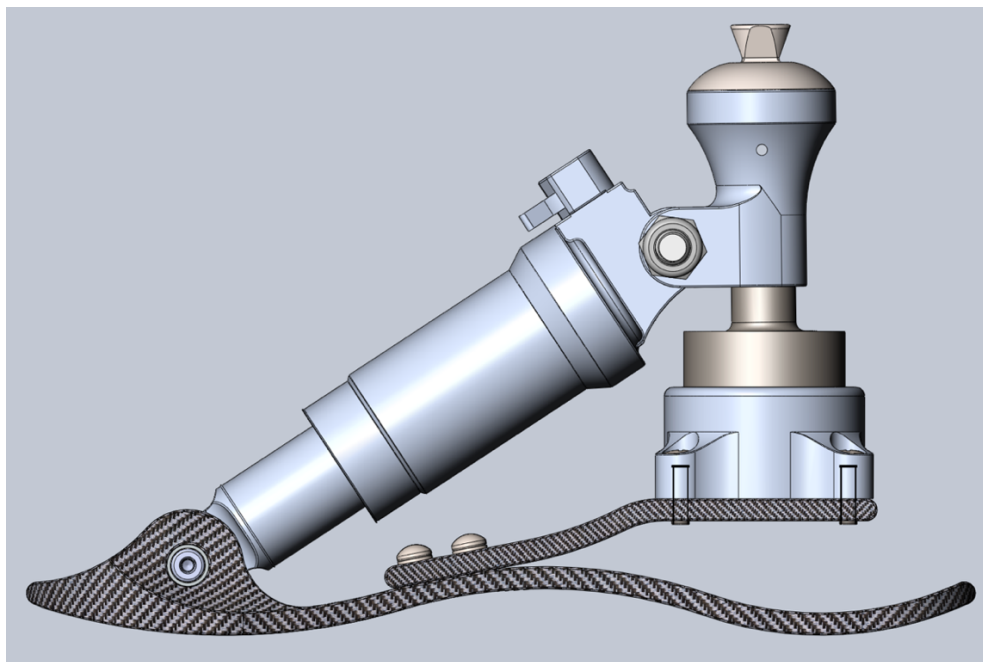


Figure 11 - Profile View of Prosthetic Design

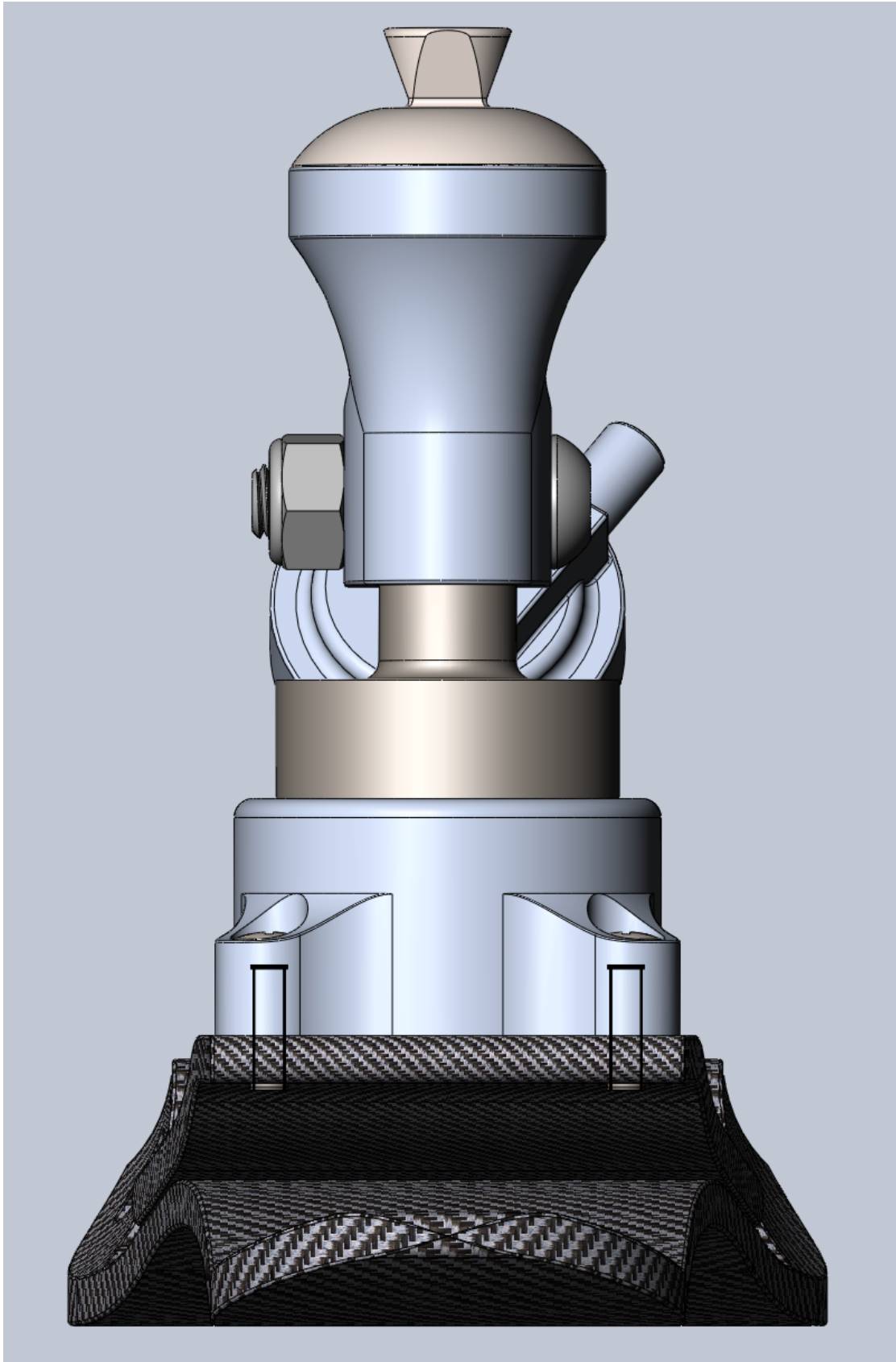


Figure 12 - Rear View of Prosthetic Design

3.3. Design Features

3.3.1. Foot Plates



Figure 13 - Isometric View of Foot Plates

The base of this prosthetic design comprises two carbon fiber foot plates that are bolted together. The lower-foot plate contacts the ground and is one of the connection points for the Fox Float DPS piston. The upper-foot plate is the connection point for the ball joint mechanism. The foot plates cambered and cantilevered designs, as well as the stiff carbon fiber, provide some passive shock absorption to the prosthetic. Both plates have been designed to fulfill multiple functions in a simple design that is easy to manufacture.

Both foot plates are made from Zoltek PX35 multi-directional fabric. PX35 fabric is useful for forming complex shapes and can be machined to the final foot plate forms. Areas that need additional thickening can use PX35 prepreg tapes to meet different composite properties at different foot plate areas. The material properties of PX35 are listed in Table 2 below.

Simulations for the upper- and lower-foot plates and can be seen in Section 4.1. A manufacturer for the upper- and lower-foot plates was unable to be located. Future production of this design will require fabrication by a carbon fiber manufacturer specializing in custom small batch components.

| Property | Multi-Directional Fabric | Prepreg Tape |
|---------------------------------|---------------------------------|---------------------|
| Tensile Strength | 4137 MPa | 1850 MPa |
| Tensile Modulus | 242 GPa | 130 GPa |
| Density | 1.81 g/cc | - |
| Compressive Strength | - | 1320 MPa |
| Compressive Modulus | - | 125GPa |
| Interlaminar Shear Strength | - | 70 MPa |
| +/- 45° In-Plane Shear Strength | - | 59 MPa |
| +/- 45° In-Plane Shear Modulus | - | 4.8 GPa |

Table 2 - Zoltek PX35 Material Properties [21]

The foot plates are connected to one another by four M5 bolts and washers, which are held in place by threaded standoffs on the underside of the lower foot plate (Figure 14). The standoffs are press-fitted into the lower foot plate and provide a clean connection without bulky hardware. The threaded standoffs used are an M5 size manufactured by S.W. Anderson, and both the washers and bolts are manufactured by McMaster-Carr. Using more hardware distributes the forces so that each bolt encounters lower stresses. In addition, the connection points between each plate are chosen at an area of minimal foot flexure, reducing the chance of potential stress points.

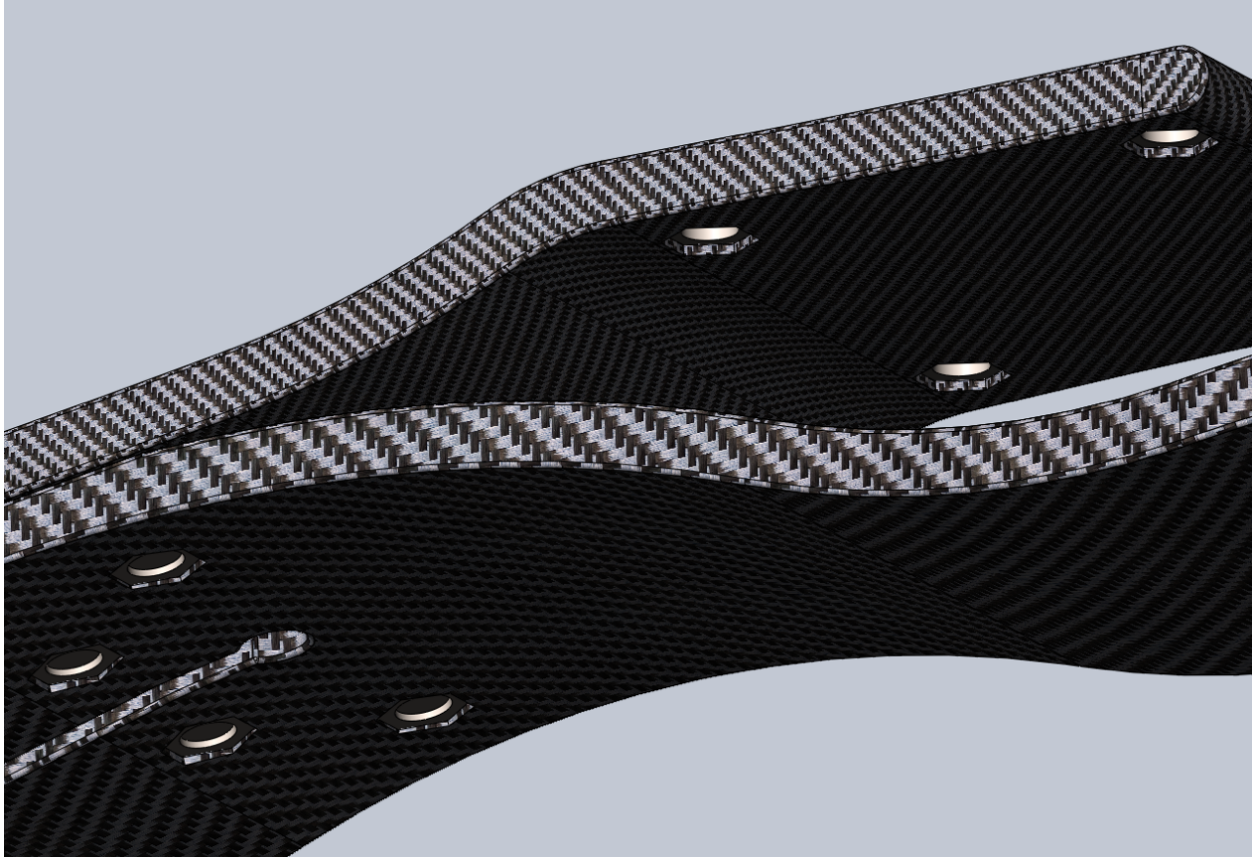


Figure 14 - Detail of Threaded Standoffs in Upper- and Lower-Foot Plates

The lower foot plate is shaped to both improve toe clearance for the user while also providing passive shock absorption. The symmetrical design allows the prosthetic to be used for either foot, with a cosmetic cover used to differentiate the left or right foot as needed. The plate curves upwards at the toe and heel to improve ground clearance when moving (Figure 15). The middle of the foot plate has a central camber, allowing foot flexure and shock absorption. Recesses for the threaded standoffs are located on the underside of the foot, near the central camber (Figure 14). These recesses are countersunk to hold the standoff in place and prevent rotation once inserted.

The front of the foot plate features a split toe design, which enables the foot to invert and evert (Figure 16). The tops of the toe area have rounded portions which house spherical bearings

on either side (Figure 17Figure 18). The spherical bearings, manufactured by McMaster-Carr, are corrosion resistant and have a PTFE liner. The liner eliminates the need to lubricate the bearings, and the corrosion resistance allows the bearings to be used in harsh environments. The spherical bearings are press-fitted into recesses in the rounded portions of the toe area (Figure 17). Using spherical bearings enables the toes of the foot plate to invert and evert while maintaining the position of the front axle (Figure 17Figure 18). As the toes offset from one another, the bearings are able to keep the axle in place up to 27° from the horizontal position. The spherical bearings are connected by a spiral vent dowel pin (Figure 18a), which has a breaking strength of 14,300 lbs. The dowel pin is held in place by friction, while the spiral vent allows air to escape. One end of the pin has a threaded opening to facilitate pin removal for repairs. The Fox Float shock remains centered on the dowel pin by a 40 mm-width mount kit sized to fit between the spherical bearings. This kit is sealed to prevent contamination and contains a stainless-steel mount pin nested within a low friction bushing to allow free rotation of the shock [22].

Mounting one end of the Fox Float shock to the foot plate toe area provides the greatest source of shock absorbance for the prosthetic foot. The finished prosthetic will have a fitted cover for the axle hole to both protect the spherical bearing as well as give the prosthetic a clean, finished appearance.

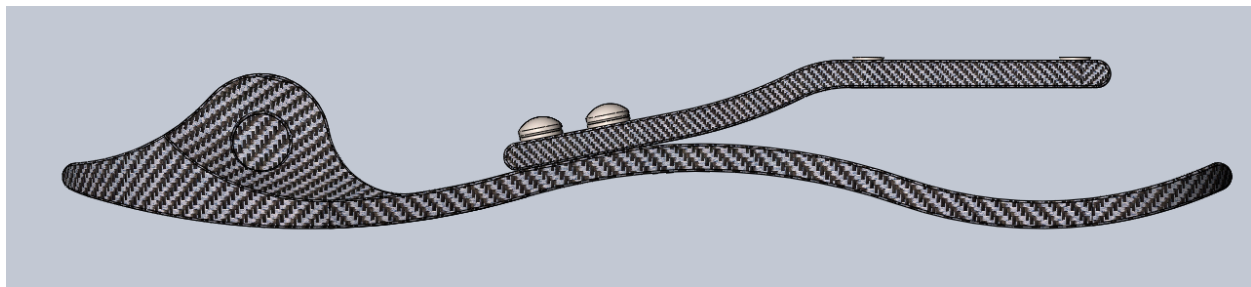


Figure 15 - Profile View of Foot Plates

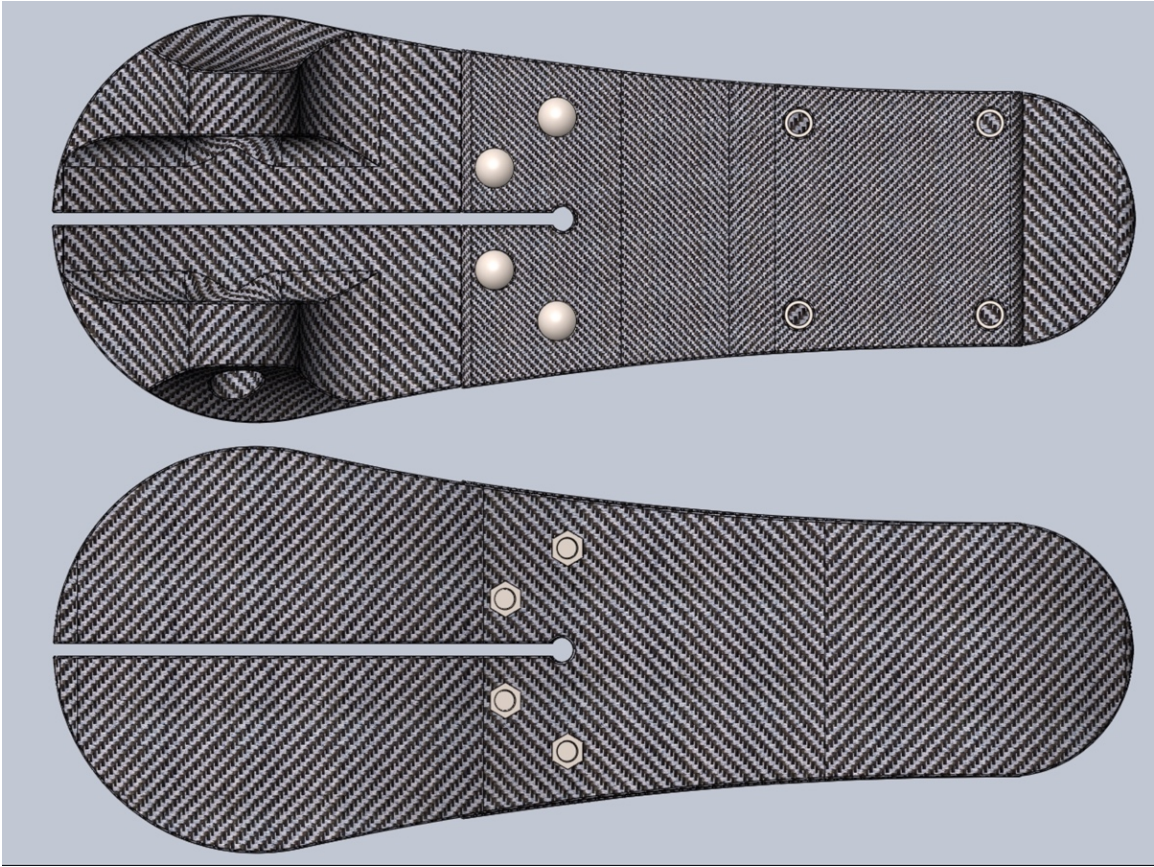


Figure 16 - Top and Bottom Views of Foot Plates

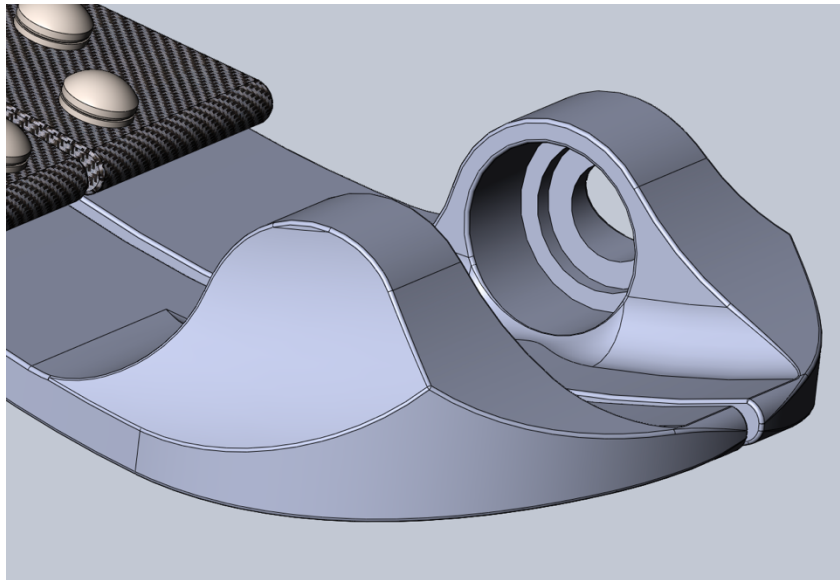


Figure 17 - Detail of Spherical Bearing Recess and Axle Pass-through (cosmetic skin removed for clarity)

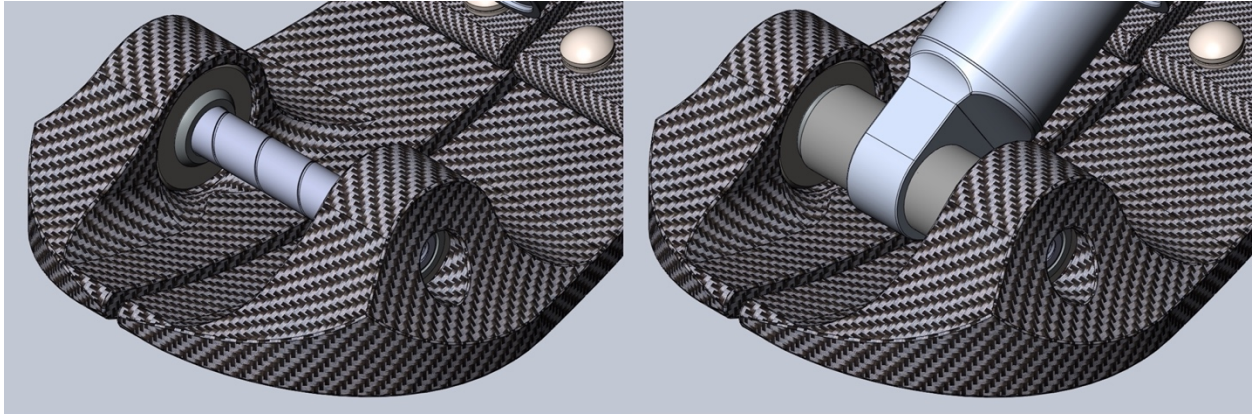


Figure 18 - a) Foot Dowel Pin inserted in Spherical Bearings. b) Full front assembly with Fox Float Shock and Mount Kit.

The design of the upper foot plate is much simpler compared to the lower foot plate. The upper foot plate is a cantilevered design that suspends from the lower foot plate. In addition to providing shock absorption through flexure, the upper plate is sized to place the ball joint in a similar position to a natural ankle (Figure 19). By placing the ball joint in this location, the prosthetic will move more like a natural foot. It is believed that doing so will enable amputees to acclimate to the prosthetic faster and will make the prosthetic feel more comfortable. The underside of the cantilevered portion has recesses to fit threaded standoffs, similarly to the lower foot plate (Figure 14). The threaded standoffs used here are also size M5 and manufactured by S.W. Anderson. These are used to connect the upper foot plate to the attachment bracket, which holds the ball joint in place.

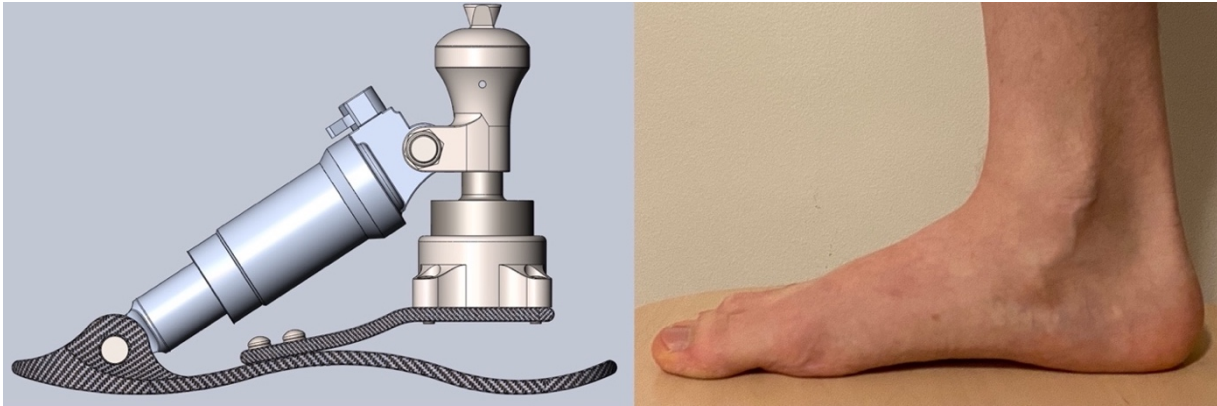


Figure 19 - Profile Comparison of Prosthetic and Natural Foot

3.3.2. Fox Float DPS

<https://www.ridefox.com/family.php?m=bike&family=float>

Figure 20 - Fox Float DPS piston [23]

This prosthetic design utilizes a Factory Series Fox Float DPS shock for energy storage and return. This model is known primarily in the world of mountain biking as one of the best possible choices for rear suspension. The shocks are known for their active engagement and smooth movement throughout the stroke length. However, these shocks are not limited to mountain biking, but have had success in prosthetics as well. The Fox Float DPS has been used successfully by BioDapt for their VF2 prosthetic foot (Figure 7). The wide range of compression settings make the Float DPS a good candidate for users who wish to fine-tune the foot for different applications.

The Fox Float DPS performs best when the air pressure is adjusted to the proper “sag setting.” Sag is the amount of compression the shock experiences under bodyweight, and should be between 25-30% of total shock travel [24]. Sag is based upon bodyweight, with the proper psi set equal to the user’s bodyweight as a starting point. The sag can then be raised or lowered

slightly based on personal preference. Since the Float DPS has a maximum pressure of 350 psi, it is reasonable to assume anyone below 350 lb will be able to use this shock safely [24]. Despite this robustness, the shock is surprisingly lightweight. The shock used for this design weighs only 221 g [23]. The shock uses a lever-controlled dual piston system (DPS) to cycle between three main compression modes: Open, Medium, and Firm (Figure 21). The main piston is used during the Open and Medium modes, and a second lockout piston engages in Firm mode to restrict fluid travel [25]. These modes can be switched on the fly as compression demands change throughout the day. In addition to the three main modes, there is an additional three position selector specifically for Open mode (Figure 21). This selector controls the amount of low-speed compression while in Open mode, further fine tuning the amount of compression available [24]. The Float DPS also integrates an EVOL air spring into the design. The air spring is a sleeve that creates a negative air chamber to significantly reduce the force needed to initiate travel. It also has a more linear progression, which improves mid-stroke support and bottom-out resistance [24]. Volume spacers are available that change the amount of mid-stroke and bottom-out resistance if needed. The Float DPS also has rebound adjustment, which controls the rate at which the shock extends after compressing (Figure 21). Rebound damping increases with higher air pressure settings, with higher damping resulting in slower shock rebound to full extension.

<https://www.ridefox.com/fox17/help.php?m=bike&id=1079#usingtheevolairsleeve>.

Figure 21 – (left to right) Fox Float 3-Position Lever, Open Mode Adjust, and Rebound Adjustment [24]

Another benefit to using the Fox Float DPS is that the shock can be serviced relatively easily. Fox's website contains a number of resources providing the information necessary to service or completely rebuild the shock if necessary. This allows the user to repair their

prosthetic foot more easily if any issues would occur and increases the service life of the prosthetic.

As described in the previous section, one end of the Fox Float connects to a dowel pin in the lower foot plate. Connecting the prosthetic foot in this manner will allow it to use the shock while still allowing inversion and eversion of the foot (Figure 18). The other end of the shock will be connected to the ball joint stud connection bracket, which is covered in the following section. Connecting the shock in this fashion allows easy access to the 3-position lever controlling the compression modes. Moreover, this position enables the shock to absorb and release energy during walking and running while offering good range of motion.

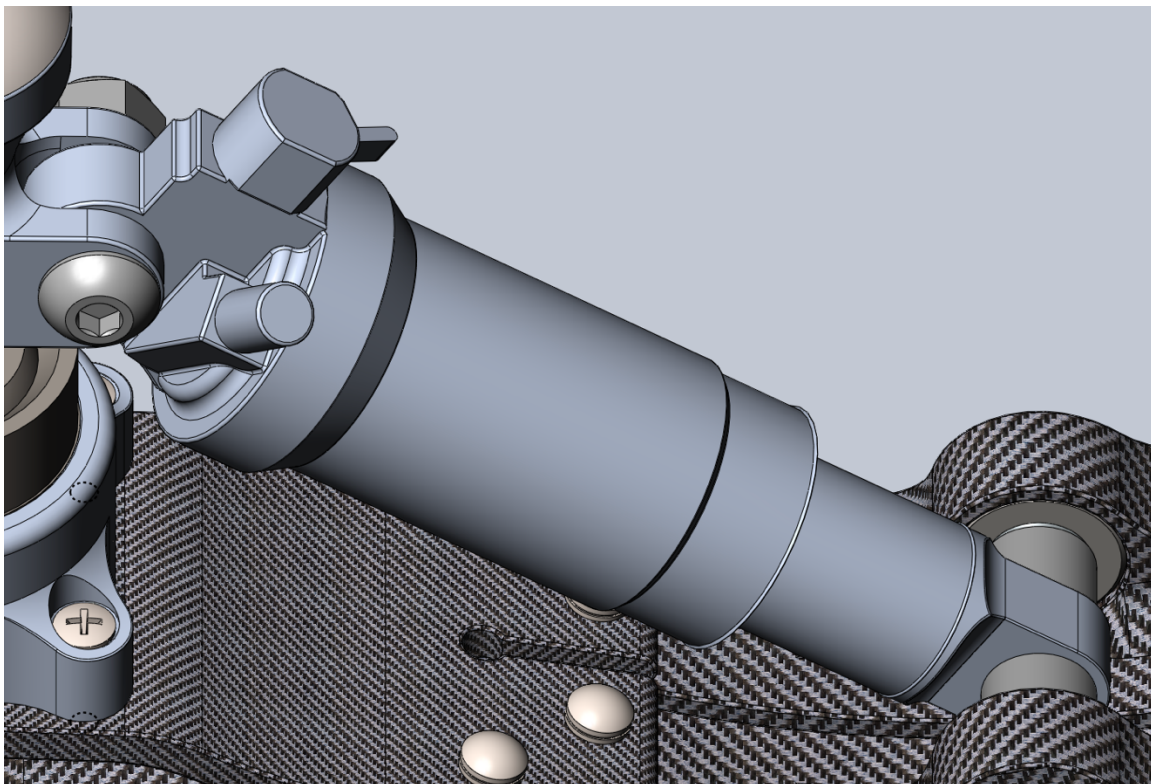


Figure 22 - Detail View of Fox Float DPS shock Connection Points

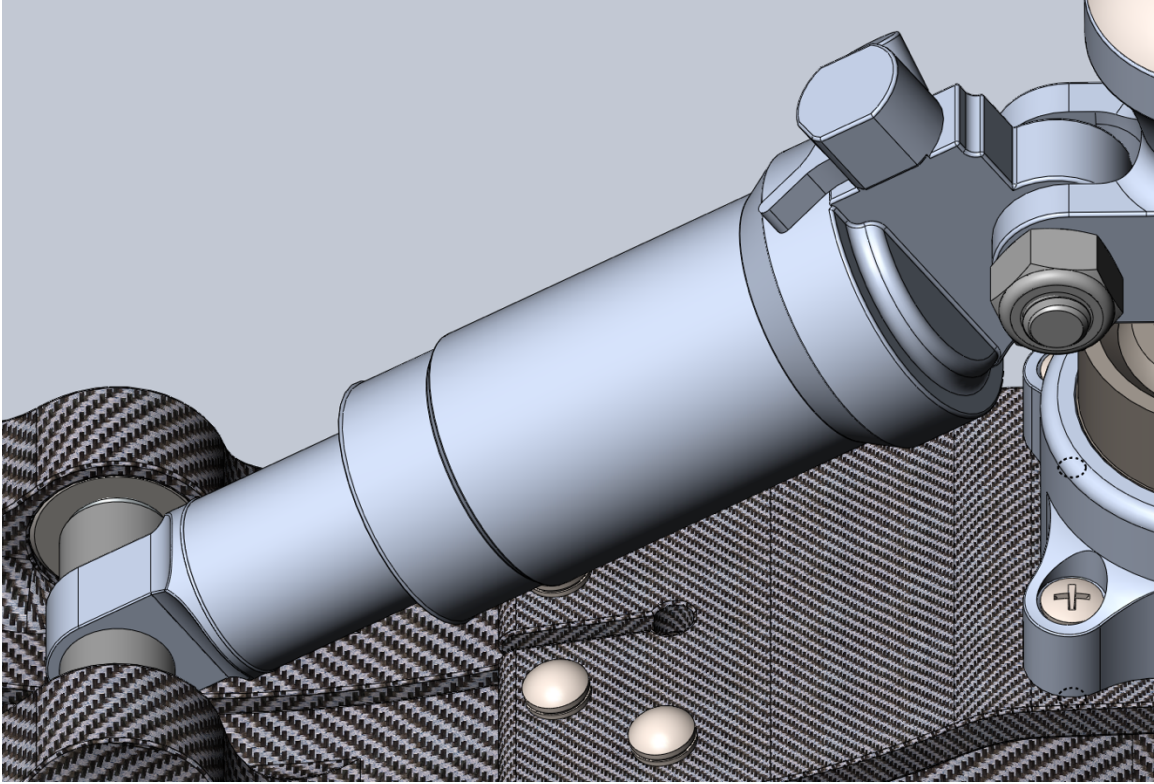


Figure 23 - Alternate Detail View of Fox Float DPS Shock Connection Points

3.3.3. Ball Joint Stud Attachment Bracket

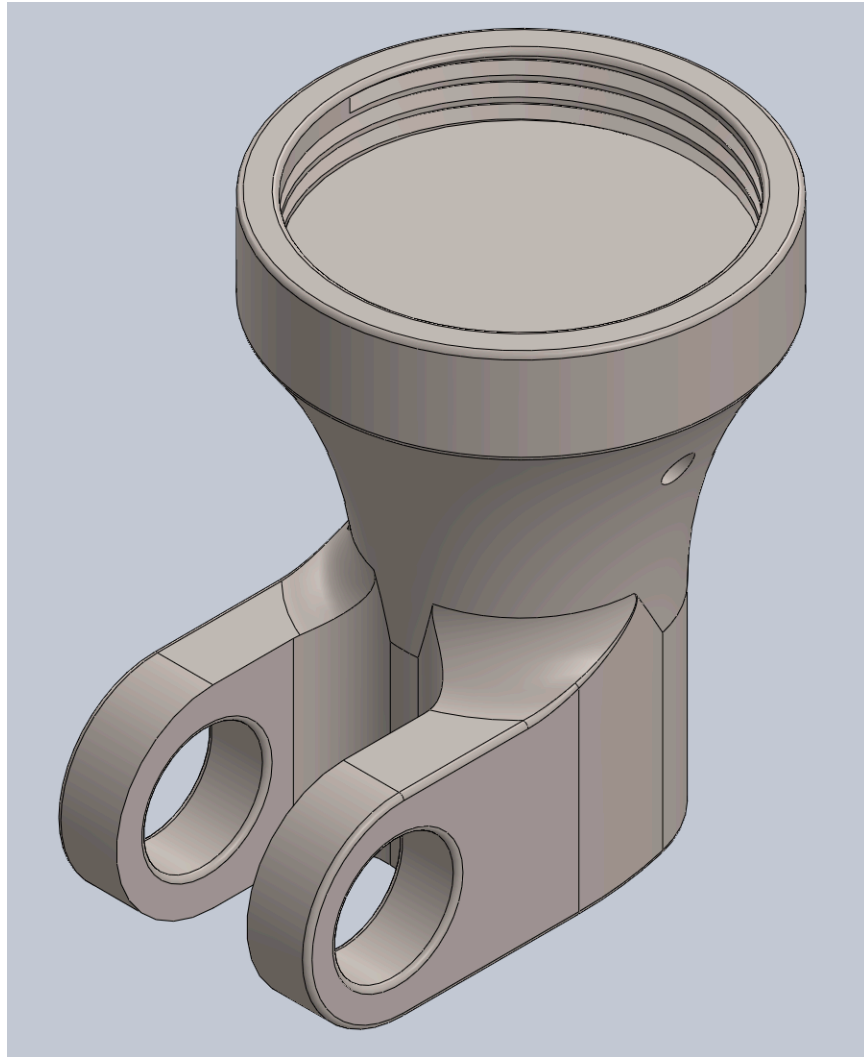


Figure 24 - Ball Joint Stud Attachment Bracket

Despite its small size, this bracket has one of the most important functions in the prosthetic design. Designed specifically for this project, this bracket serves as the connection point between the Fox Float DPS, the QA1 ball joint, and the pyramid adapter, which attaches the prosthetic foot to the prosthetic socket (Figure 8). This component was designed to use as little material as possible while being able to safely withstand the forces experienced during use. The bracket is made from Aluminum 7075-T651, and weighs only 103 g. This material was

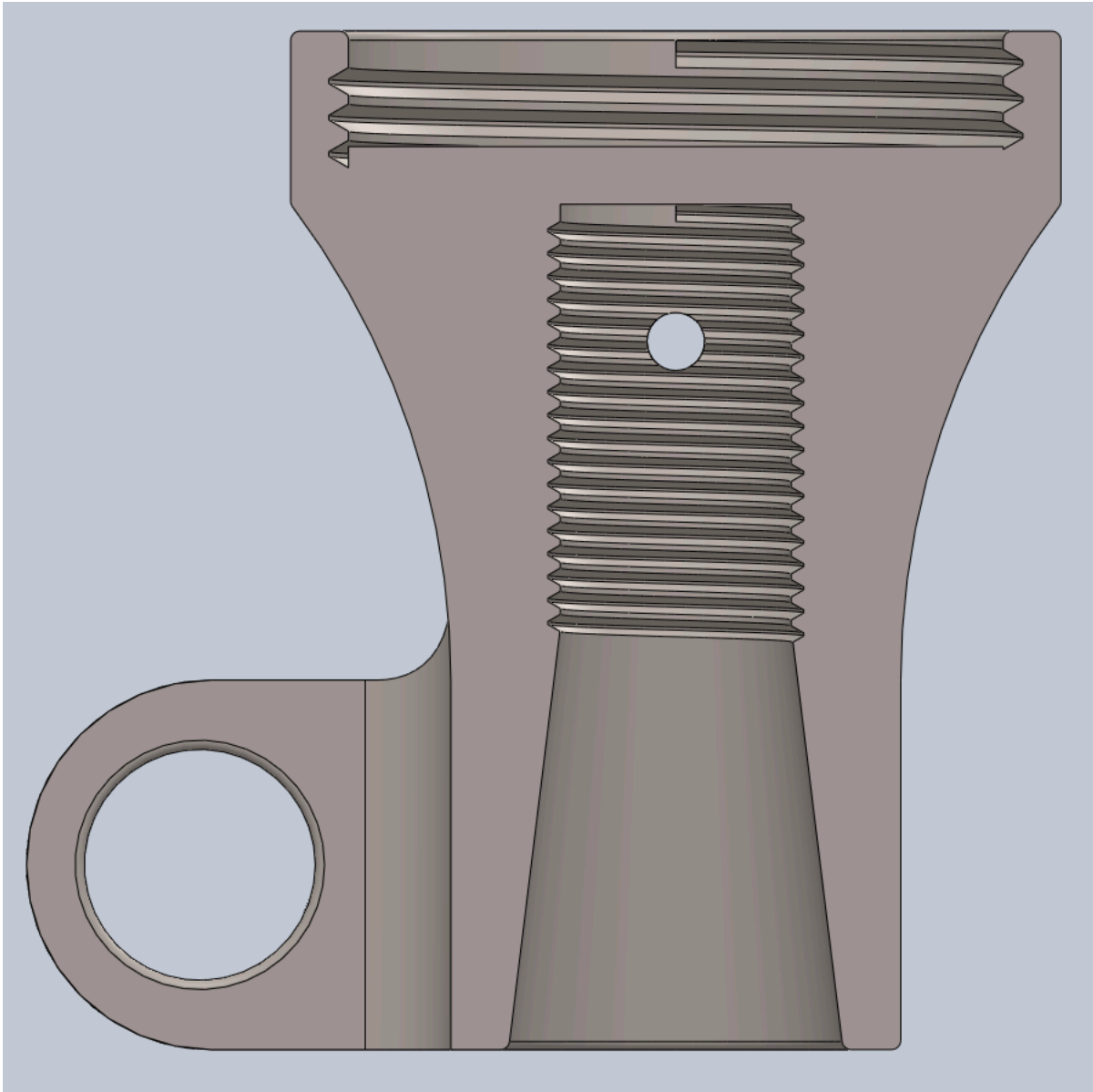
chosen because of its high strength-to-weight ratio, and its ability to be easily machined at an affordable price.

The top of the bracket is threaded to accept the pyramid connector (Figure 25b). This standardized component is compatible with most prosthetic connection systems. The pyramid connector is used to connect the prosthetic foot to a prosthetic socket that covers the residual limb. This particular pyramid connector is the PTM-WH, manufactured by Bulldog Tools Inc. This pyramid adapter is made from titanium and weighs 43 g [26].

Similar to the pyramid connector, the inside of the ball joint stud attachment bracket is threaded to accept the ball joint stud (Figure 25a). Once fully threaded in place, there is a hole to accept a cotter pin to fix the stud inside the bracket. The ball joint is described in further detail in Section 3.3.4.

The final connection points for the ball joint stud attachment bracket are the arms, which serve as connection points for the Fox Float DPS shock. The shock connects to the bracket with a nut and bolt that also acts as a shaft for the shock. Like the foot plate toe area, the Fox Float shock is centered in place with a mount kit. This kit measures 15 mm wide and is functionally identical to the mount kit used in the toe area. To ensure the component could withstand the forces it would experience during use, this part of the bracket was tested using Solidworks Simulation Xpress. The results of these tests can be found in Section 4.2.

By connecting several parts of the prosthetic together, this bracket fulfills an important role in the prosthetic assembly. It allows the prosthetic to have the mobility granted by the ball joint as well as the energy storage and return capabilities of the Fox Float DPS shock. In addition, the bracket serves to connect the prosthetic foot to a standard prosthetic socket, enabling more people to use this device.



http://www.bulldogtools.com/prosthetic/rotating-pyramid-insert-hole-titanium_p_5479.html?osCsid=1e3dbf010b0becb3b0f812d0548c8327

Figure 25 - a) Section View of Ball Joint Stud Attachment Bracket, b) PTM-WH Pyramid Connector [26]

3.3.4. QA1 Ball Joint



Figure 26 - QA1 1210-105 Upper Ball Joint [20]

An upper ball joint manufactured by QA1 will be used for this prosthetic design. This ball joint was made for use in automobile suspension systems but has applications in prosthetics too. Although a ball joint does not appear to have been used in previous prosthetic designs, using one as an ankle mechanism should result in a prosthetic with greater ankle mobility than seen in other designs.

The ball joint used in this design has a screw-in style housing (Figure 26). This style was chosen over the other styles, press-in and bolt-in, for several reasons. Press-in styles were impractical due to their size and due to carbon fiber failing to successfully hold the housing in place. The upper foot plate would need to be substantially thicker and would require high levels of consistent precision to ensure a tight press fit between foot plate and ball joint housing. Bolt-

in housings are also larger than screw-in style housings, which would make the foot bulkier. In addition, the height of the bolt-in housing would require a larger space between the upper- and lower-foot plates to avoid contact. This would cause the ball joint to move out of position from the natural ankle, making the prosthetic's movement feel more unnatural. The screw-in housing has a smaller diameter than the other styles, allowing a more compact prosthetic overall. This housing style is held in place by the housing attachment bracket (Section 3.3.5) to the upper foot plate. The ball joint is located in the same position as a natural ankle, allowing the prosthetic to move more like a natural foot.

The ball joint housing contains several components (Figure 27). The race seats the top of the ball joint stud in place, limiting vertical movement and improving the longevity of the stud. The ball joint stud is the most important component of the joint. The stud has a wide range of movement. It can rotate 32° from a vertical position in a 360° inverted cone and can also pivot about the vertical axis. The stud has a black oxide coating to improve strength and reduce wear. Two pieces hold the bottom of the stud in place: a molded polymer cup and a steel spider. The cup is molded out of a high-density polymer and provides movement in low-load applications. During high loads, the oil-impregnated steel spider allows free movement of the stud. The ball joint has a torque nut that allows the joint to be pre-loaded, varying how freely the stud moves within the housing. These components are all held in place with a jam nut.

Another reason this ball joint was chosen for this project is because it can be completely rebuilt. If the torque nut is loosened, all the parts can be cleaned or replaced as needed. By using an adjustable torque nut, the prosthetic can be fine-tuned to the individual's preferences. For example, some users will prefer the ball joint stud to have some resistance before moving, while others will prefer totally free movement of the stud. In addition to customizing the prosthetic to

each user's preference, the ability to disassemble and rebuild the ball joint can extend its usable life. Extending the ball joint's usable life should also increase the lifespan of the whole prosthetic, making it more cost-effective to the user over time.



Figure 27 - Exploded View of QAI Ball Joint [20]

3.3.5. Ball Joint Housing Attachment Bracket

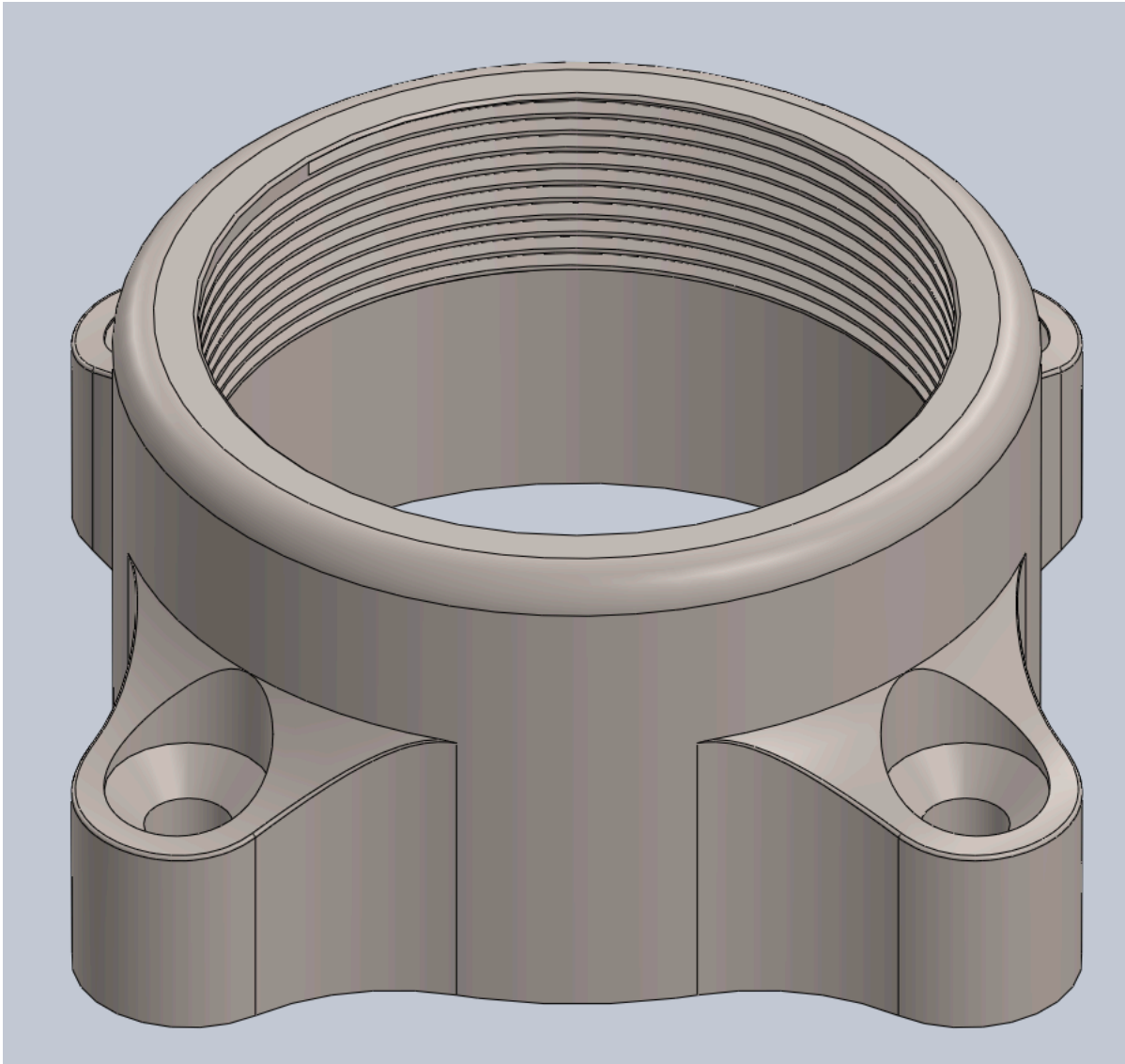


Figure 28 - Ball Joint Housing Attachment Bracket

The ball joint housing attachment bracket is another part that was designed specifically for this prosthetic foot. The bracket's primary function is to, as its name suggests, connect the ball joint to the prosthetic foot. It does so in a simple, lightweight design that is still durable enough to withstand the abuse expected of a prosthetic foot.

The ball joint housing attachment bracket attaches to the ball joint by screwing onto the threads of the ball joint housing. Once the ball joint bracket and ball joint have been connected, the whole apparatus is held in place on the upper foot plate with bolts and threaded standoffs. The bolts go through the four outer holes of the bracket and connect with the threaded standoffs that protrude through the underside of the upper foot plate (Figure 29). The bracket's bolt holes have recesses cut into the underside of the upper foot plate to seat the threaded standoffs and ensure a consistent fit (Figure 29).

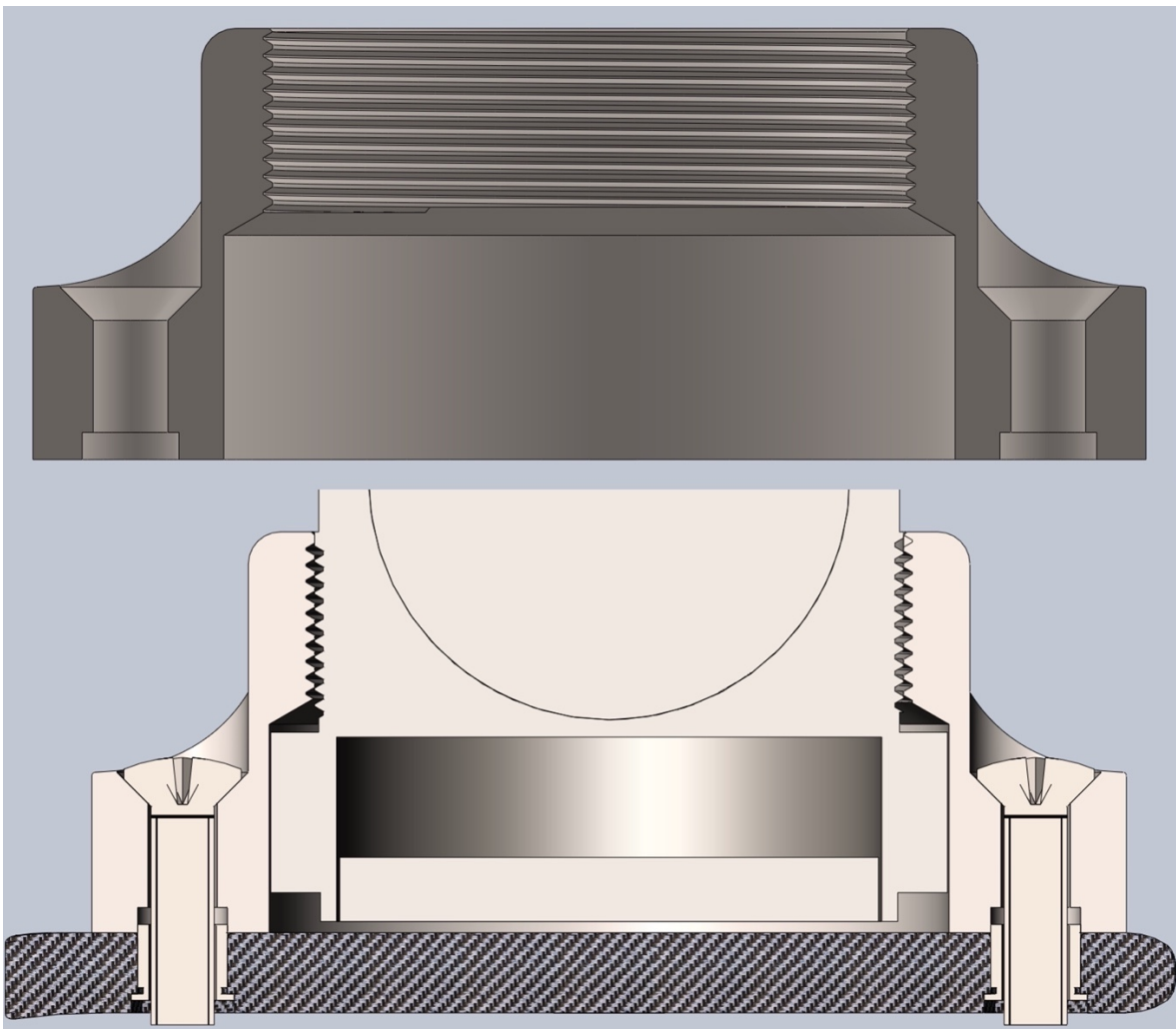


Figure 29 - a) Ball Joint Housing Attachment Bracket Section View, b) Ball Joint Assembly Section View

The ball joint housing attachment bracket is made from Aluminum 7075-T651 and weighs only 73 g. As with the stud attachment bracket, this material was chosen because for its high strength-to-weight ratio, and the ability to easily machine the material at an affordable price. Multiple simulations were run on the ball joint housing attachment bracket, the results of which can be seen in Section 4.3. This bracket serves a simple but important purpose and keeps an integral part of the prosthetic solidly connected.

3.4. Design Cost

Prosthetic devices are very expensive. As stated earlier, the prices for prosthetics can range from \$5,000 up to \$70,000, with health insurance usually only covering a fraction of those costs [6]. Given that many amputees have the financial burden of surgeries and physical therapy, the affordability of prosthetics is especially important, with any savings contributing to a less stressful transition. This project seeks to create a prosthetic that costs significantly less than other available prosthetics while still providing improved mobility and comfort to the user.

To be included in the final design, the components had to meet several requirements. The first requirement was that the components must be able to withstand the forces encountered when walking and running. The foot experiences significant forces when moving, so it stands to reason that any prosthetic foot must be able to do the same. The components were chosen to meet or exceed the forces expected to be encountered in an amputee's daily life. The components must also be relatively lightweight, so that the prosthetic is not overly cumbersome. This device's components are lightweight while meeting the necessary strength requirements.

The availability of components was another integral design consideration. As often as possible, this design attempted to use readily available components over components that would

need to be made specifically for this device. Using readily available components reduces the overall cost of the prosthetic and makes it easier to source parts for the prosthetic. Using easily sourced parts also makes component repairs or replacement easier as well.

The next requirement was robust design of the components. The prosthetic is expected to be used in all types of environments, so the components that make up the prosthetic must also be able to function properly in various environments. Components should be corrosion-resistant to prevent degradation from water or sweat and have sufficient fatigue resistance to prevent failure. Moving parts should either be self-lubricating or have seals to prevent contamination ingress. By ensuring the various components meet these requirements, prosthetic maintenance is minimized, and the device can be trusted to function properly.

While the majority of the components used in the proposed design are readily available, some components need to be manufactured specifically for this device. In this design, there were four design-specific parts that need to be custom manufactured: the upper- and lower-foot plates, the ball joint stud attachment bracket, and the ball joint housing attachment bracket. A manufacturer was sourced that could create the brackets, and a cost estimate was determined for their manufacturing (Table 3).

The attachment brackets for the ball joint stud and the ball joint housing can be manufactured by Protolabs, a rapid prototyping and production company that can make components with various materials and manufacturing techniques. Parts can be uploaded to the site, and a quote for different manufacturing methods can be compared to find the most cost-effective option. These parts were initially intended to be made from Grade 5 titanium (Ti 6Al-4V) due to its high strength-to-weight ratio, biocompatibility, and its ability to be machined via CNC or 3D printing. The 3D printed quotes were available immediately, and prices for both the

standard resolution and high resolution were determined (Table 3). For the CNC machining option, it was found that the ball joint stud attachment bracket could not be made from titanium in this way. This began an exploration of other available material options. It was determined that the next best material option would be aluminum alloy 7075-T651, which is most commonly used for aircraft structural parts. This material was found to be as capable of withstanding the expected forces as titanium. This alloy has an ultimate tensile strength of 570 MPa, and a yield strength of 500 MPa. In addition, 7075-T651 aluminum has good fatigue and corrosion resistance. Using aluminum proved to be significantly more cost effective than titanium, costing between 65-80% less than 3D printed titanium. The prices listed in Table 3 reflect the costs of manufacturing each component. In the end, CNC machining both components from aluminum 7075-T651 proved to be the most cost-effective method.

| | Stud Attachment Bracket | Housing Attachment Bracket |
|----------------------------|--------------------------------|-----------------------------------|
| 3D Printed Titanium | | |
| - Normal Resolution | 1389.00 | 1094.46 |
| - High Resolution | 1865.82 | 1805.75 |
| CNC Machining | | |
| - Titanium Ti-6Al-4V | N/A | 1313.51 |
| - Aluminum 7075-T651 | 448.98 | 312.93 |

Table 3 - Price Comparison of Ball Joint Attachment Bracket Manufacturing Methods (USD)

A manufacturer for the upper- and lower-foot plates was unable to be located. The foot plates can potentially be made by hand; however, this limits the construction methods available without specialized equipment. Future researchers will either need to manufacture the foot plates independently or find a carbon fiber company that is willing to manufacture custom small batch components.

An exploded view of the prosthetic assembly can be seen in Figure 30, with the full list of the parts and their cost listed in Table 4. The total price is how much would be needed to make one prototype of the prosthetic foot. Finalized versions of the prosthetic should cost less as the design is further refined. Refining the design would remove unnecessary parts and optimize the remaining parts as well. In addition, as the scale of manufacturing increases, the costs of the various components will become less expensive due to economies of scale. Custom manufactured components will become more affordable as more are made, and readily available components will also become more affordable as larger volume orders are placed.

As Table 4 shows, even with the relatively expensive custom components, this prosthetic device is still much more affordable than many other prosthetics that are currently available. Not only that, but the prosthetics that do come close to this price point are missing many of the features found in this device. This prosthetic device has a greater range of mobility and is able to store and return energy with a pneumatic piston, all for significantly lower cost than other devices. The ability to repair the device as needed helps to lower its long-term cost as well. Solidworks has estimated the prosthetic's total weight at 4.45 lb (2018 g), although this result is somewhat inaccurate. The simplified component models may weigh more than their physical counterparts, which would cause the prosthetic model's weight to be higher. The finished prototype should be slightly lighter. While this prototype device's weight is higher than the prosthetics listed in Table 1, future versions of the prosthetic will optimize the design, resulting in a lighter device.

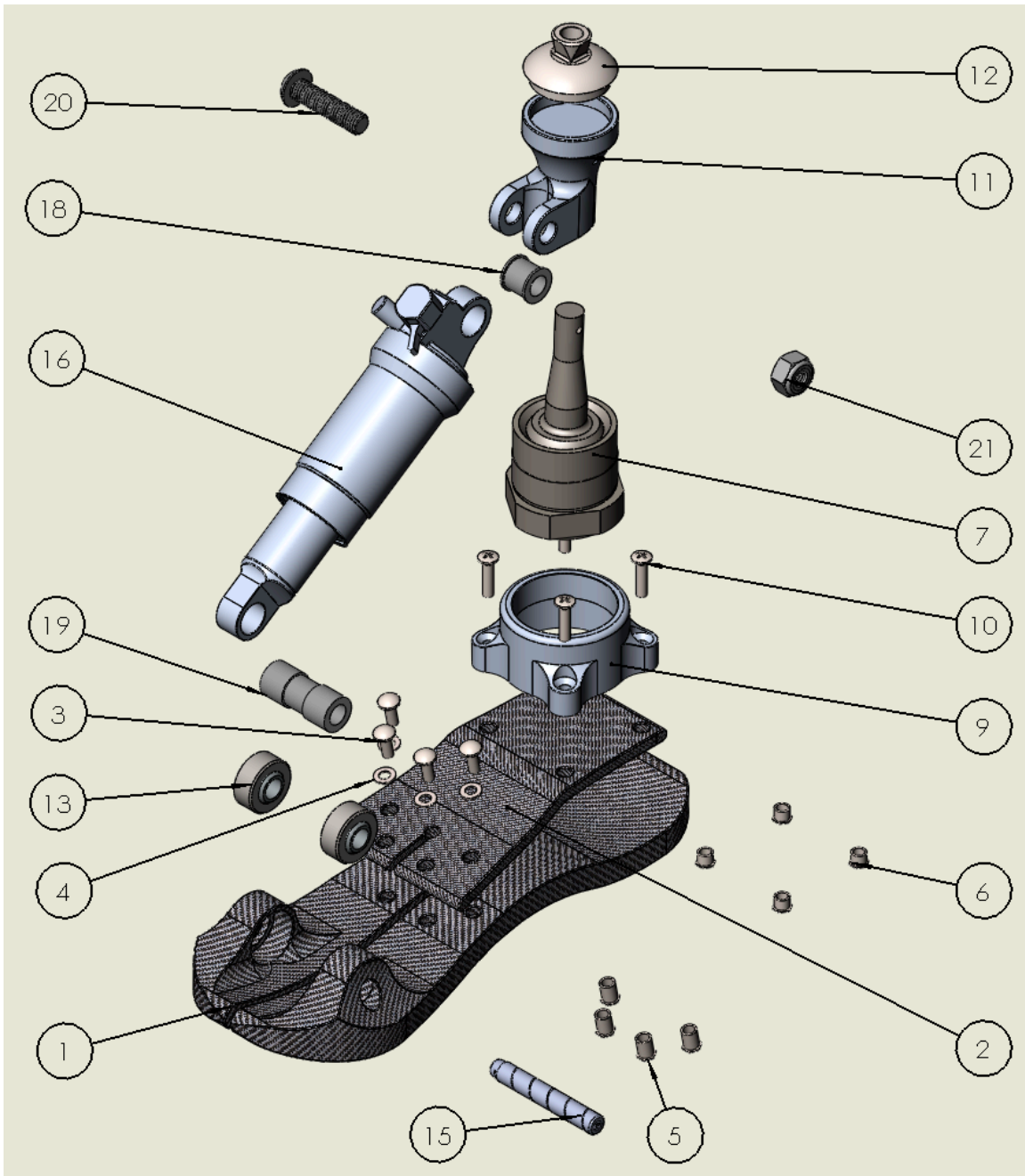


Figure 30 - Exploded View of Prosthetic Assembly

| Part # | Component | Manufacturer | Qty | Weight | Cost |
|---------------------|------------------------------------------|---------------------|------------|-------------------------|--------------------|
| 1 | Lower Foot Plate | N/A | 1 | 1.24 lb (565 g) | N/A |
| 2 | Upper Foot Plate | N/A | 1 | 0.56 lb (252 g) | N/A |
| 3 | Foot Plate Bolts (90604A748) | McMaster-Carr | 8 | 0.01 lb (3 g) | \$12.05/pkg of 100 |
| 4 | Foot Plate Washers (93475A240) | McMaster-Carr | 4 | 0.41 g | \$2.57/pkg of 100 |
| 5 | Threaded Standoffs (SO4-M5-10) | S.W. Anderson Co. | 4 | 1.41 g | \$0.57/ea |
| 6 | Threaded Standoffs (SO4-M5-6) | S.W. Anderson Co. | 4 | 0.85 g | \$0.57/ea |
| 7 | QA1 Ball Joint 1210-105 | QA1 | 1 | 1.34 lb (607 g) | \$59.99/ea |
| 9 | Ball Joint Housing Attachment Bracket | Protolabs | 1 | 0.16 lb (73 g) | \$312.93 |
| 11 | Ball Joint Stud Attachment Bracket | Protolabs | 1 | 0.23 lb (103 g) | \$448.98 |
| 12 | Pyramid Connector PTM-WH | Bulldog Tools Inc. | 1 | 0.09 lb (43 g) | \$42.10/ea |
| 13 | Spherical Bearings (2995K33) | McMaster-Carr | 2 | 0.18 lb (86 g) | \$12.96/ea |
| 15 | Foot Plate Dowel Pin (97352A310) | McMaster-Carr | 1 | 0.07 lb (33 g) | \$8.30/ea |
| 16 | Fox Float DPS | Fox Factory Inc. | 1 | 0.49 lb (221 g) | \$479.00 |
| 18 | Fox Float Mount Kit (10x15) | TF Tuned | 1 | N/A | \$24.82 |
| 19 | Fox Float Mount Kit (10x40) | TF Tuned | 1 | N/A | \$24.82 |
| 20 | Stud Attachment Bracket Bolt (94500A336) | McMaster-Carr | 1 | 0.06 lb (28 g) | \$10.63/pkg of 10 |
| 21 | Stud Attachment Bracket Nut (94645A220) | McMaster-Carr | 1 | 0.03 lb (14 g) | \$10.48/pkg of 25 |
| Total Weight | | | | 4.45 lb (2018 g) | |
| Total Cost | | | | | \$1467.15 |

Table 4 – Prosthetic Component Costs and Manufacturers (Note: Sections marked “N/A” were unable to be determined.)

4. Simulations

Nearly all of the parts designed for this prosthetic were tested in Solidworks to ensure their strength, given that the parts must be capable of withstanding the intense forces experienced when walking and running. The foot experiences the greatest forces during running. For instance, a 250 lb person will experience forces up to 13x their bodyweight, or approximately 15kN. Unless otherwise stated, this force value (15kN) was used as the standard force that all parts must be capable of withstanding. Additionally, each of these parts was also tested to ensure that they had a minimum factor of safety of 2. Simulation details for each tested part are listed in the following sections. For each simulation, the minimum and maximum of three different values were reported: von Mises stress, displacement, and factor of safety. For the former two, the maximum value is the value of importance, while for the factor of safety, the minimum value is the important value. These values are provided in Table 5 in the following sections, with the most important values italicized.

Some parts, such as the Fox Float DPS shock and the QA1 ball joint, were not tested in Solidworks. These parts were not tested for several reasons, the first of which is modeling inaccuracies in Solidworks. The models made in Solidworks to represent these parts are not completely accurate: rather, they are simply approximations of the real parts used for visualization purposes. Using these approximations for simulation purposes would create completely inaccurate results. Furthermore, these parts have already shown to be successful for their intended purpose. The Fox Float DPS has been used successfully in the VF2 by BioDapt and can be expected to perform well in this foot's design as well. The QA1 ball joint, while not explicitly used in a prosthetic application before, is used successfully in the automobile industry.

The forces experienced in that application would be significantly larger than any experienced in a foot, and so can be expected to perform well as the ankle mechanism in this design.

4.1. Foot Plates

The upper- and lower-foot plates were made from carbon fiber composites, specifically Zoltek PX 35 multi-directional fabric and PX35 prepreg tape. Carbon fiber composites are made from multiple layers of carbon fiber strands woven in different patterns and held together by resin. Areas that are expected to experience higher forces are reinforced with the prepreg tape for added strength. Once the rough form is obtained, the component is baked at high temperatures and pressure to obtain the final composition, then machined to its finished shape. Carbon fiber composite have anisotropic material properties that are highly dependent on the direction of the carbon fiber strand direction, as well as the weave pattern and the orientation of each layer of carbon fiber. Other factors that affect the material properties are the carbon fiber/resin ratio, as well as the number of voids left from the different manufacturing methods. All of this to say that it is incredibly difficult to accurately simulate a composite material. While Solidworks is capable of performing simulations for composite materials, there is not enough data to accurately perform a simulation. Although several material properties were able to be obtained, there are still several missing pieces of information. The number of layers needed for the composite, the orientation of each layer's weave pattern, and the carbon fiber/resin ratio are all unknown. Using the material properties available, simplified simulation can be performed that treat the composite as a bulk material. These simulations will give approximations values for the components and will help to determine whether the components need significant remodeling or whether they simply need more accurate simulations performed.

The majority of the simulations were performed on the lower foot plate. Six shearing stress simulations were performed on the toe area housing the spherical bearings, since this area will experience significant forces from a number of directions. In addition, a bending force simulation was performed on the split toe area of the lower foot plate, to ensure that this part of the component is capable of withstanding the expected forces without failure. A bending force simulation was also performed for the upper foot plate to ensure it could also perform well without failing.

The first pair of simulations performed on the lower foot plate were a shearing force on the toe area housing the spherical bearings. The shearing force was directed both towards the front of the foot plate and towards the back, with a total force of 15 kN. The area connecting the upper- and lower-foot plates and the bottom of the lower foot plate were set as the fixed surfaces for these simulations. Visual results of the von Mises stress, displacement, and factor of safety can be seen for the forward (Figure 31Figure 33) and rearward (Figure 34Figure 36) shear stresses, and the minimum and maximum values can be seen in Table 5.

| | Forward | | Rearward | |
|--------------------------|----------------|----------------|-----------------|----------------|
| | Min | Max | Min | Max |
| von Mises Stresses (psi) | $3.287e^{-05}$ | $1.602e^{+04}$ | $3.287e^{-5}$ | $1.602e^{04}$ |
| Displacement (mm) | 0 | $3.252e^{-02}$ | 0 | $3.252e^{-02}$ |
| Factor of Safety | <i>11.14</i> | $5.427e^{+09}$ | <i>11.14</i> | $5.427e^{+09}$ |

Table 5 - Lower Foot Plate 1st and 2nd Toe Shear Simulations

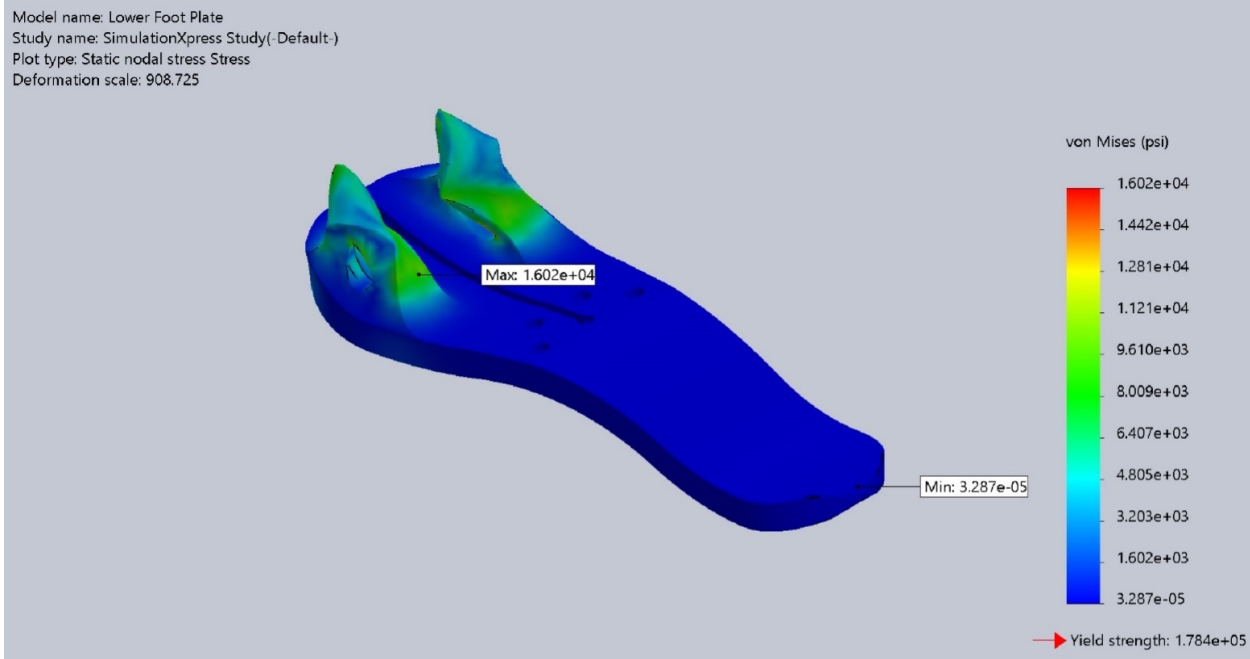


Figure 31 – Lower Foot Plate Forward Toe Shear von Mises Stress (psi)

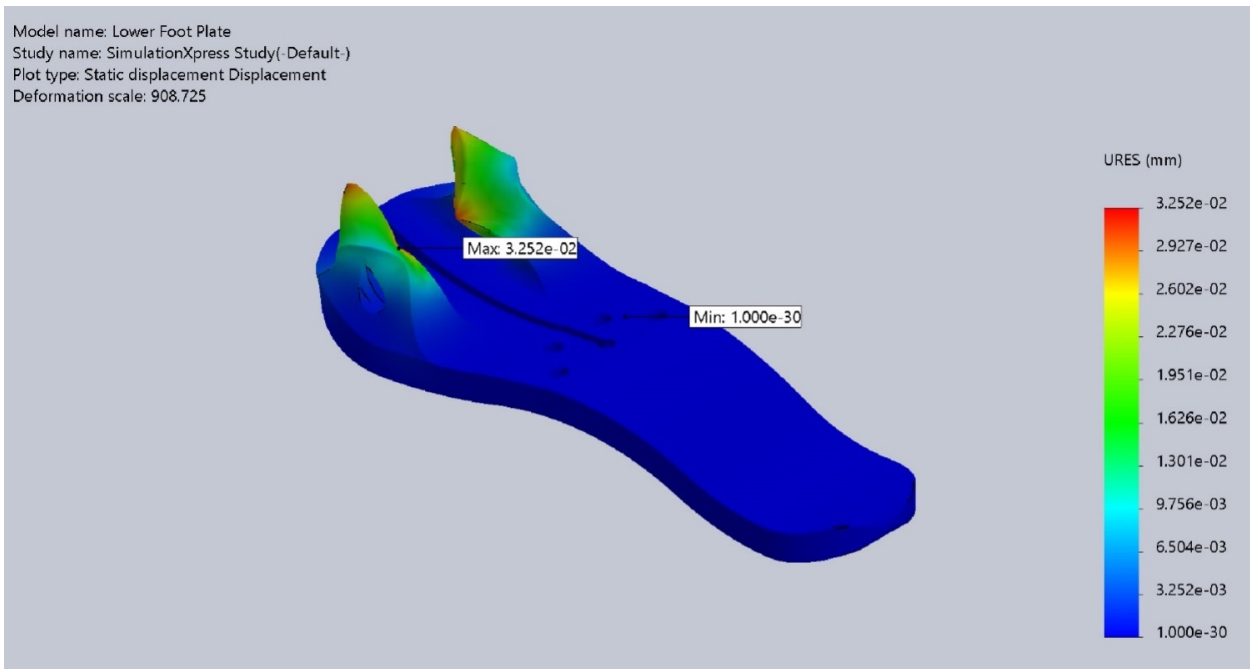


Figure 32 - Lower Foot Plate Forward Toe Shear Displacement (mm)

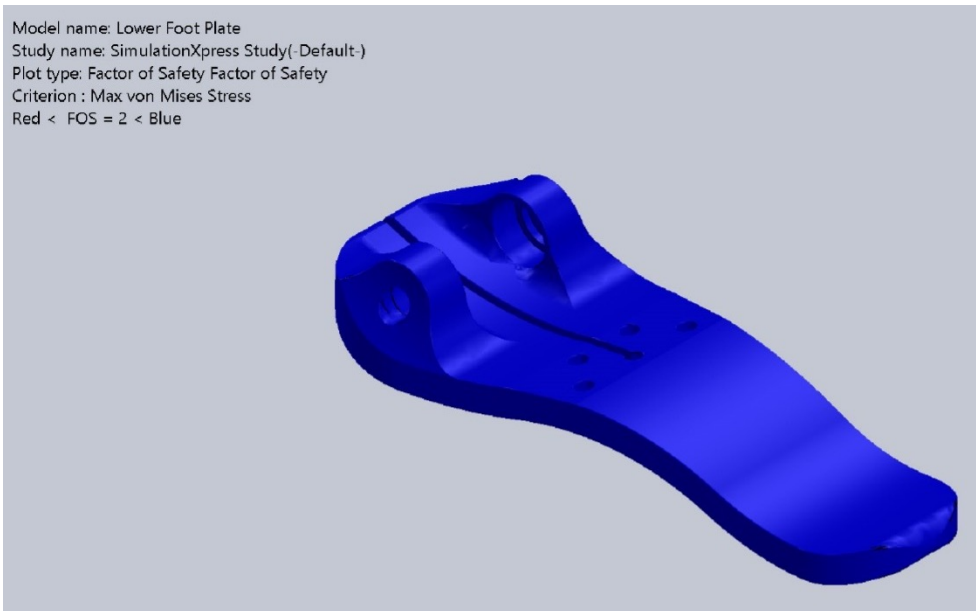


Figure 33 - Lower Foot Plate Forward Toe Shear Factor of Safety

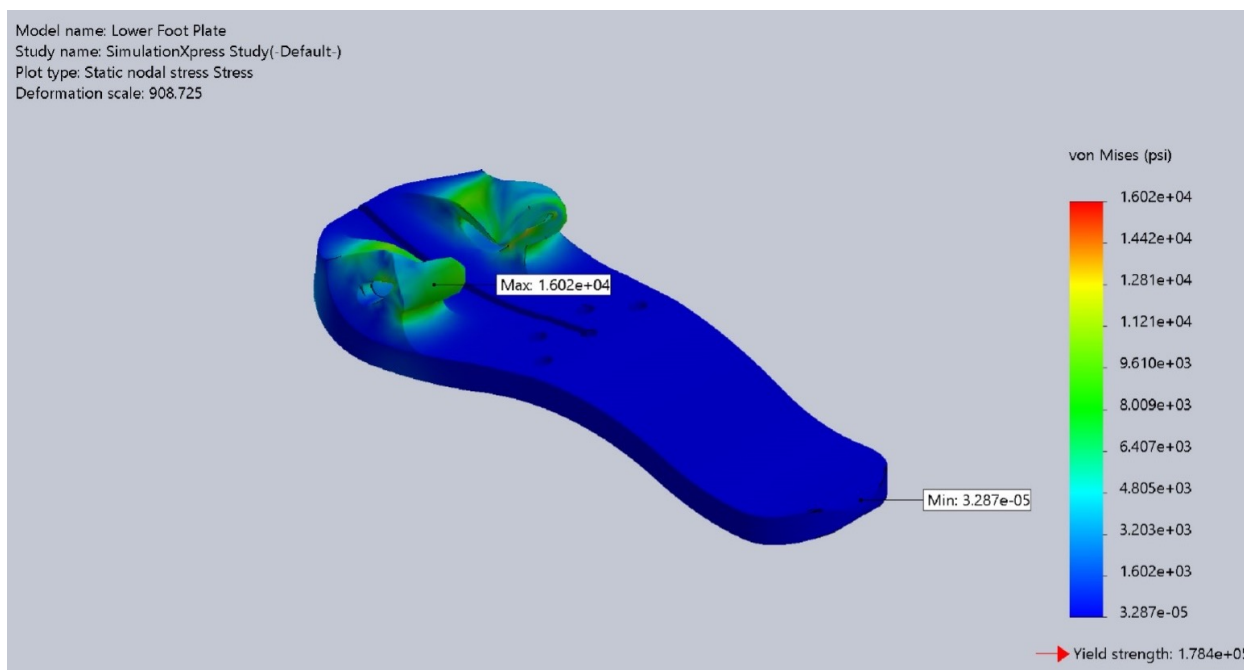


Figure 34 - Lower Foot Plate Rearward Toe Shear von Mises Stress (psi)

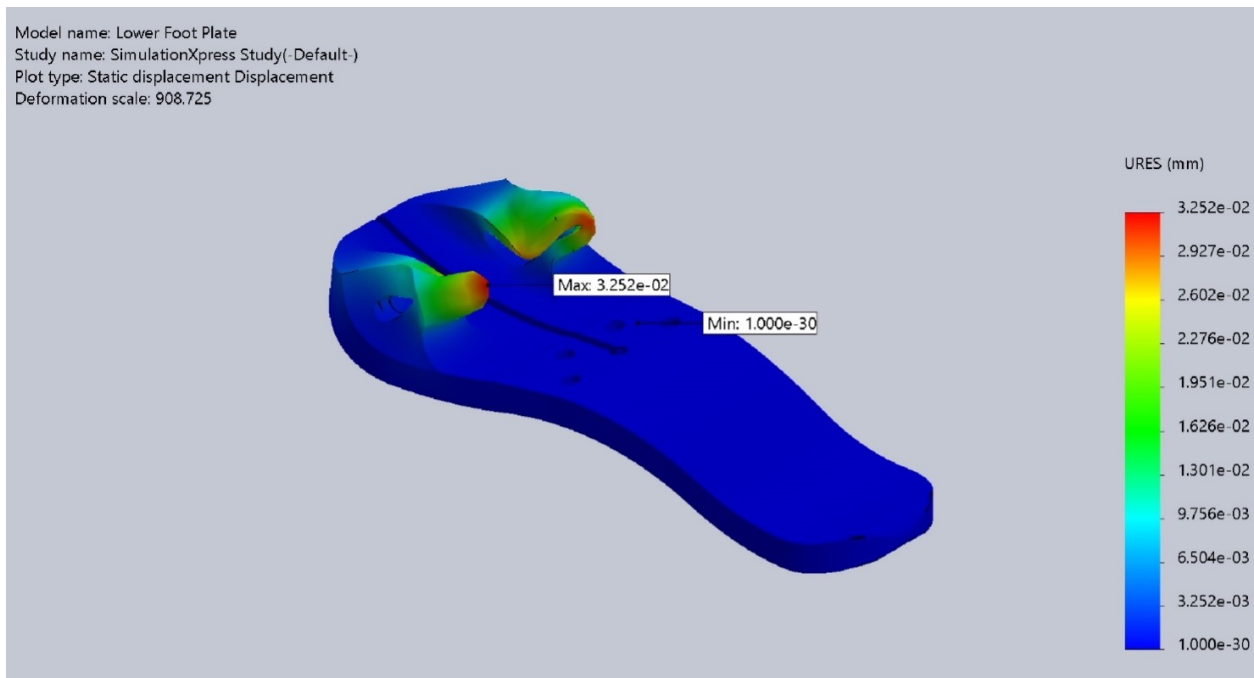


Figure 35 - Lower Foot Plate Rearward Toe Shear Displacement (mm)

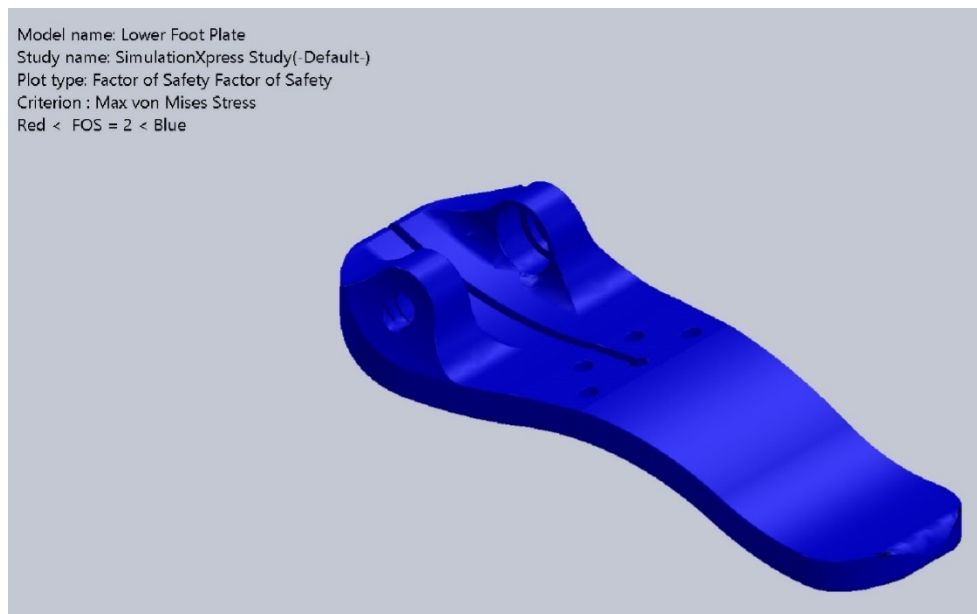


Figure 36 - Lower Foot Plate Rearward Toe Shear Factor of Safety

The initial results show that the toa area is more than capable of withstanding shearing forces in the forward and rearward directions. For both simulations, the maximum von Mises

stresses experienced were $1.602e^{+04}$ psi, safely below the yield strength of $1.784e^{+05}$ psi. The maximum displacement was only $3.252e^{-02}$ mm, and the minimum factor of safety was 11.14.

The next pair of simulations performed on the toe area were shearing forces pointed up and down. The value for these simulations was also a total force of 15 kN, with the connecting area and the bottom of the foot plate used as fixed surfaces. The results of the von Mises stresses, displacement, and factor of safety can be seen for the upwards (Figure 37) and downwards (Figure 40) shearing forces, with the minimum and maximum values listed in Table 6.

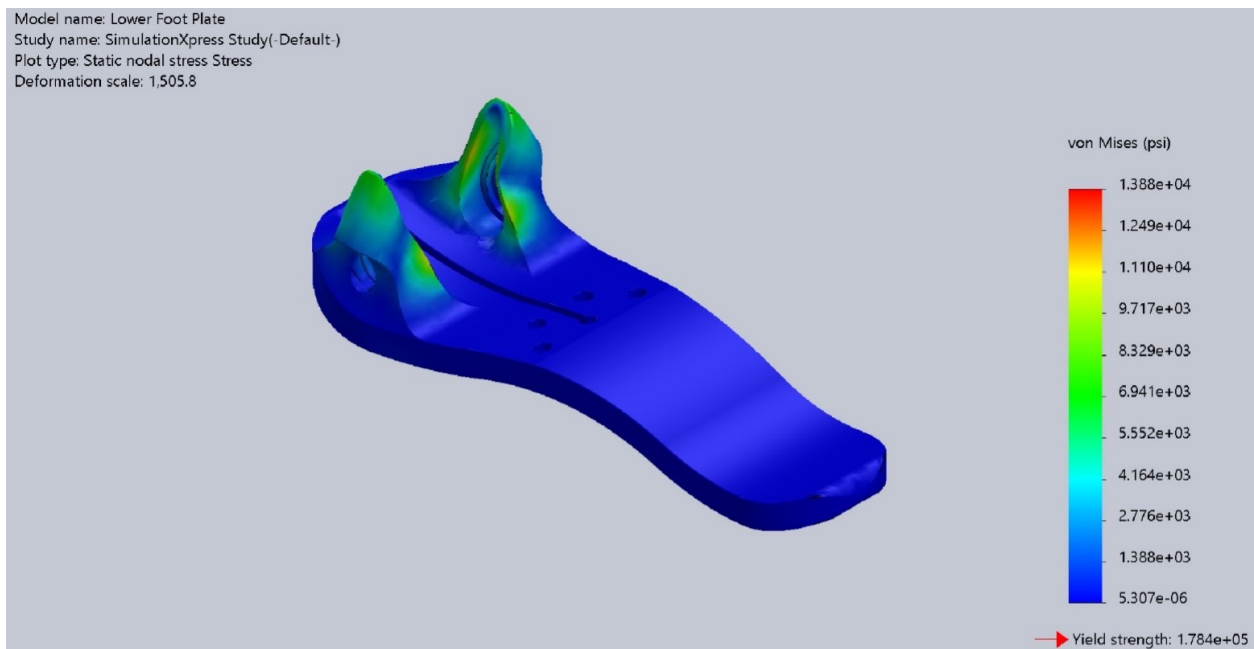


Figure 37 - Lower Foot Plate Upward Toe Shear von Mises stress (psi)

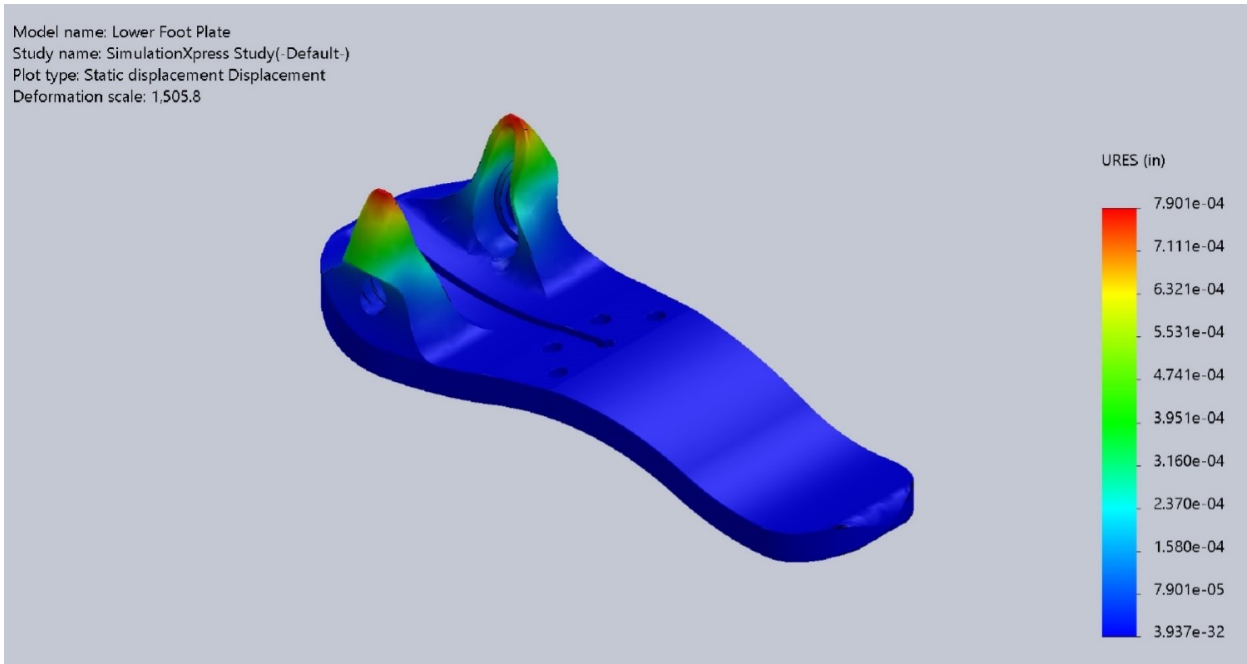


Figure 38 - Lower Foot Plate Upward Toe Shear Displacement (in)

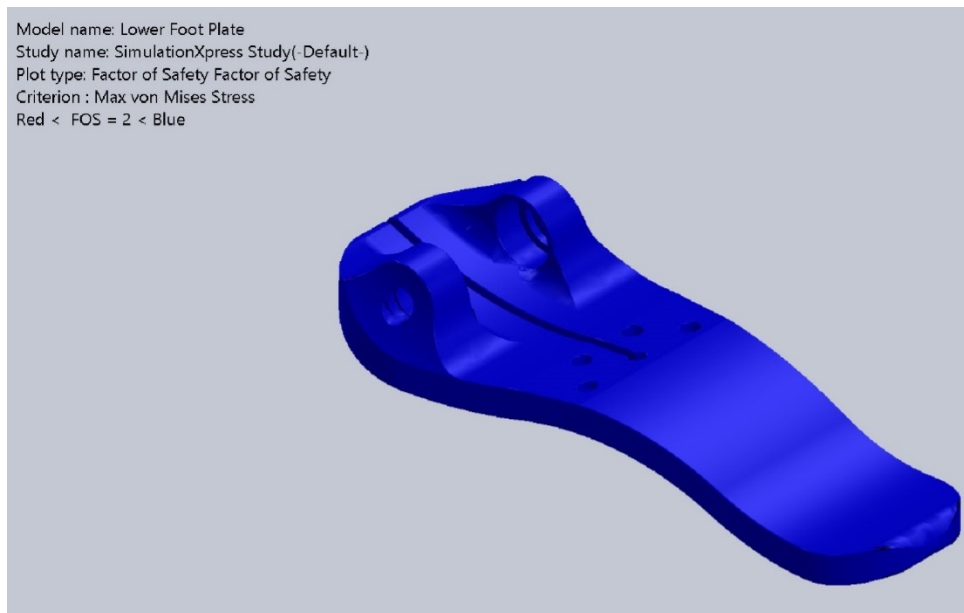


Figure 39 - Lower Foot Plate Upward Toe Shear Facto of Safety

| | Upward | | Downward | |
|--------------------------|----------------|----------------|----------------|----------------|
| | Min | Max | Min | Max |
| Von Mises Stresses (psi) | $5.307e^{-06}$ | $1.388e^{+04}$ | $5.307e^{-06}$ | $1.388e^{+04}$ |
| Displacement (in) | 0 | $7.901e^{-04}$ | 0 | $7.901e^{-04}$ |
| Factor of Safety | 12.85 | $3.361e^{+10}$ | 12.85 | $3.361e^{+10}$ |

Table 6 - Lower Foot Plate 3rd and 4th Toe Shear Simulations

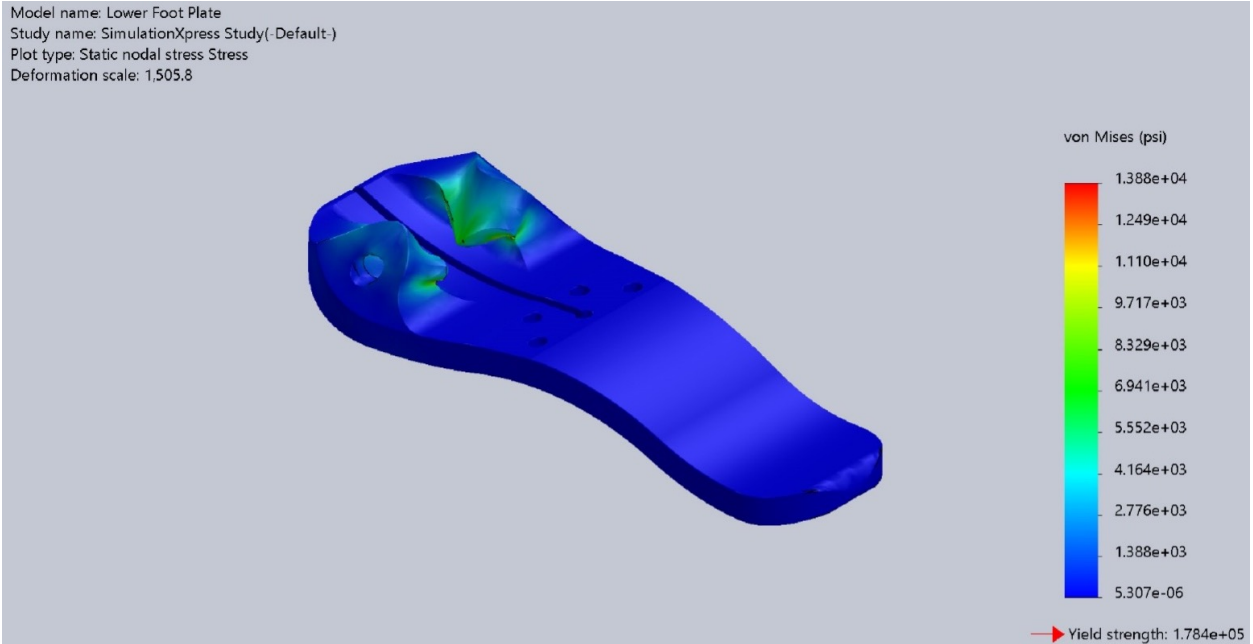


Figure 40 - Lower Foot Plate Downward Toe Shear von Mises Stress (psi)

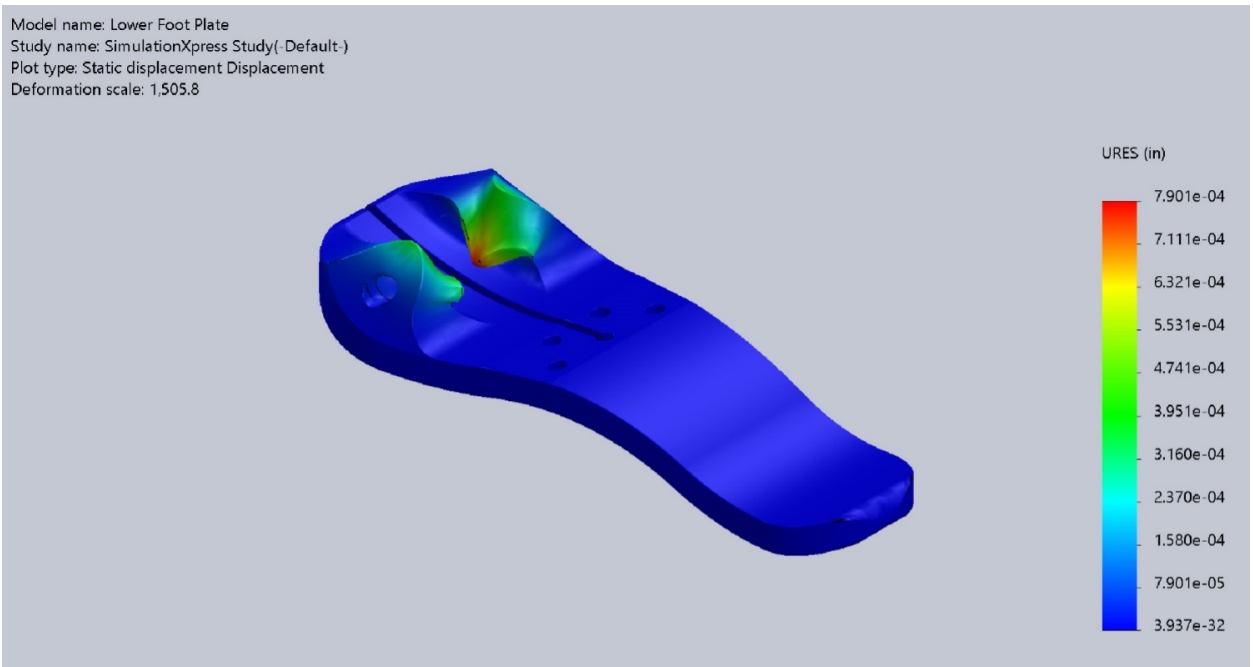


Figure 41 - Lower Foot Plate Downward Toe Shear Displacement (in)

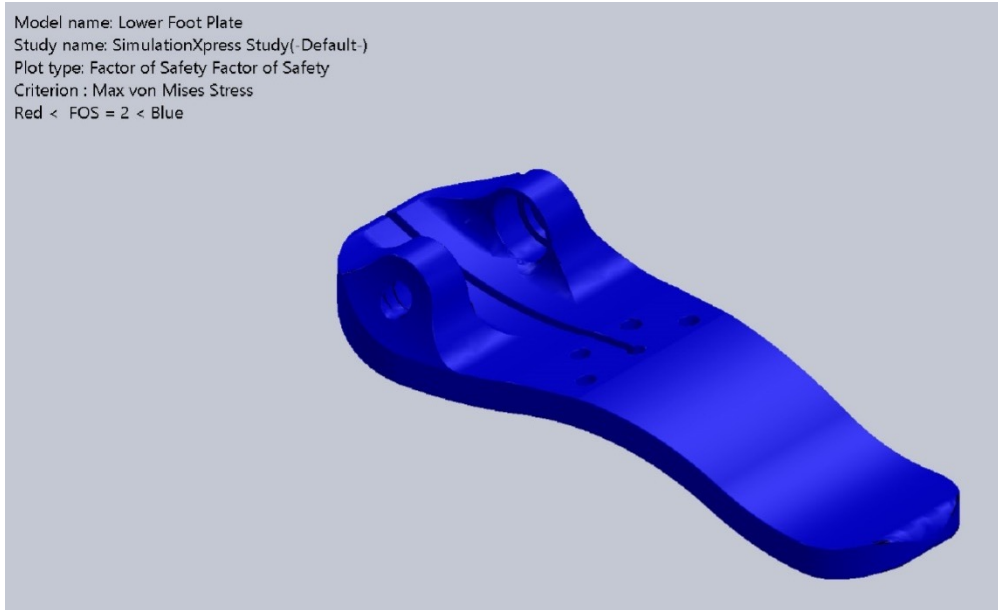


Figure 42 - Lower Foot Plate Downward Toe Shear Factor of Safety

As with the first pair of simulations, the toe area seems more than capable of withstanding the forces that are expected at this area. In both simulations, the maximum von Mises stress experienced was $1.388e^{+04}$ psi, below the yield strength of $1.784e^{+05}$ psi. The maximum displacement was $7.901e^{-04}$ in, and the minimum factor of safety was 12.85.

The final pair of simulations performed on the toe area were shearing forces directed outwards from the center of the foot plate. Each simulation used a force of 7,500 N and used the same fixed surfaces as the previous shearing simulations. The results for the von Mises stress, displacement, and factor of safety can be seen for the left (Figure 43Figure 45) and right (Figure 46Figure 48), with Table 7 listing the minimum and maximum values.

| | Left | | Right | |
|--------------------------|----------------|-------------------|----------------|-------------------|
| | Min | Max | Min | Max |
| Von Mises Stresses (psi) | $1.535e^{-07}$ | $1.753e^{+04}$ | $3.706e^{-06}$ | $9.853e^{+03}$ |
| Displacement | 0 | $2.686e^{-02}$ mm | 0 | $8.202e^{-04}$ in |
| Factor of Safety | 10.17 | $1.163e^{+12}$ | 18.11 | $4.745e^{+10}$ |

Table 7 - Lower Foot Plate 5th and 6th Toe Shear Simulations

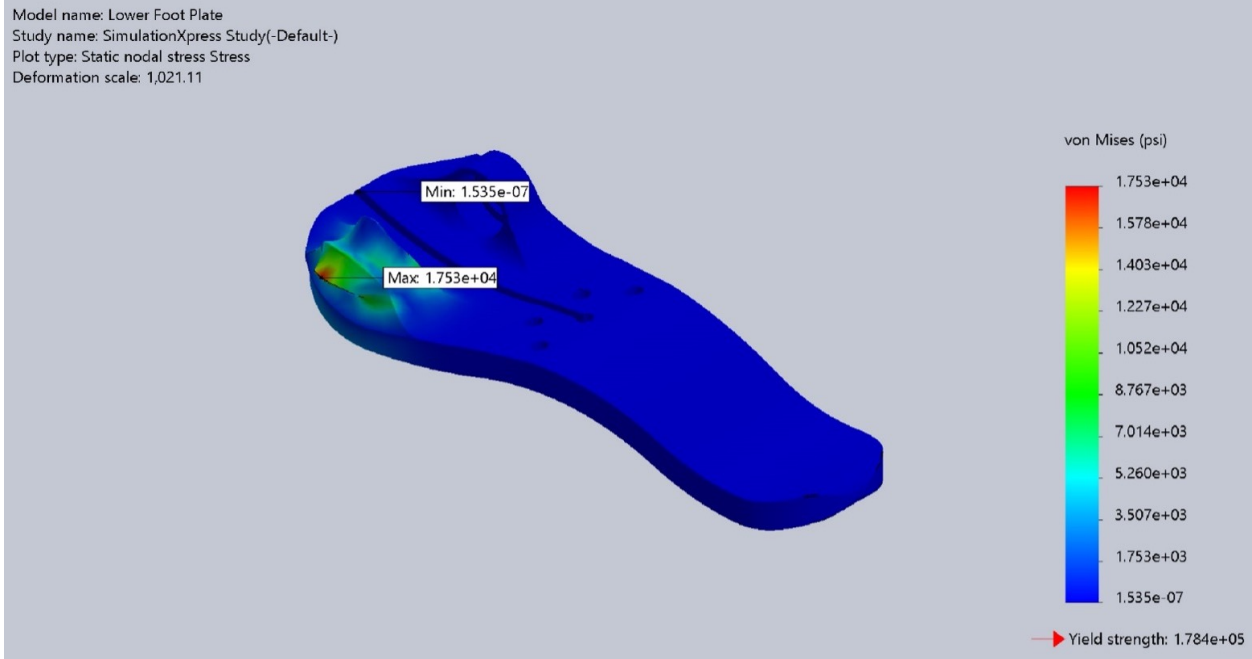


Figure 43 - Lower Foot Plate Left Toe Shear von Mises Stress (psi)

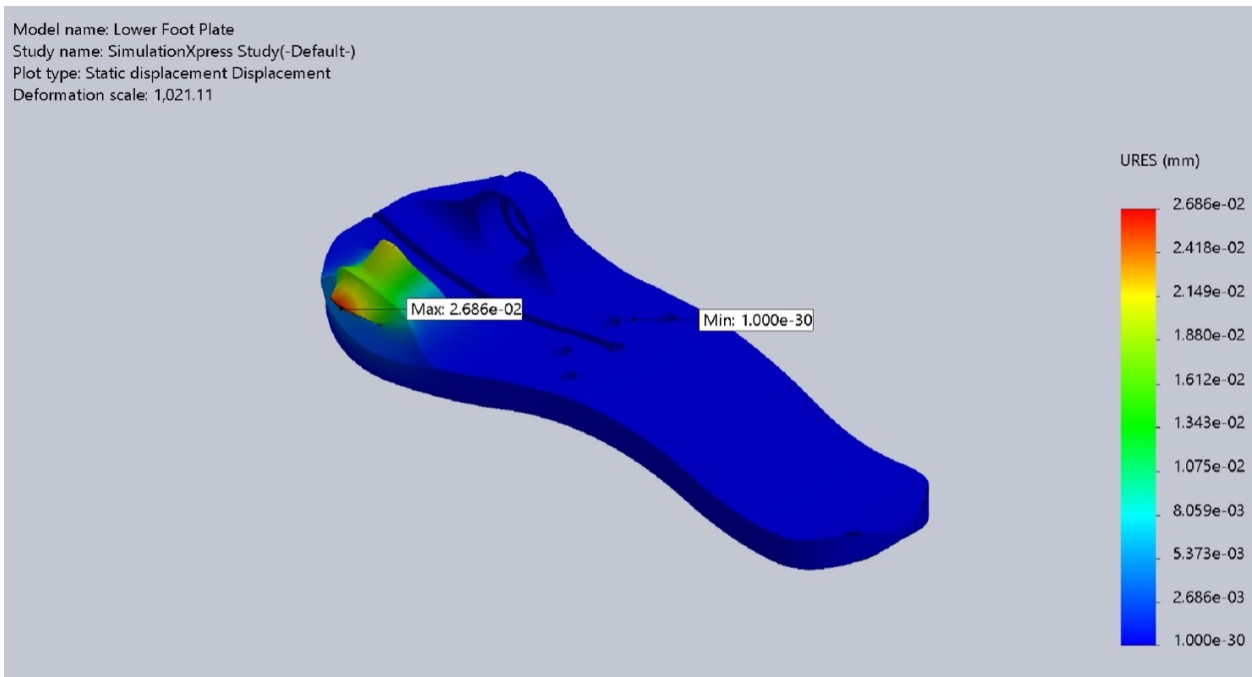


Figure 44 - Lower Foot Plate Left Toe Shear Displacement (mm)

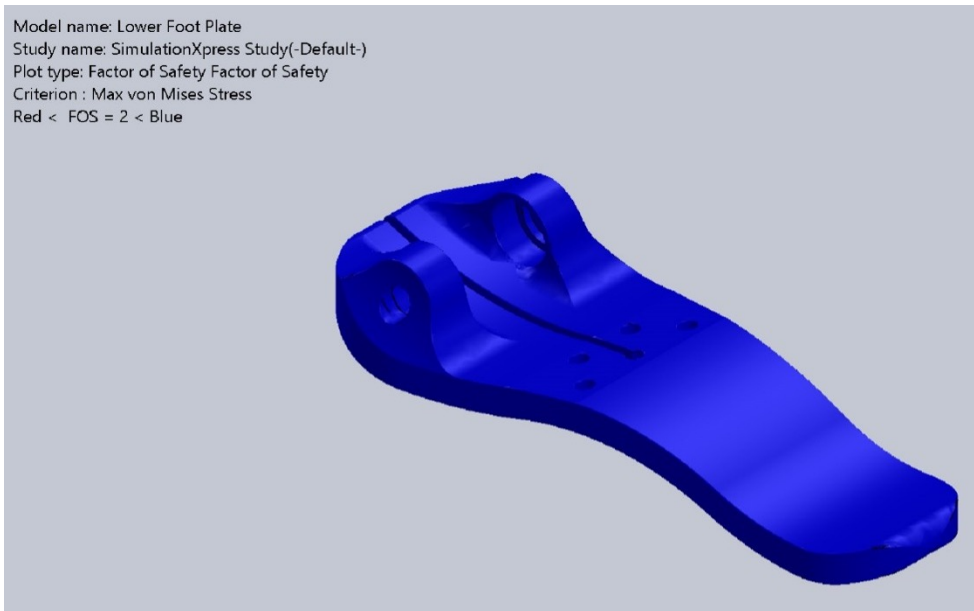


Figure 45 - Lower Foot Plate Left Toe Shear Factor of Safety

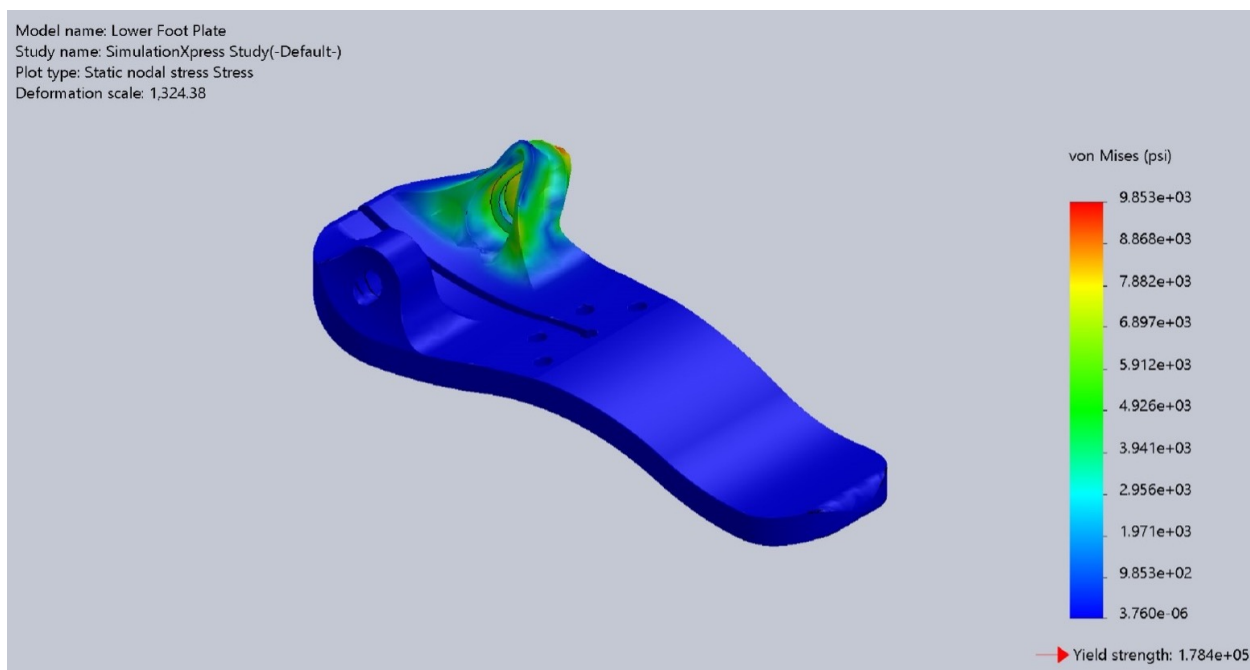


Figure 46 - Lower Foot Plate Right Toe Shear von Mises Stress (psi)

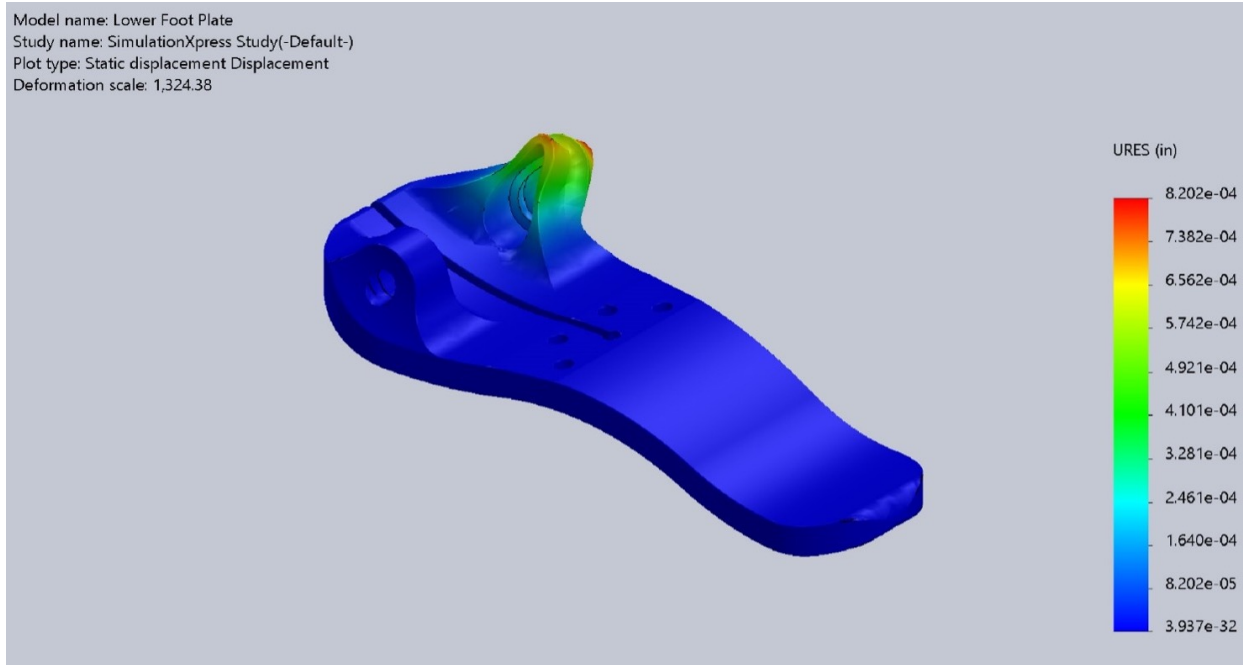


Figure 47 - Lower Foot Plate Right Toe Shear Displacement (in)

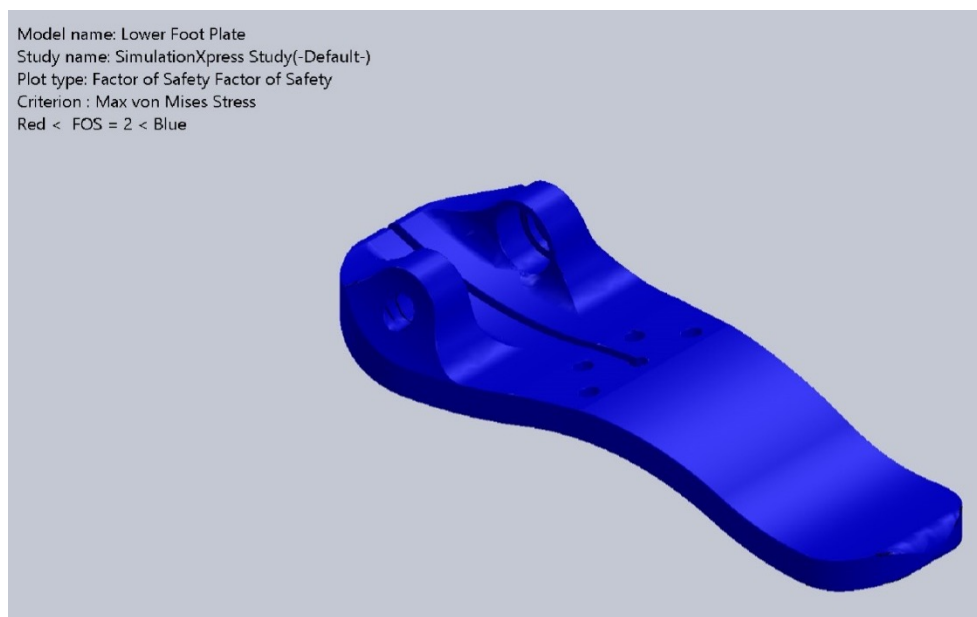


Figure 48 - Lower Foot Plate Right Toe Shear Factor of Safety

These simulation results show the toe area is capable of withstanding large forces perpendicular to the direction forces are expected to come from. The shearing force to the left

resulted in a minimum factor of safety of 12.85, and a maximum displacement of $2.686e^{-02}$ mm. The maximum von Mises stress encountered was $1.753e^{+04}$ psi. The shear force towards the right was similarly robust, with a maximum von Mises stress of $9.853e^{+03}$ psi, and a maximum displacement of $8.202e^{-04}$ in. The minimum factor of safety for this simulation was 18.11. These initial results indicate that the toe area housing the spherical bearings has been robustly designed and is more than capable of withstanding the expected forces without failure.

In addition to the many simulations on the toe area, a bending force was also applied to the split toes of the lower foot plate. For this simulation, a total force of 15 kN was applied to the underside of the toe areas, with the foot plate connection area and the rear bottom portion of the lower foot plate serving as fixed surfaces. Visual results of the von Mises stress (Figure 49), displacement (Figure 50), and factor of safety (Figure 51) are below, with the minimum and maximum values listed in Table 8.

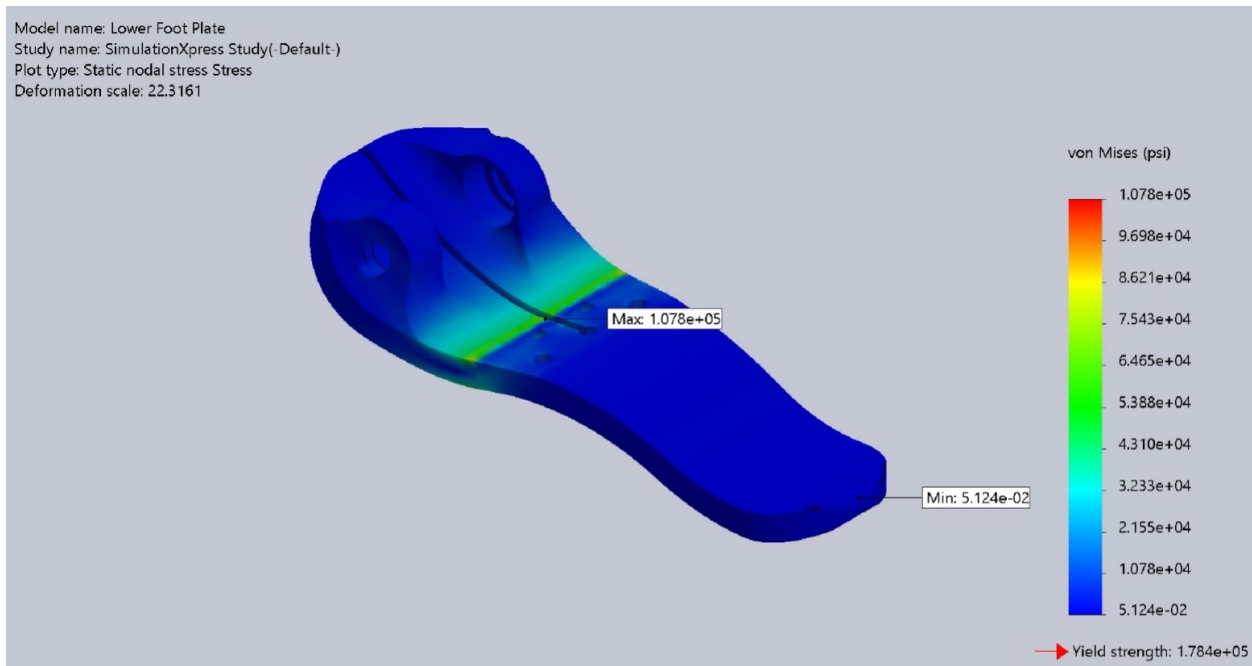


Figure 49 - Lower Foot Plate Bending Force von Mises Stress (psi)

| | Minimum | Maximum |
|--------------------------|----------------|----------------|
| Von Mises Stresses (psi) | $5.124e^{-02}$ | $1.078e^{+05}$ |
| Displacement (mm) | 0 | 1.228 |
| Factor of Safety | 1.656 | $3.482e^{+06}$ |

Table 8 - Lower Foot Plate Bending Force Simulation

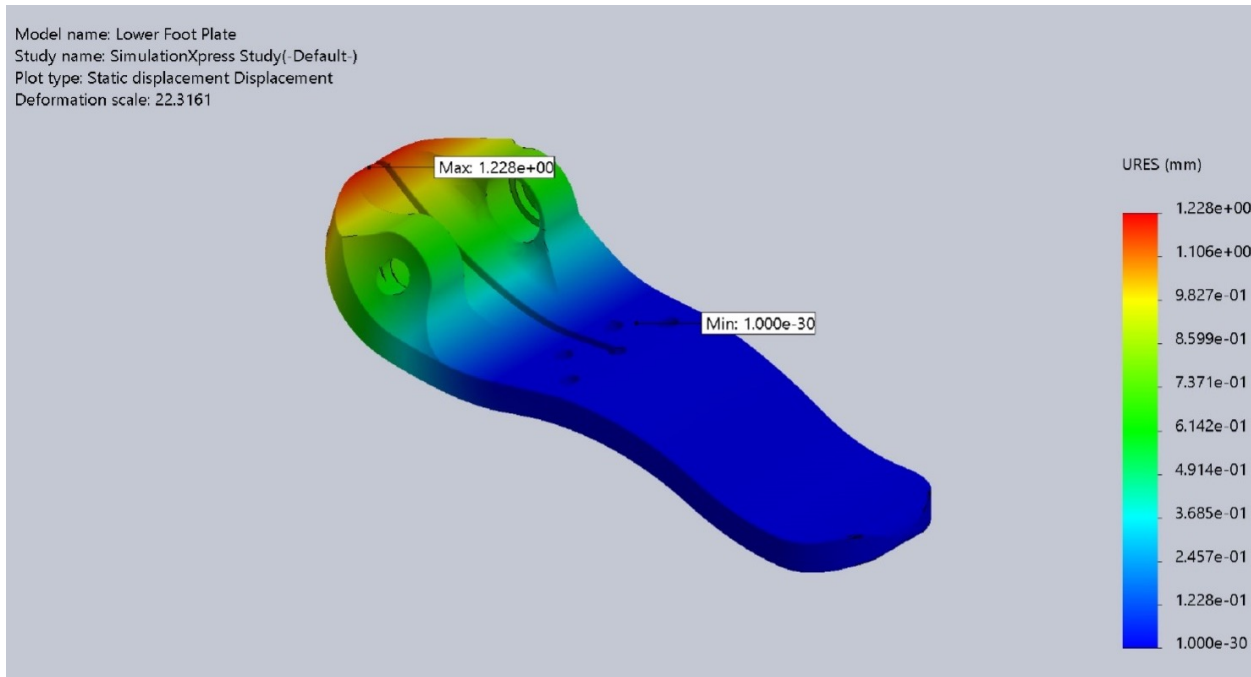


Figure 50 - Lower Foot Plate Bending Force Displacement (mm)

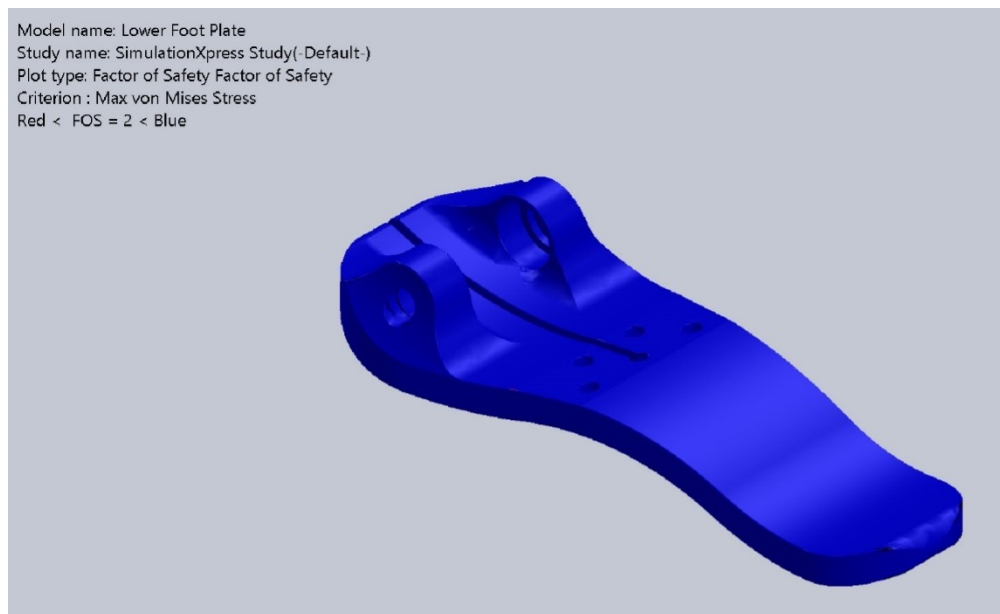


Figure 51 - Lower Foot Plate Bending Force Factor of Safety



Figure 52 - Lower Foot Plate Bending Force Factor of Safety Detail

The results show that the current design will need to be refined to withstand the expected forces. The maximum von Mises stress experienced was $1.078e^{+05}$ psi, dangerously close to the yield strength of $1.784e^{+05}$ psi. This resulted in a minimum factor of safety of 1.656, and a maximum displacement of 1.228 mm. As can be seen in Figure 52, the areas that are above a factor of safety of 2 are quite small and may simply need further reinforcement when making the foot plate. Another possibility could be a calculation error made by Solidworks while performing the simulations. More advanced simulations would reveal whether the red areas are an actual concern or simply an error caused by simplified simulations.

The upper foot plate has a similar bending force simulation applied to it. A force of 15kN was applied downward on the top surface of the foot plate, with the foot plate connection area serving as the fixed surface. The maximum and minimum values are listed in Table 9, with the von Mises stress (Figure 53), displacement (Figure 54), and factor of safety (Figure 55) shown below.

| | Minimum | Maximum |
|--------------------------|----------------|----------------|
| Von Mises Stresses (psi) | $1.670e^{-01}$ | $9.569e^{+04}$ |
| Displacement (mm) | 0 | 2.090 |
| Factor of Safety | 1.864 | $1.068e^{+06}$ |

Table 9 - Upper Foot Plate Bending Force Simulation

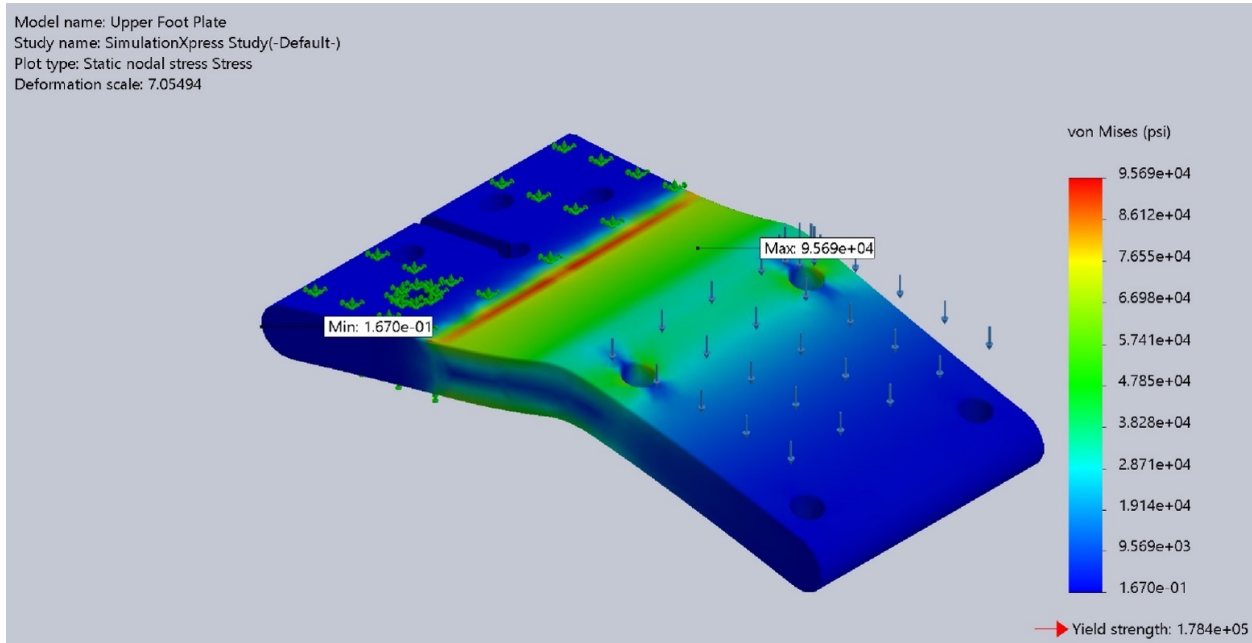


Figure 53 - Upper Foot Plate Bending Force von Mises Stress (psi)

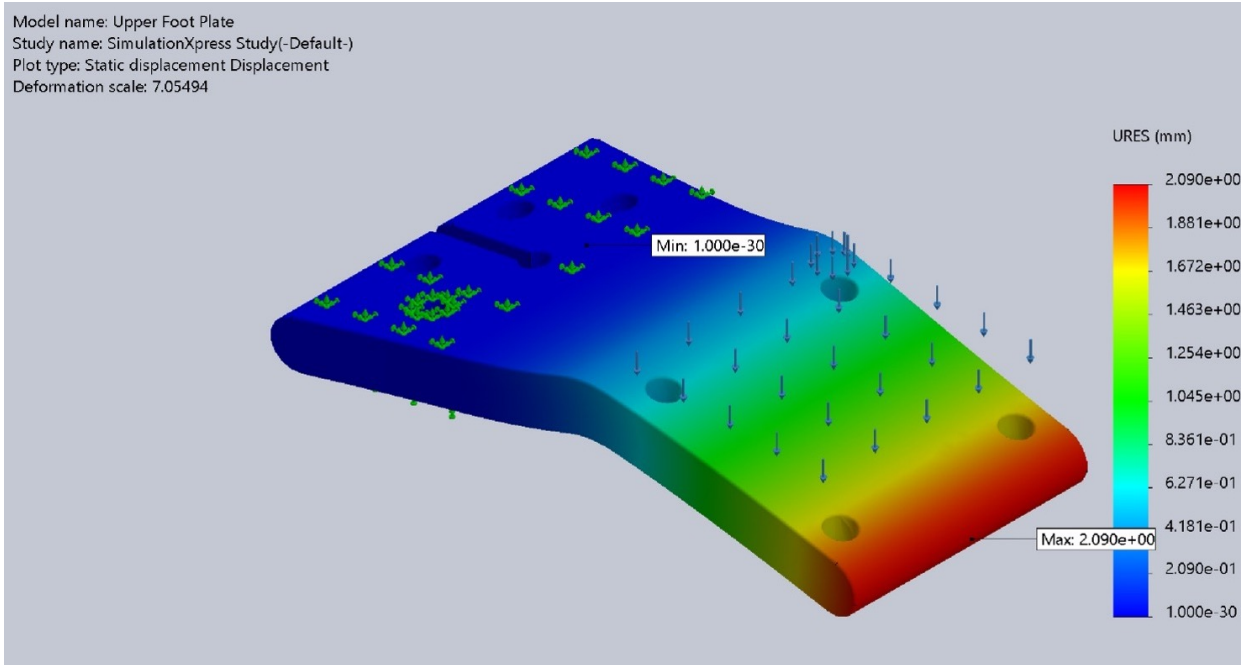


Figure 54 - Upper Foot Plate Bending Force Displacement (mm)

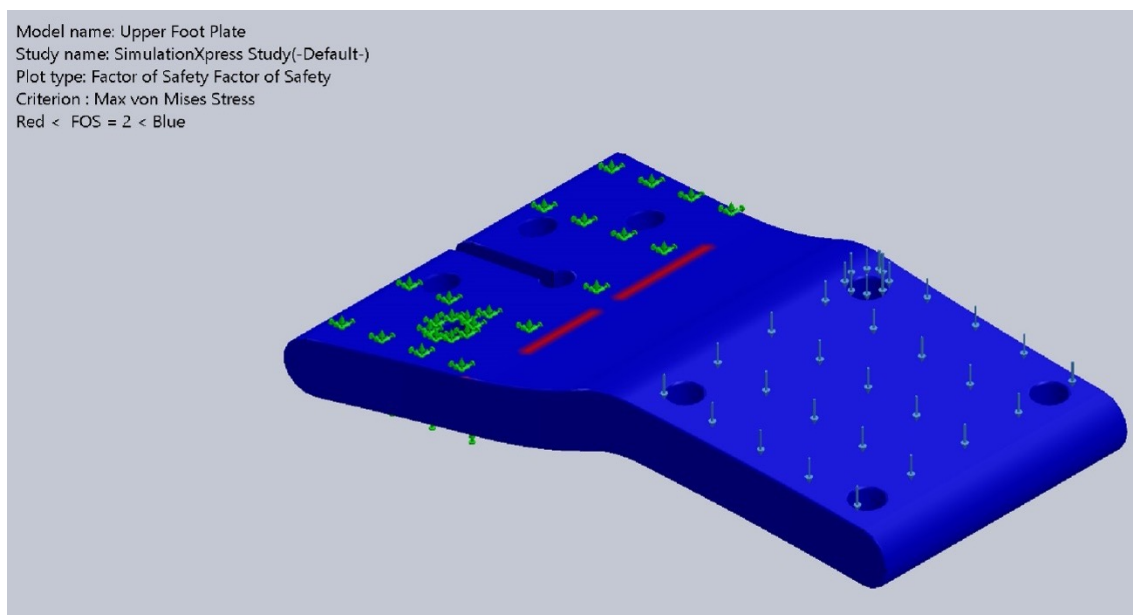


Figure 55 - Upper Foot Plate Bending Force Factor of Safety

Similar to the lower foot plate, the upper foot plate will likely need to be refined to better withstand the expected forces. The upper foot plate experienced a maximum von Mises stress of $9.569e^{+04}$ psi, with a minimum factor of safety of 1.864. The maximum displacement was 2.090

mm. The area of maximum stress was at the bend, indicating that reinforcement in that area or a design modification will be necessary for this component.

Despite the collected values showing simplified approximations of carbon fiber composite's material properties, the collected values indicate these designs should be sufficient for the prosthetic design. The toe area in particular seems more than capable of withstanding the expected forces, and with some reinforcement the foot plates will be able to safely withstand the expected bending forces as well. More realistic simulations that can accurately replicate the material properties will provide a fuller picture of the benefits and drawbacks of the upper- and lower-foot plates' designs.

4.2. Ball Joint Stud Attachment Bracket

For the ball joint stud attachment bracket, the highest expected forces will occur on the arms for the Fox hydraulic shock. In particular, the bolt holes in the arms will be the areas in which high forces will occur. Another area in which forces are of concern is the area that connects the pyramid connector. Several simulations were performed for the stud attachment bracket. Multiple simulations tested shearing forces on the bolt holes for the Fox shock connection point, and another simulation tested the force required to push the connection arms apart. A shearing simulation was also performed for the pyramid connector area to ensure the stud attachment bracket would not fail at that location. Finally, a shearing simulation was performed on the stud attachment area of the attachment bracket.

The first pair of simulations deal with a shearing force on the bolt hole towards and away from the main body of the stud attachment bracket. The Fox shock may be pushing on this part with substantial forces during motion of the prosthetic foot, so it is important to ensure that the

bracket can withstand large forces in these directions. The arms were subjected to a 15 kN force on the inside of the bolt hole, similar to what would be experienced by the shock axle pushing into the arms. The stud connection area and the pyramid adapter connection area were the fixed surfaces for these simulations. The minimum and maximum values are listed in Table 10 and the visualizations for the von Mises stresses, displacement, and factor of safety for the forward (Figure 56Figure 58) and rearward (Figure 59Figure 61) are shown below.

| | Forward | | Rearward | |
|--------------------------|----------------|----------------|----------------|----------------|
| | Min | Max | Min | Max |
| von Mises Stresses (psi) | $8.951e^{-01}$ | $2.502e^{+04}$ | $8.951e^{-01}$ | $2.502e^{+04}$ |
| Displacement (mm) | 0 | $4.776e^{-02}$ | 0 | $4.776e^{-02}$ |
| Factor of Safety | 2.928 | $8.182e^{+04}$ | 2.928 | $8.182e^{+04}$ |

Table 10 - Stud Attachment Bracket Arm 1st and 2nd Simulations

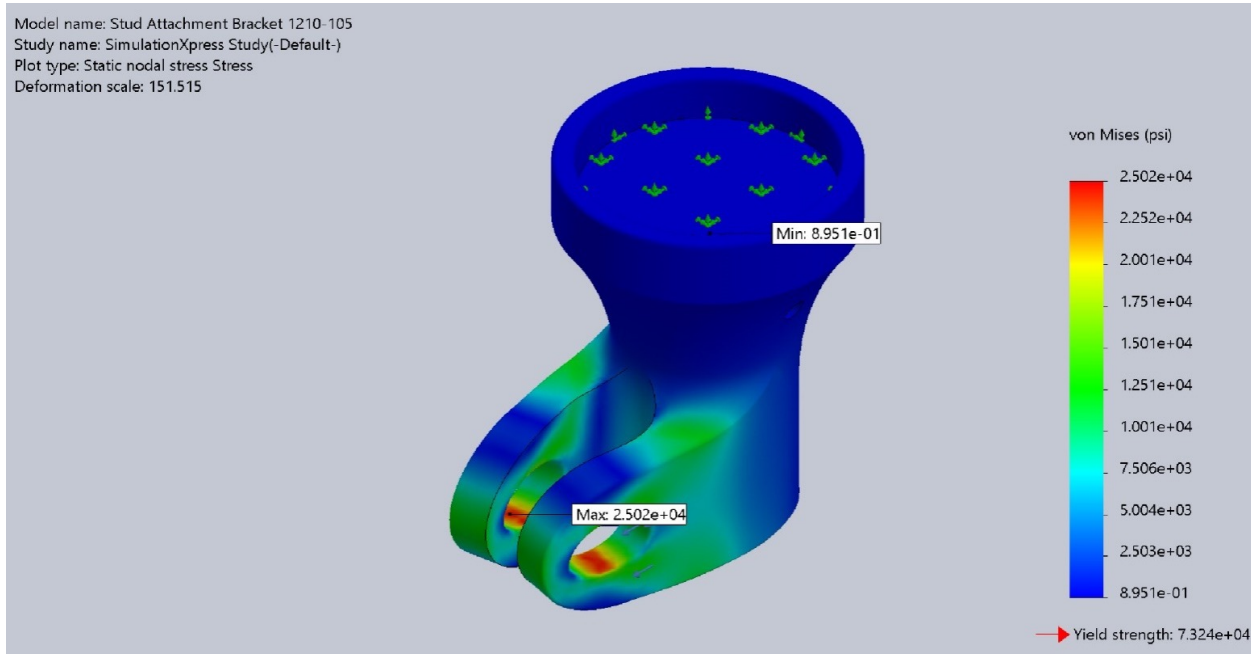


Figure 56 - Stud Attachment Bracket Forward Shearing Force von Mises Stress (psi)

Model name: Stud Attachment Bracket 1210-105
Study name: SimulationXpress Study(-Default-)
Plot type: Static displacement Displacement
Deformation scale: 151.515

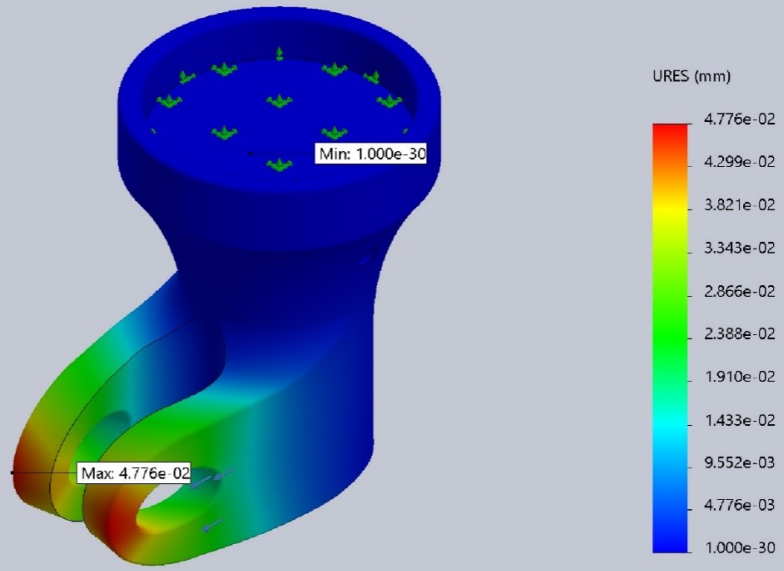


Figure 57 - Stud Attachment Bracket Forward Shearing Force Displacement (mm)

Model name: Stud Attachment Bracket 1210-105
Study name: SimulationXpress Study(-Default-)
Plot type: Factor of Safety Factor of Safety
Criterion : Max von Mises Stress
Red < FOS = 2 < Blue

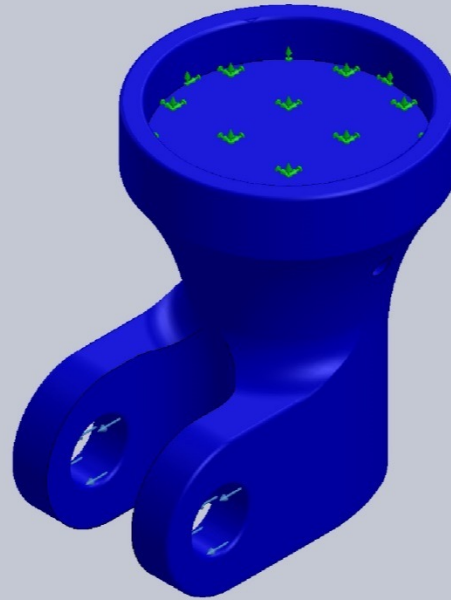


Figure 58 - Stud Attachment Bracket Forward Shearing Force Factor of Safety

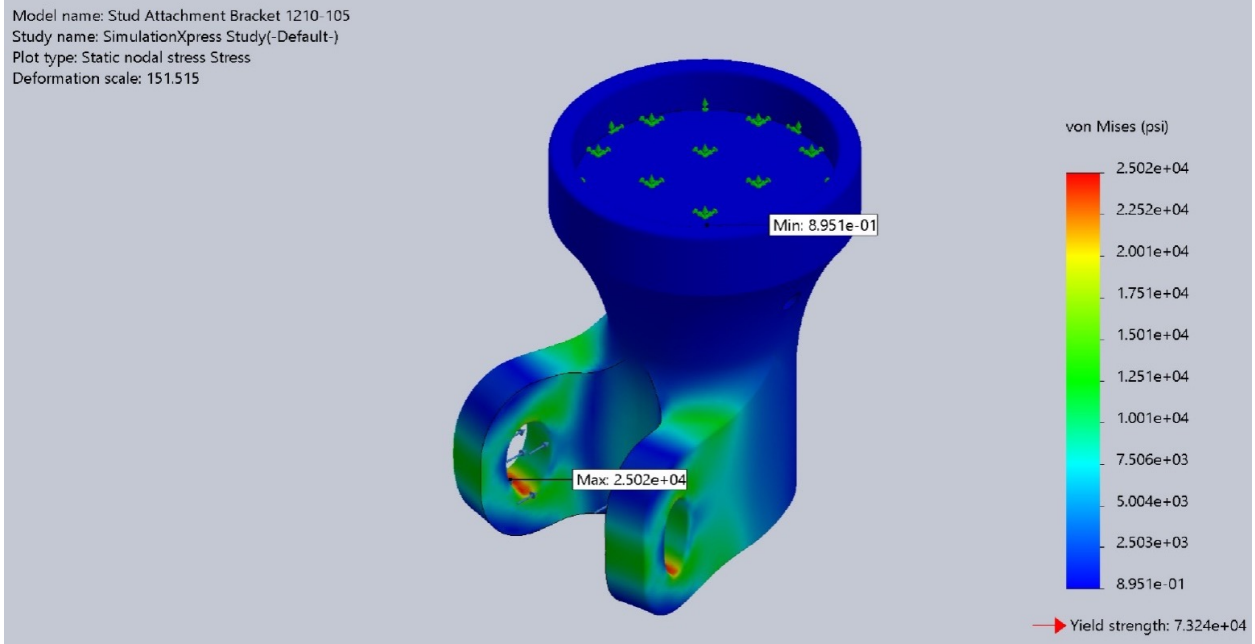


Figure 59 - Stud Attachment Bracket Rearward Shearing Force von Mises Stress (psi)

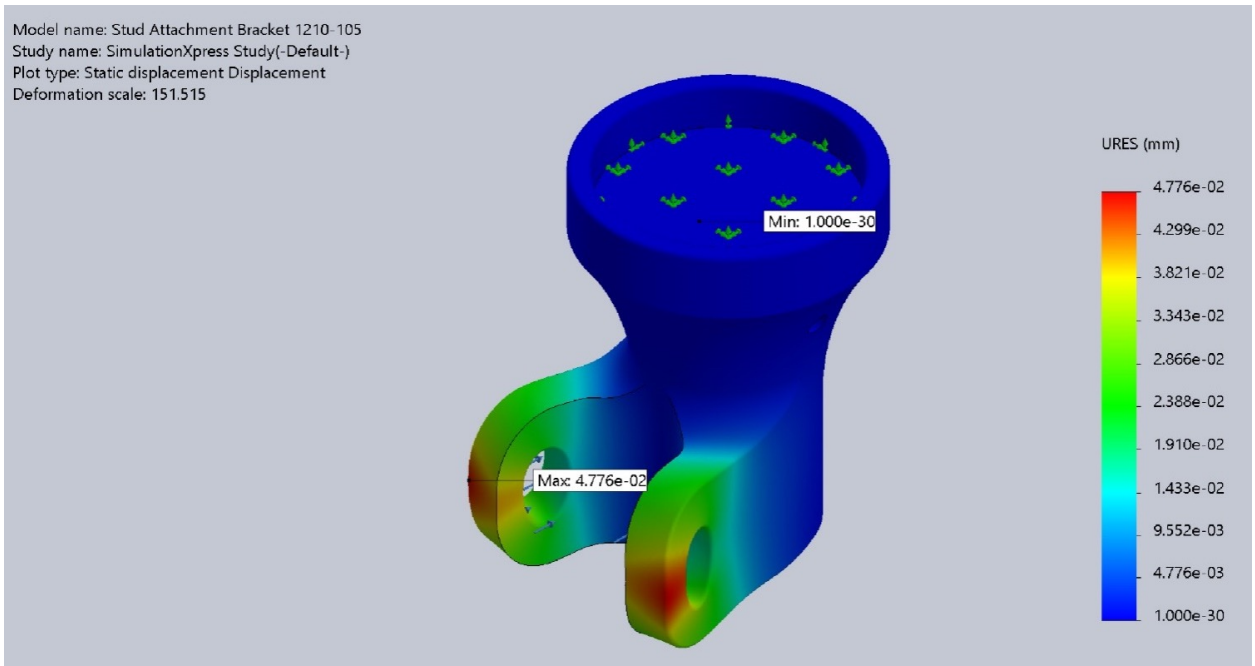


Figure 60 - Stud Attachment Bracket Rearward Shearing Force Displacement (mm)

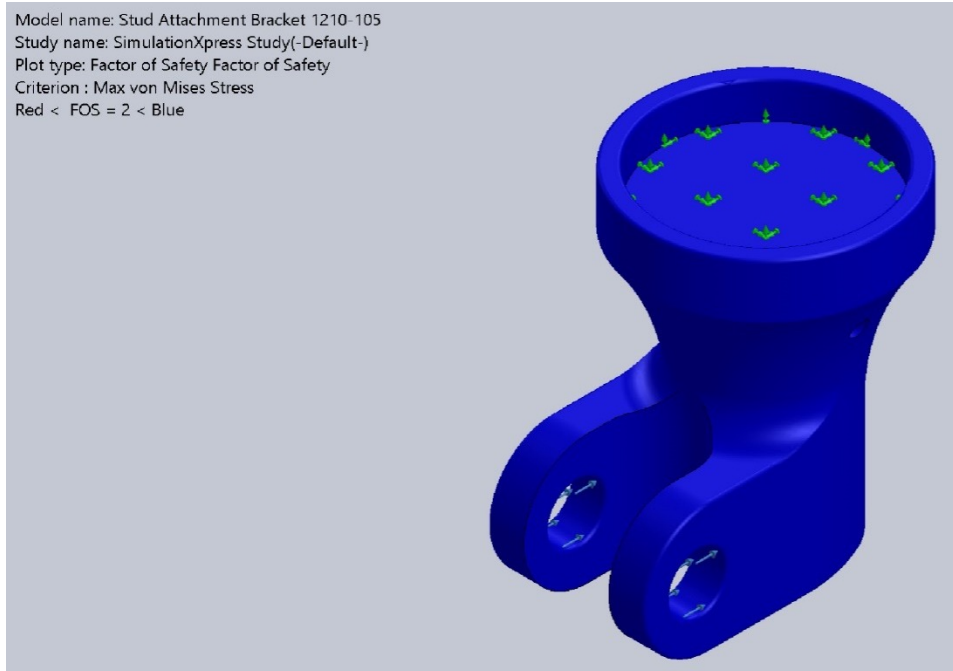


Figure 61 - Stud Attachment Bracket Rearward Shearing Force Factor of Safety

The results show the stud attachment bracket will withstand the expected forces without failure. The largest displacement is $4.776e^{-02}$ mm. The highest von Mises stress experienced are below the yield strength, with a maximum of $2.502e^{+04}$ psi. The lowest factor of safety is 2.928, which is acceptable for safe use.

The next pair of simulations were also shearing simulations on the axle hole, this time pointed up and down. A 15 kN force was applied to the interior of the axle hole as before, with the same fixed surfaces used as the first pair of simulations. The results for von Mises stress, displacement, and factor of safety for upwards (Figure 62Figure 64) and downwards (Figure 65Figure 67) are below, as well as the minimum and maximum values listed in Table 11.

| | Upward | | Downward | |
|--------------------------|----------------|----------------|----------------|----------------|
| | Min | Max | Min | Max |
| von Mises Stresses (psi) | $9.924e^{-01}$ | $4.896e^{+04}$ | $9.924e^{-01}$ | $4.896e^{+04}$ |
| Displacement (mm) | 0 | $1.311e^{-01}$ | 0 | $1.311e^{-01}$ |
| Factor of Safety | 1.496 | $7.381e^{+04}$ | 1.496 | $7.381e^{+04}$ |

Table 11 - Stud Attachment Bracket Arm 3rd and 4th Simulations

Model name: Stud Attachment Bracket 1210-105
Study name: SimulationXpress Study(-Default-)
Plot type: Static nodal stress Stress
Deformation scale: 43.1949

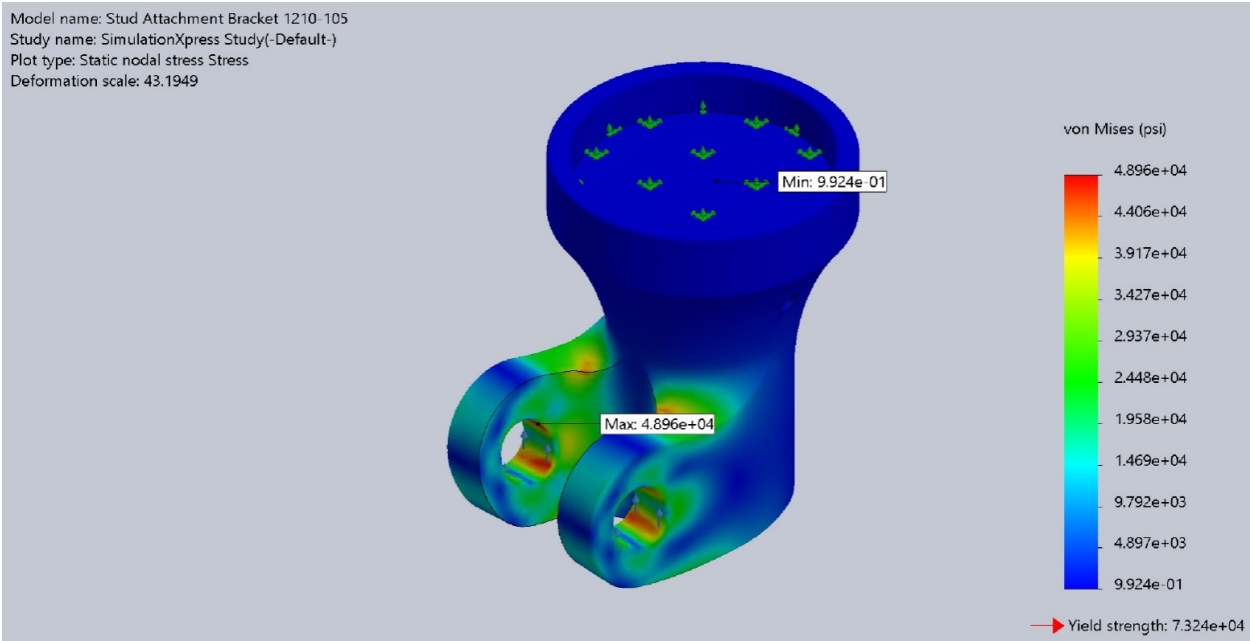


Figure 62 - Stud Attachment Bracket Upward Shearing Force von Mises Stress (psi)

Model name: Stud Attachment Bracket 1210-105
Study name: SimulationXpress Study(-Default-)
Plot type: Static displacement Displacement
Deformation scale: 43.1949

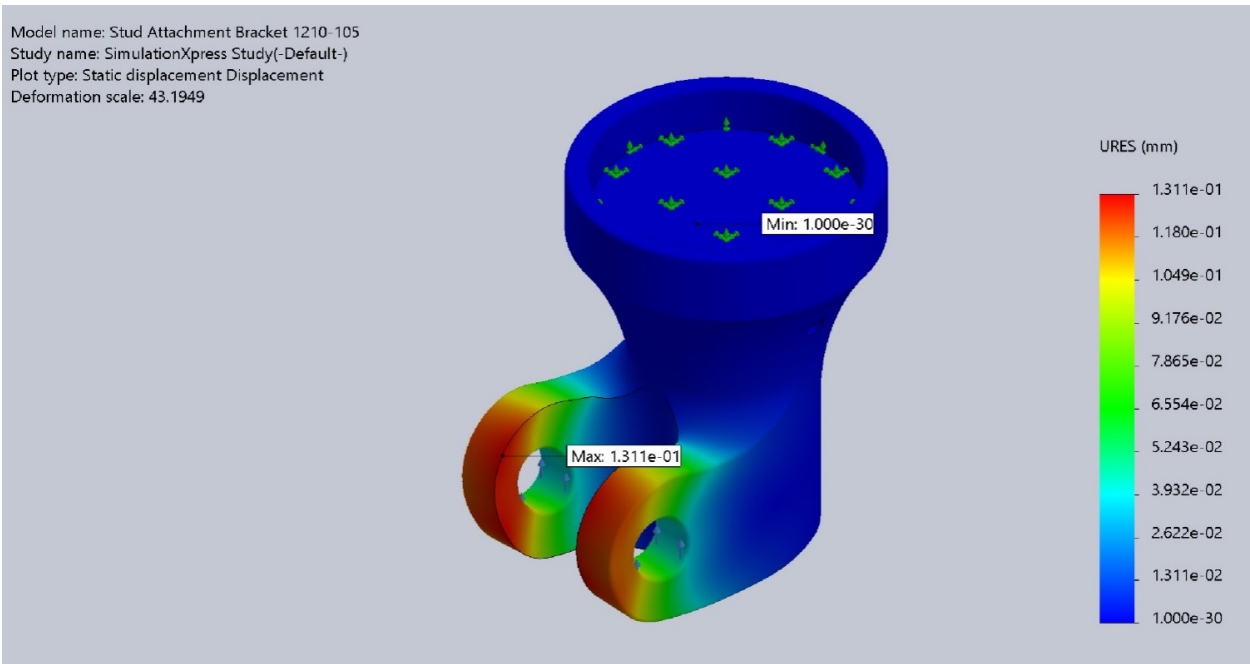


Figure 63 - Stud Attachment Bracket Upward Shearing Force Displacement (mm)

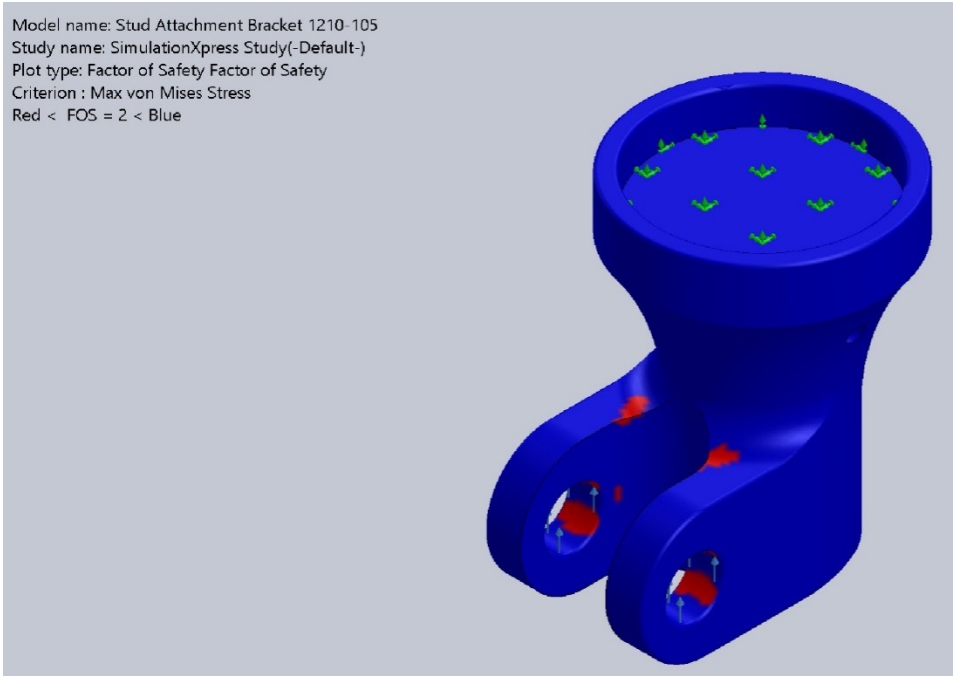


Figure 64 - Stud Attachment Bracket Upward Shearing Force Factor of Safety

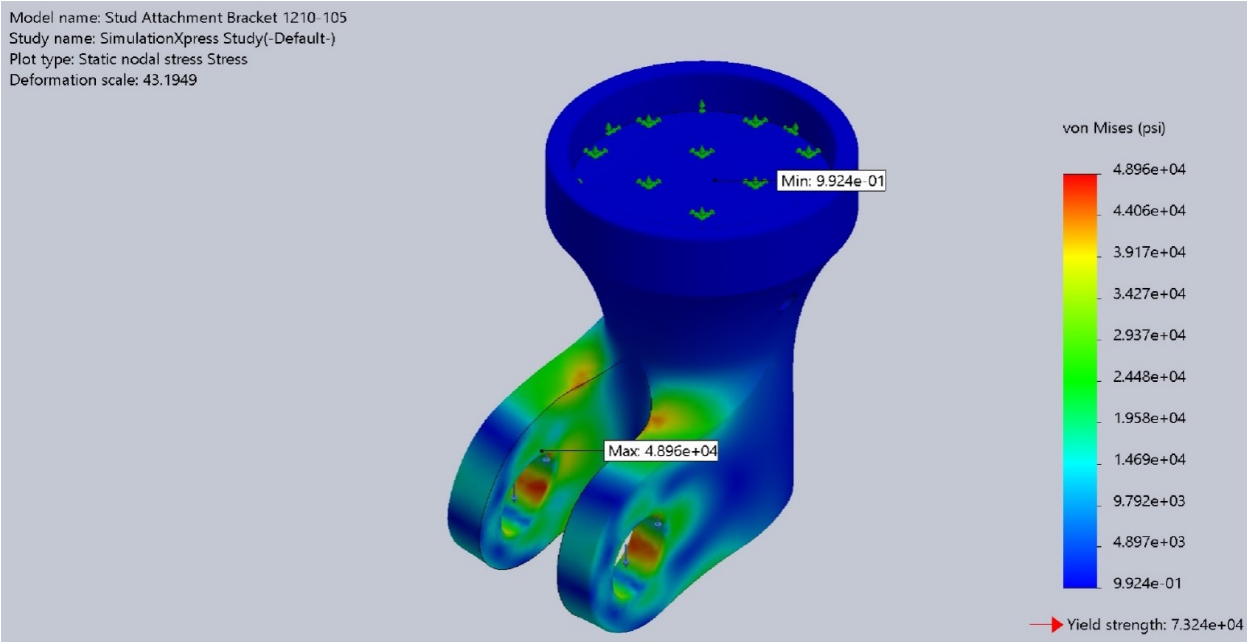


Figure 65 - Stud Attachment Bracket Downward Shearing Force von Mises Stress (psi)

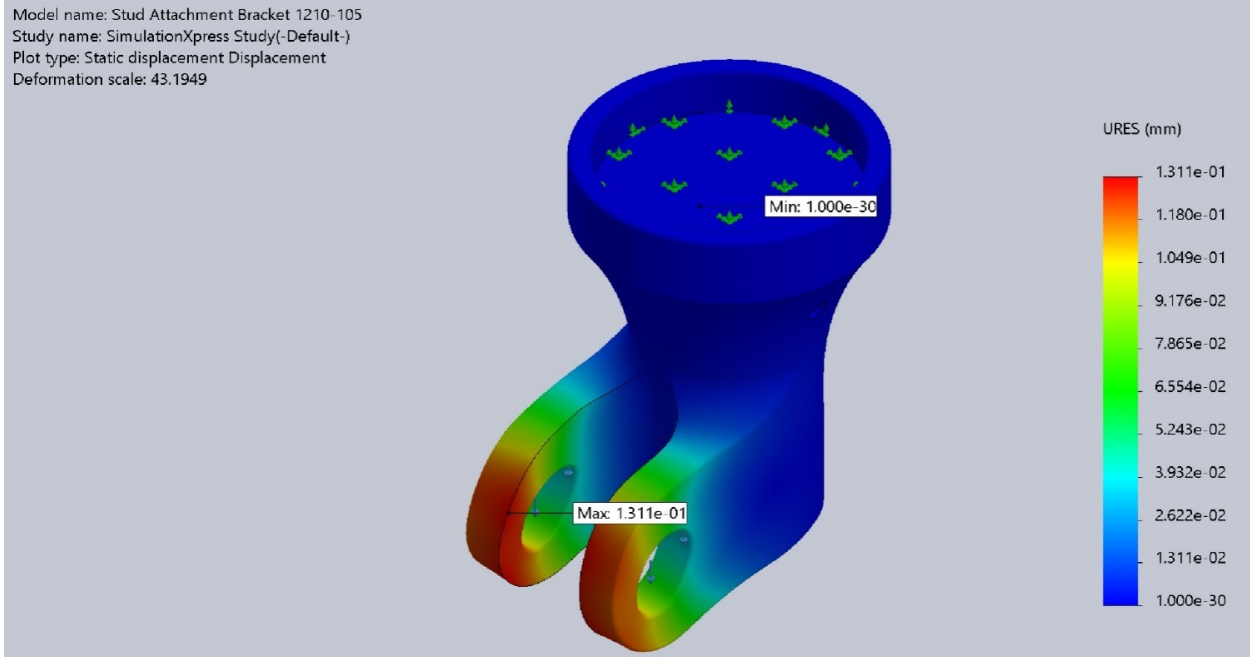


Figure 66 - Stud Attachment Bracket Downward Shearing Force Displacement (mm)

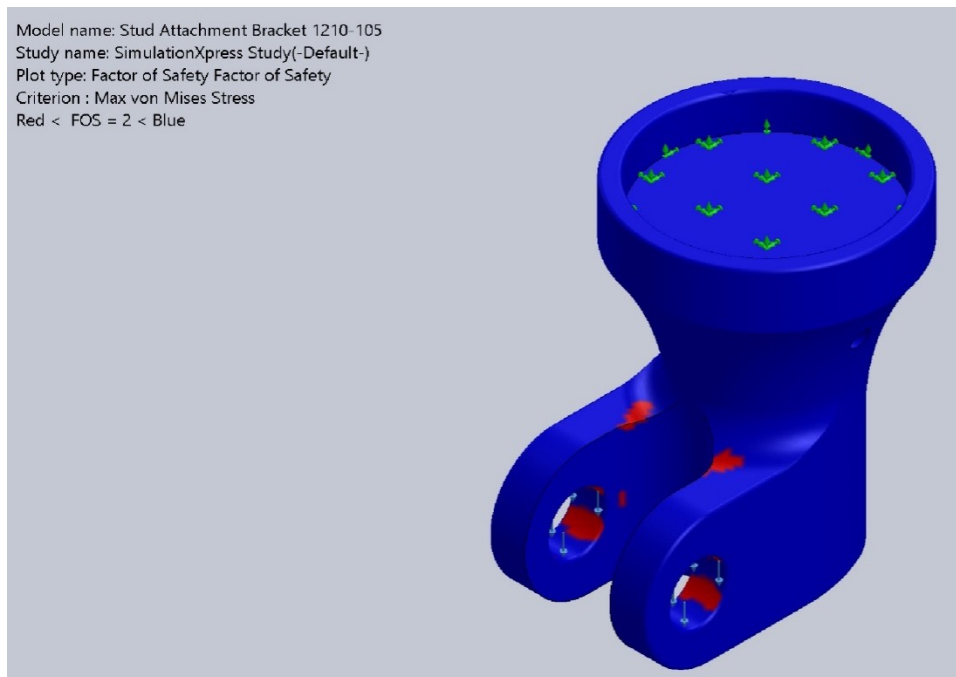


Figure 67 - Stud Attachment Bracket Downward Shearing Force Factor of Safety

The results show that the arms will not be able to sustain a purely vertical force of this magnitude. The highest von Mises stress encountered was $4.896e^{+04}$ psi, which is still safely below the yield strength of $7.324e^{+04}$ psi. The maximum displacement was $1.311e^{-01}$ mm, with a minimum factor of safety of 1.496. Future versions of the stud attachment bracket will need to be redesigned to better sustain the high levels of force expected during walking and running while using this prosthetic. Suggestions for potential modifications can be found in Section 5.3.

The next simulation performed on the arms details a normal force pushing the arms outward. This is not a direction in which high forces are expected, since most of the force will be coming in a direction perpendicular to the axle, not parallel. A simulation was still performed with a reduced force of 3750 N, one quarter of the highest expected force value. Results for the von Mises stresses (Figure 68), displacement (Figure 69), and factor of safety (Figure 70) follow, with their minimum and maximum values listed in Table 12.

| | Minimum | Maximum |
|--------------------------|----------------|----------------|
| von Mises Stresses (psi) | 1.134 | $4.819e^{+04}$ |
| Displacement (mm) | 0 | $2.693e^{-01}$ |
| Factor of Safety | 1.520 | $6.457e^{+04}$ |

Table 12 - Stud Attachment Bracket Arm 5th Simulation

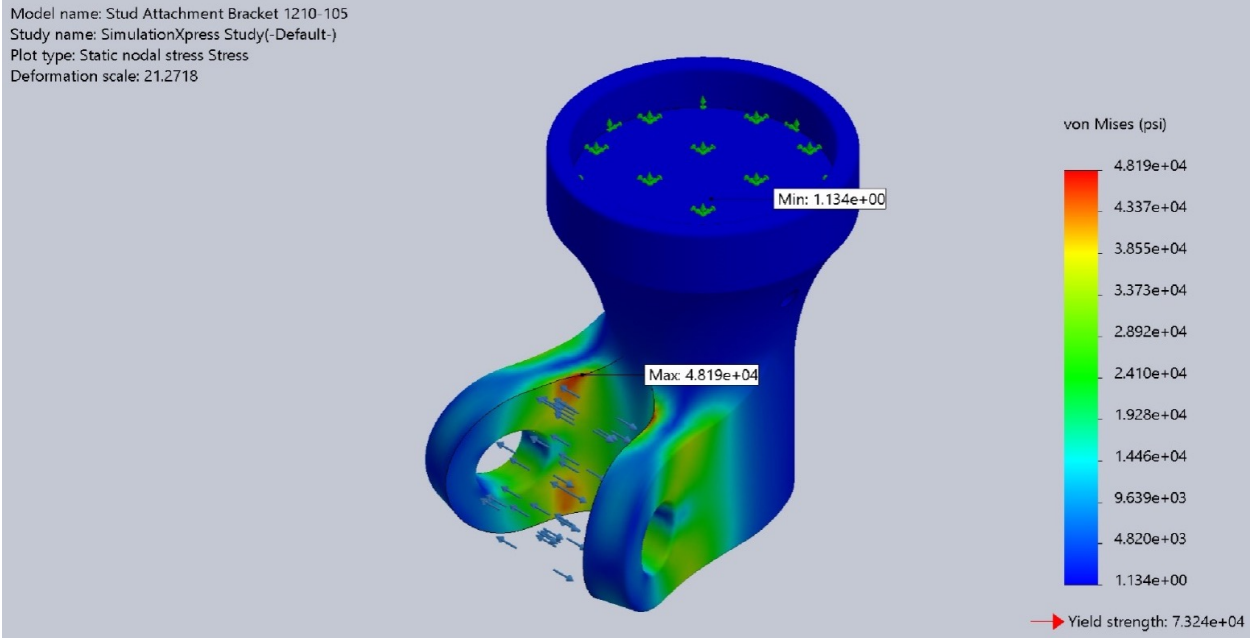


Figure 68 - Stud Attachment Bracket Normal Force Arm von Mises (psi)

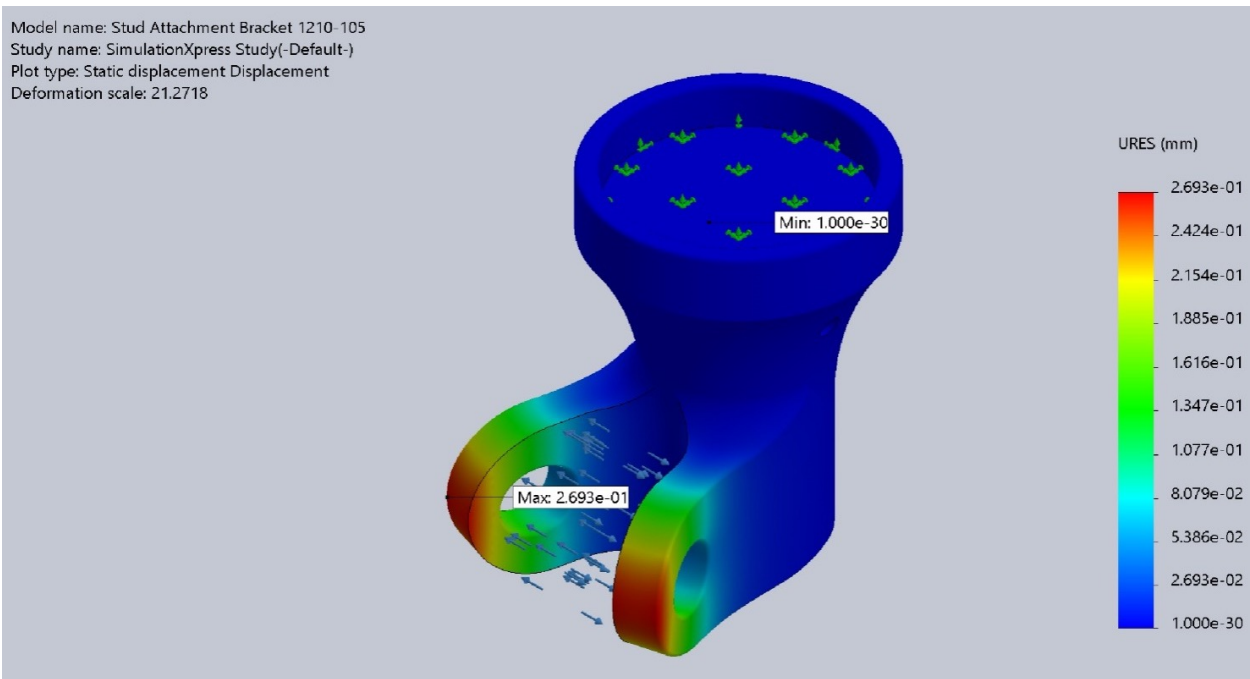


Figure 69 - Stud Attachment Bracket Normal Force Arm Displacement (mm)

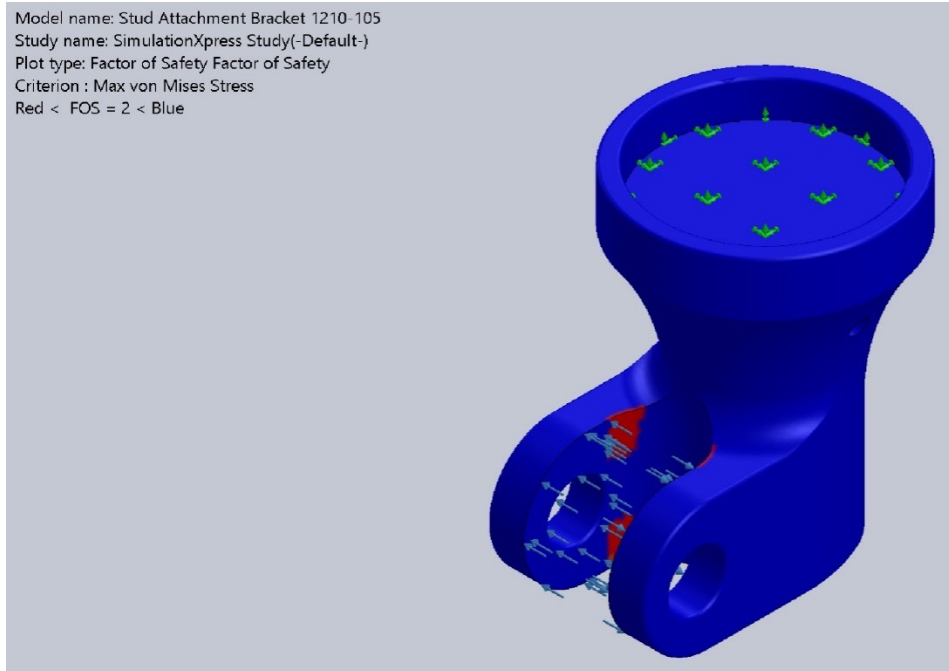


Figure 70 - Stud Attachment Bracket Normal Force Arm Factor of Safety

The results of the simulation show that the arms would not be able to sustain a large force causing the arms to be pushed outwards. Even at a force of 3750 N, the highest von Mises stress encountered was $5.577e^{+4}$ psi, coming close to the material's yield strength. Displacements as high as $3.040e^{-1}$ mm were experienced, and the lowest factor of safety was 1.313. However, since forces are not expected to come from these directions, this is not an expected cause of concern for the current design. Physical testing of the prototype would be a better judge of the forces experienced in this direction, but for now digital models will serve as preliminary testing methods for the expected reactions of this component.

Two final simulations were performed on the ball joint stud attachment bracket: a shearing force on both the pyramid connector area and on the stud attachment area. The pyramid connector area could experience significant forces during heel strike, so it is best to ensure the connection point is capable of withstanding large forces. The simulation tested a 15 kN shearing

force in the frontal plane. Since this area is symmetrical in the frontal and sagittal planes, results for the shearing force should be similar in both planes. Results for the von Mises stresses (Figure 71), displacement (Figure 72), factor of safety (Figure 73Figure 74), and minimum and maximum values (Table 13) follow.

| | Minimum | Maximum |
|------------------------|----------------|----------------|
| von Mises Stress (psi) | $2.666e^{-01}$ | $5.029e^{+04}$ |
| Displacement (mm) | 0 | $7.961e^{-02}$ |
| Factor of Safety | 1.533 | $2.783e^{+5}$ |

Table 13 - Stud Attachment Bracket Pyramid Connector Simulation

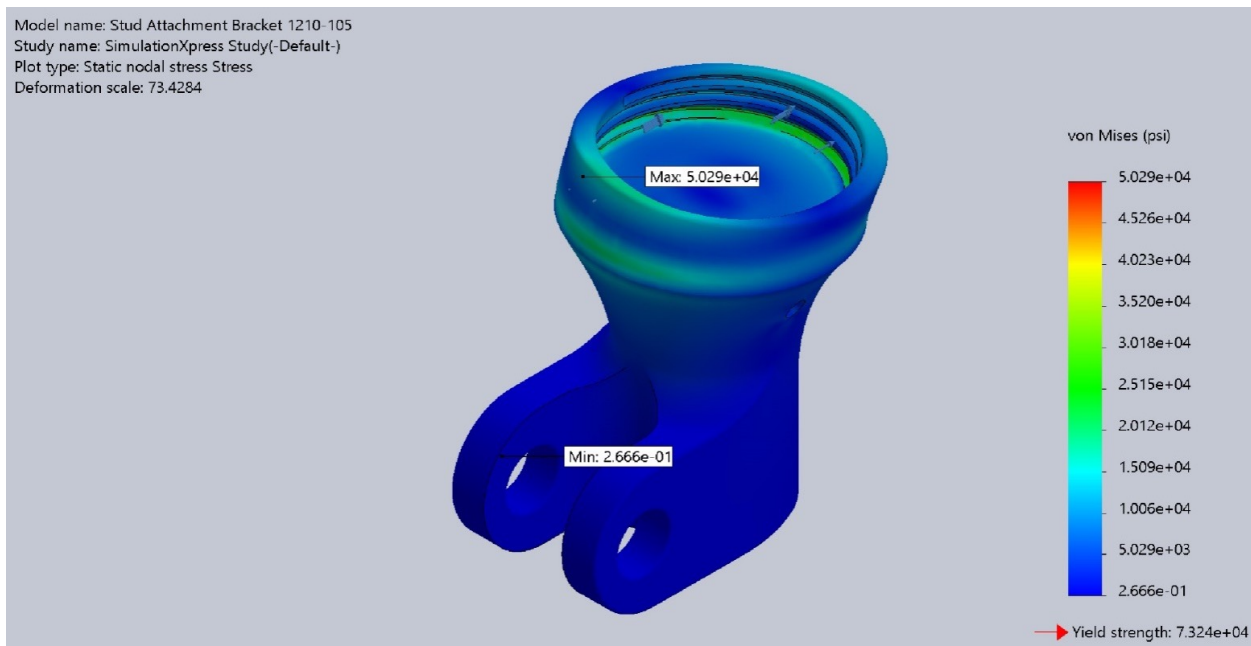


Figure 71 - Stud Attachment Bracket Pyramid Connector von Mises (psi)

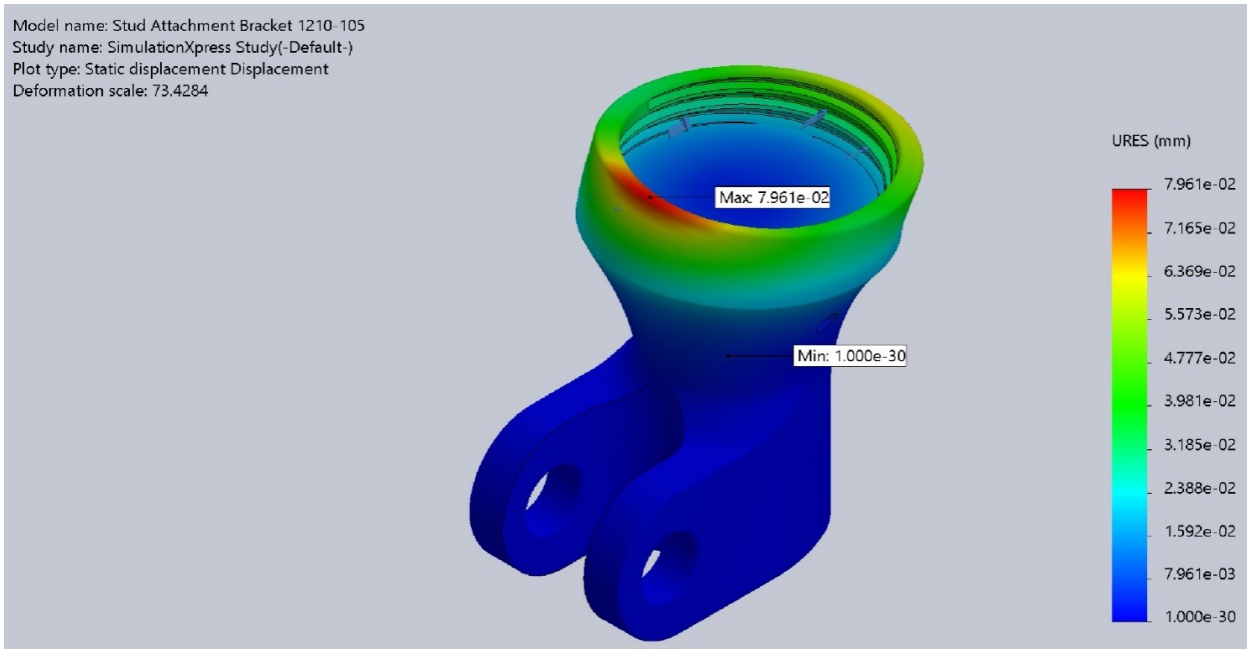


Figure 72 - Stud Attachment Bracket Pyramid Connector Displacement (mm)

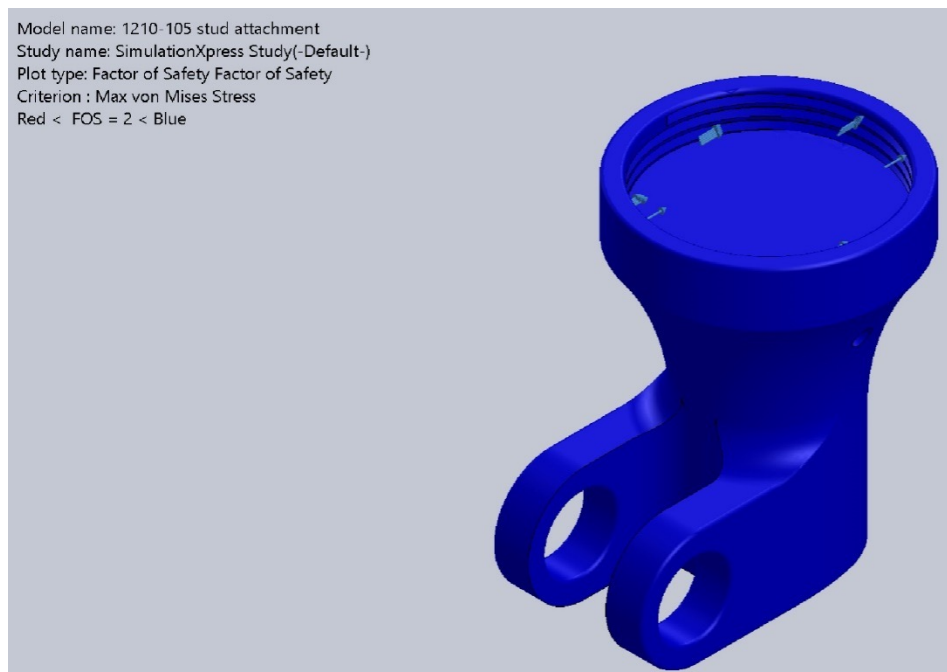


Figure 73 - Stud Attachment Bracket Pyramid Connector Factor of Safety

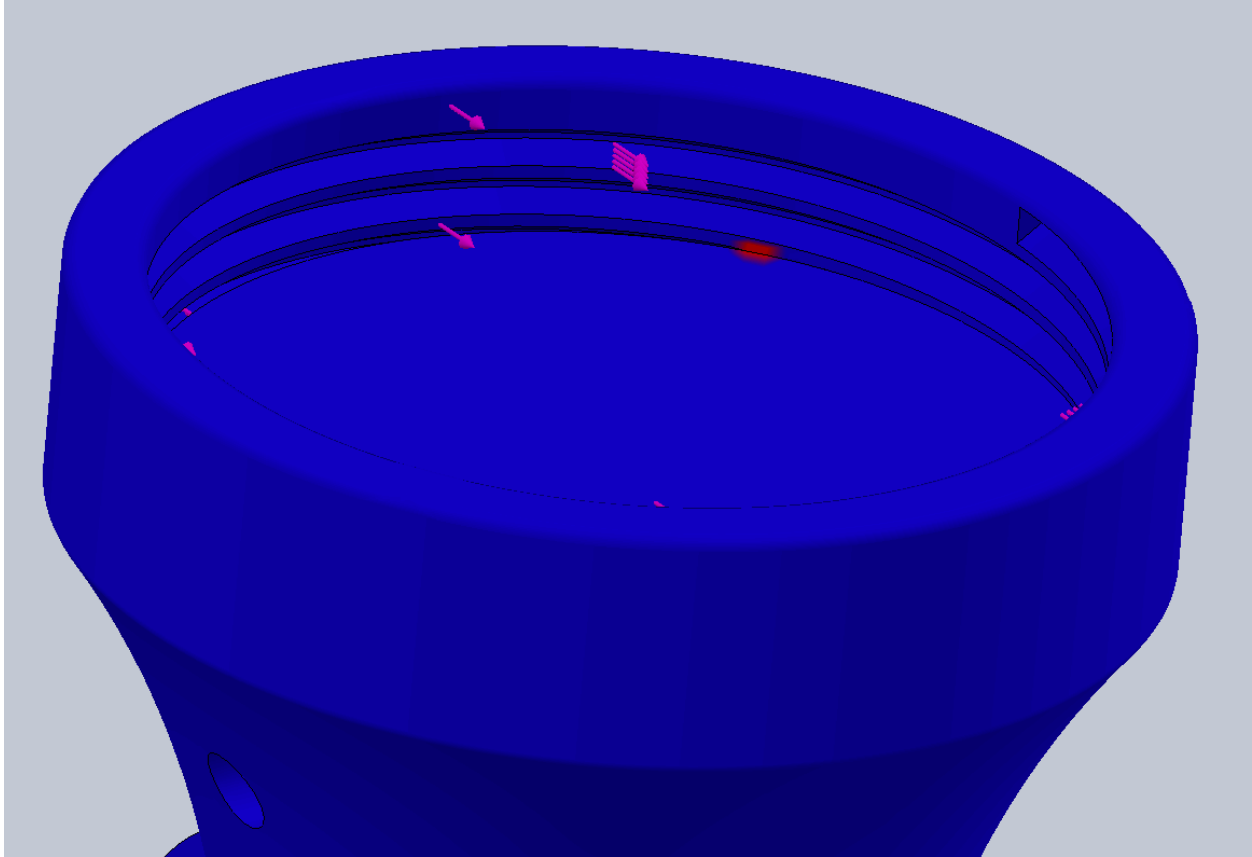


Figure 74 - Stud Attachment Bracket Pyramid Connector Factor of Safety Detail

The results show that the area holding the pyramid connector is capable of withstanding the 15 kN force. The maximum von Mises stress was $4.776e^{+4}$ psi, far enough from the yield strength for safety. The maximum displacement was only $3.141e^{-3}$ in. While the lowest factor of safety is listed at 1.533, it appears this is localized to a small area under the bottommost threads. While this is definitely a factor to consider in future designs, it does not necessarily mean this design element has failed. A different thread orientation or thread type may be all that is needed to eliminate the stress area. When the physical part is being made the threads will be examined in closer detail to ensure these stress areas are not present in the final design.

Similar to the pyramid connector area, a shearing force simulation was performed on the interior surface that will connect the ball joint stud. A 15kN force was directed towards the rear

of the frontal plane. Visual results (Figure 75Figure 77) and the table listing minimum and maximum values (Table 14) are below.

| | Minimum | Maximum |
|------------------------|----------------|----------------|
| von Mises Stress (psi) | $1.243e^{+01}$ | $1.730e^{+04}$ |
| Displacement (mm) | 0 | $1.991e^{-02}$ |
| Factor of Safety | 4.233 | $5.890e^{+03}$ |

Table 14 - Stud Attachment Bracket Ball Joint Area Simulation

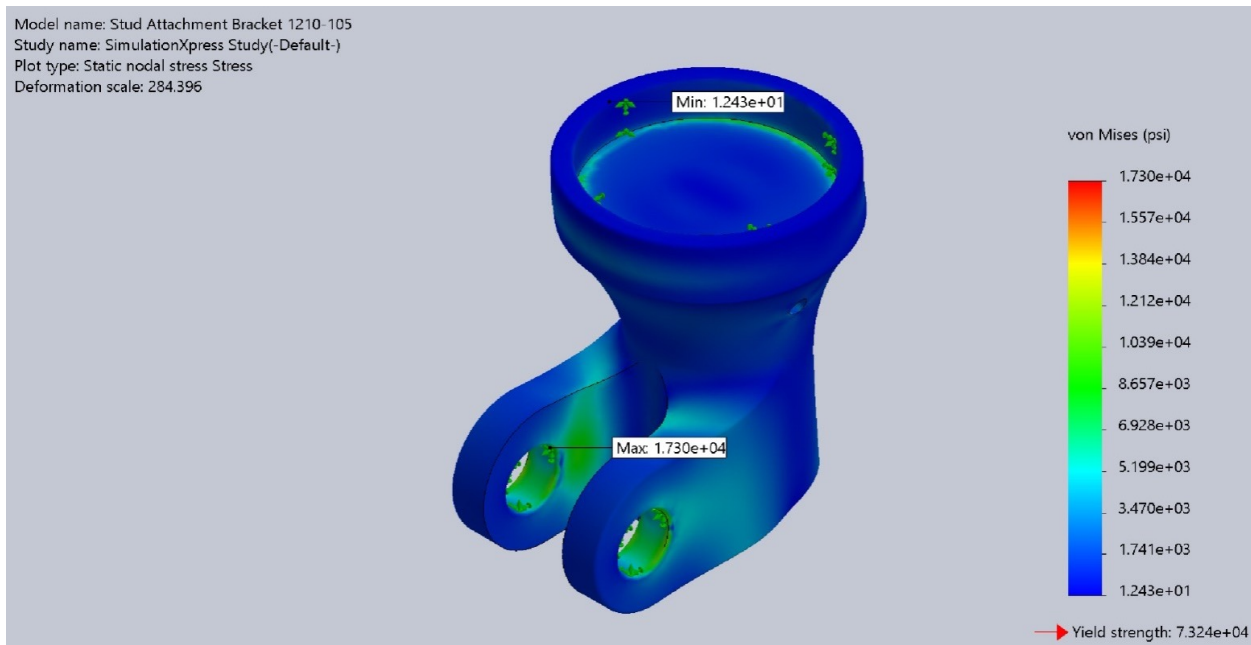


Figure 75 - Stud Attachment Bracket Ball Joint Area von Mises Stress (psi)

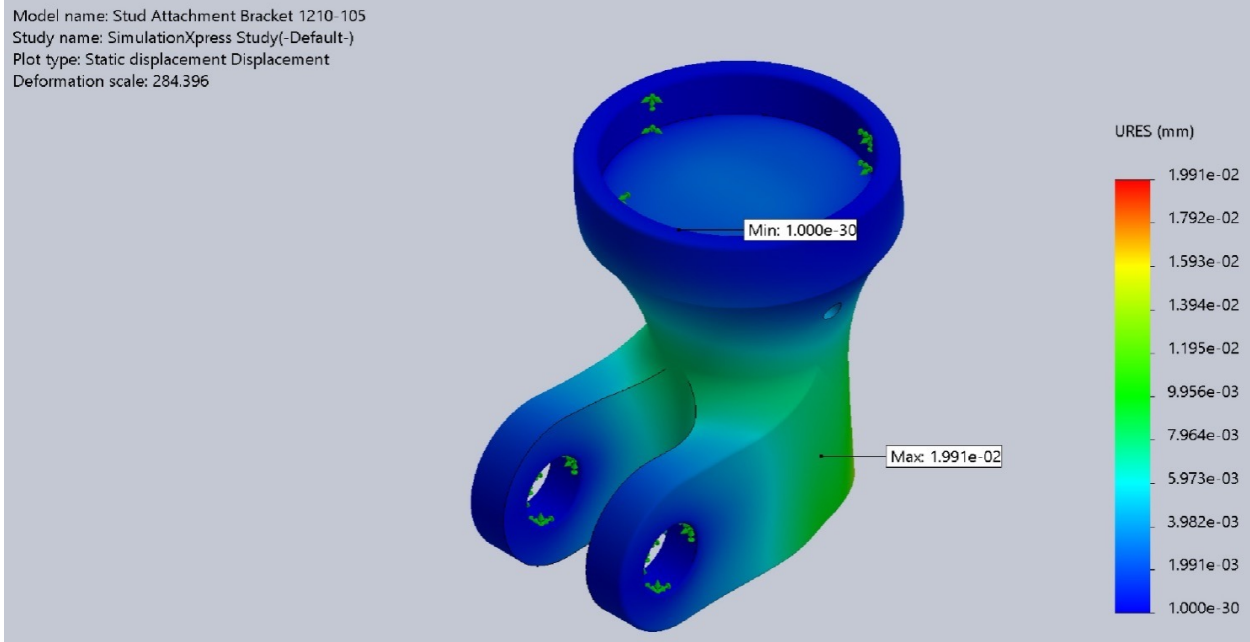


Figure 76 - Stud Attachment Bracket Ball Joint Area Displacement (mm)

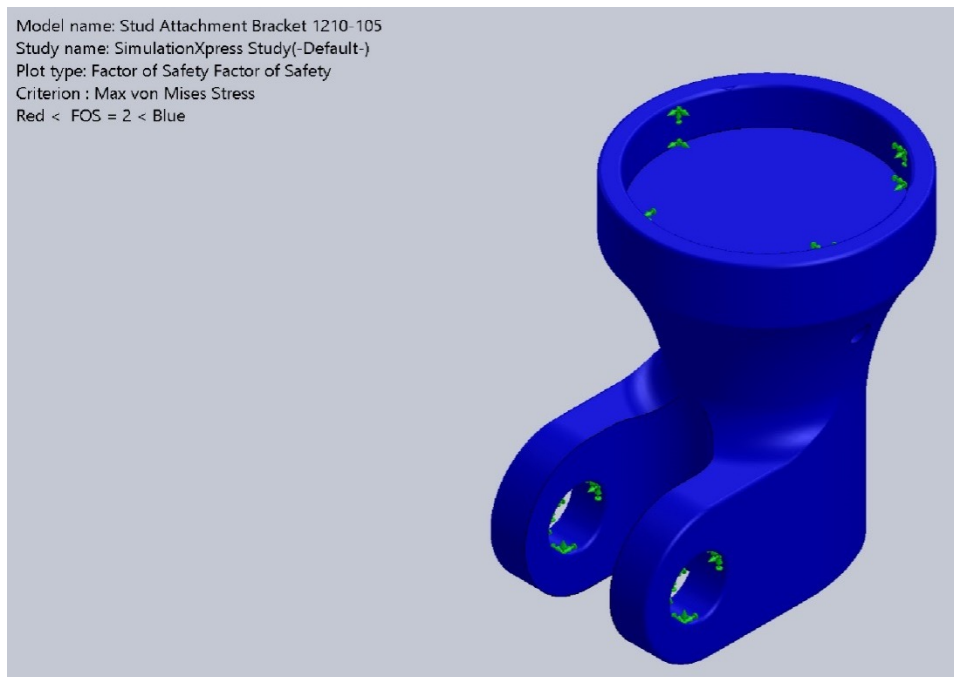


Figure 77 - Stud Attachment Bracket Ball Joint Area Factor of Safety

The results show that the ball joint connection area is more than capable of withstanding the expected forces. The minimum factor of safety for this simulation was 4.233, with a

maximum von Mises stress of $1.730e^{+04}$ psi. The maximum displacement was $1.991e^{-02}$ mm, indicating that this area of the component is robustly designed. Because it appears to be so strong, this area would serve as a good candidate for material optimization, in which the minimum amount of material is determined that can be used while still preserving its full strength.

Overall, the ball joint stud attachment bracket has a strong design that can withstand the expected forces in most areas. Minor redesigns of the arms will further strengthen this component, making it stronger and more capable. As the component is further refined and improved, the design will be optimized to be as strong and lightweight as possible.

4.3. Ball Joint Housing Attachment Bracket

The ball joint housing attachment bracket is held to the upper foot plate by four bolts. These connection points are where this component's highest expected forces will occur. The other area which is expected to experience significant forces is the top opening which connects the housing attachment bracket to the ball joint housing. Simulations testing the normal and shearing forces were performed to ensure both of these areas were capable of withstanding the expected forces.

The first simulation performed was to test the normal forces at the upper opening. This force would cause the opening to expand outward and is intended to simulate the ball joint being pulled out of the housing attachment bracket. This component was tested with a 15 kN force, with the bolt holes acting as the fixed surfaces. The minimum and maximum values are listed in Table 15, and the visualizations of the von Mises stresses (Figure 78), displacement (Figure 79), and factor of safety (Figure 80) are shown below.

| | Minimum | Maximum |
|------------------------|----------------|----------------|
| von Mises stress (psi) | $1.615e^{-02}$ | $2.301e^{+04}$ |
| Displacement (mm) | 0 | $2.544e^{-02}$ |
| Factor of Safety | 3.183 | $4.537e^{+02}$ |

Table 15 - Housing Attachment Bracket Upper Opening Normal Simulation

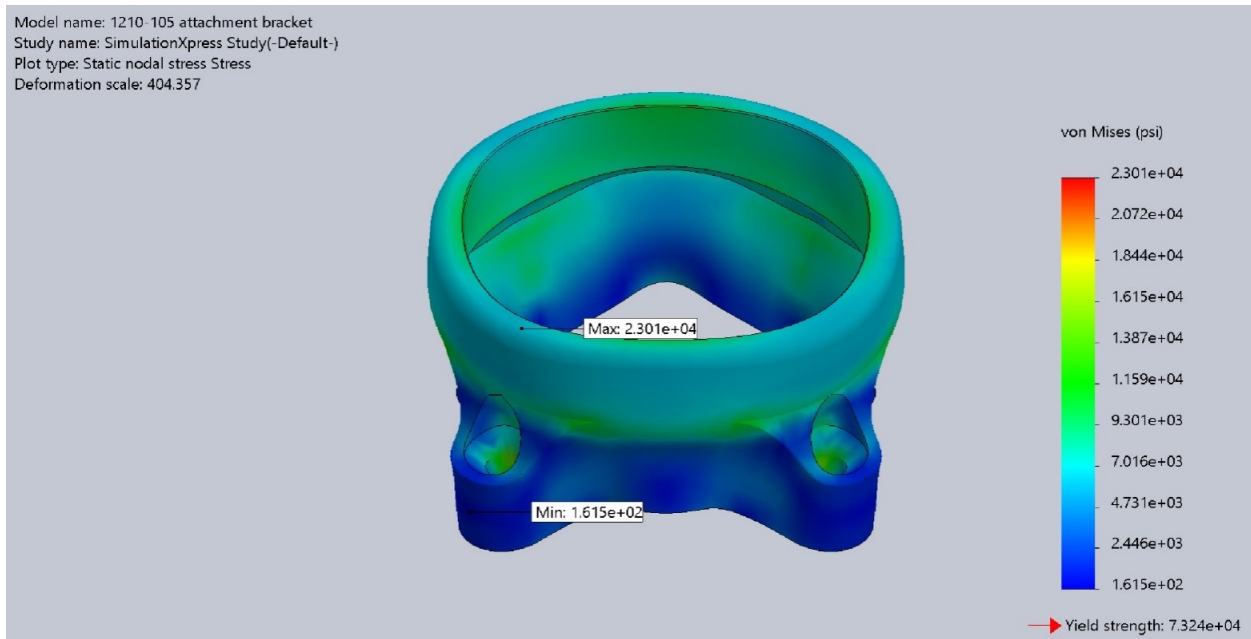


Figure 78 - Housing Attachment Bracket Opening Normal Simulation von Mises Stresses (psi)

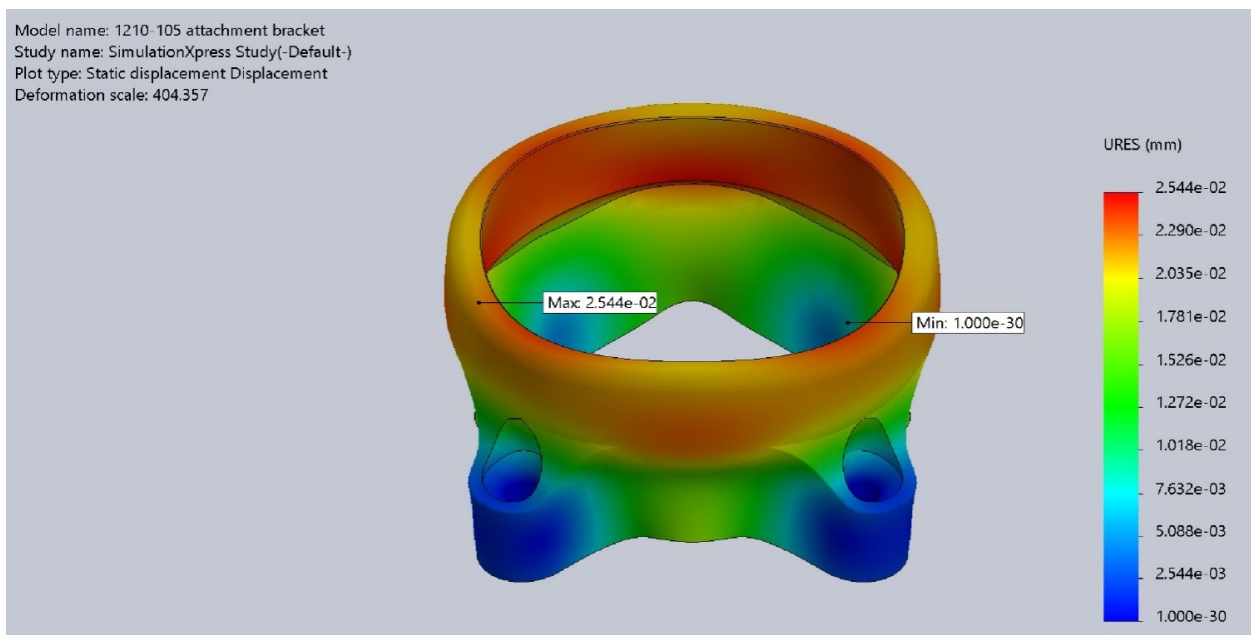


Figure 79 - Housing Attachment Bracket Opening Normal Simulation displacement (mm)

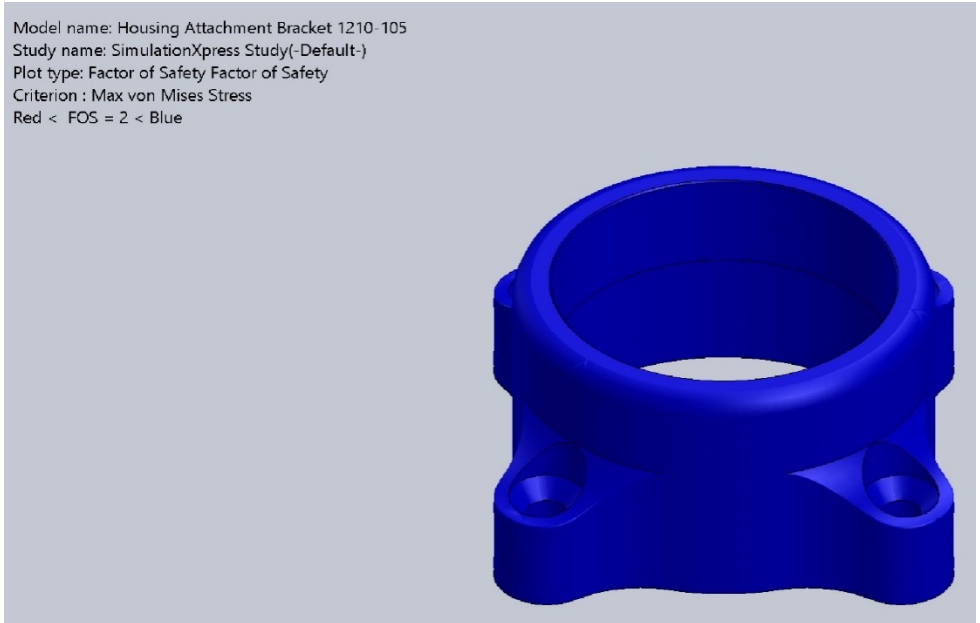


Figure 80 - Housing Attachment Bracket Opening Normal Simulation Factor of Safety

The results show the housing attachment bracket is quite capable of withstanding the normal forces, with the lowest factor of safety 3.183. The bracket experienced von Mises stresses as high as $2.301e^{+4}$ psi and only moved a displacement of $2.544e^{-2}$ mm.

The next simulation performed on the upper opening was a shearing force. Shearing forces may be experienced during certain foot movements and should therefore be tested as a precaution. The component was tested at 15kN again, and the results for this simulation are below.

| | Minimum | Maximum |
|--------------------------|----------------|----------------|
| von Mises stresses (psi) | $6.239e^{+01}$ | $3.238e^{+04}$ |
| Displacement (mm) | 0 | $6.989e^{-02}$ |
| Factor of Safety | 2.262 | $1.174e^{+03}$ |

Table 16 - Housing Attachment Bracket Upper Opening Shearing Simulation

Model name: AutoRecover Of 1210-105 attachment bracket
Study name: SimulationXpress Study(-Default-)
Plot type: Static nodal stress Stress
Deformation scale: 165.551

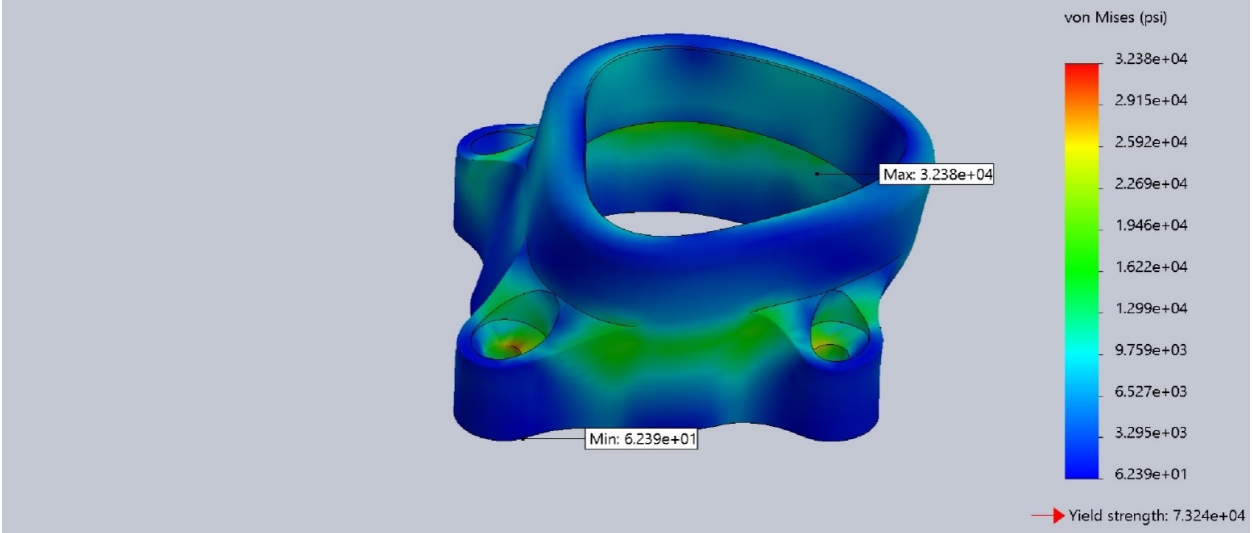


Figure 81 - Housing Attachment Bracket Opening Shearing von Mises Stresses (psi)

Model name: AutoRecover Of 1210-105 attachment bracket
Study name: SimulationXpress Study(-Default-)
Plot type: Static displacement Displacement
Deformation scale: 165.551

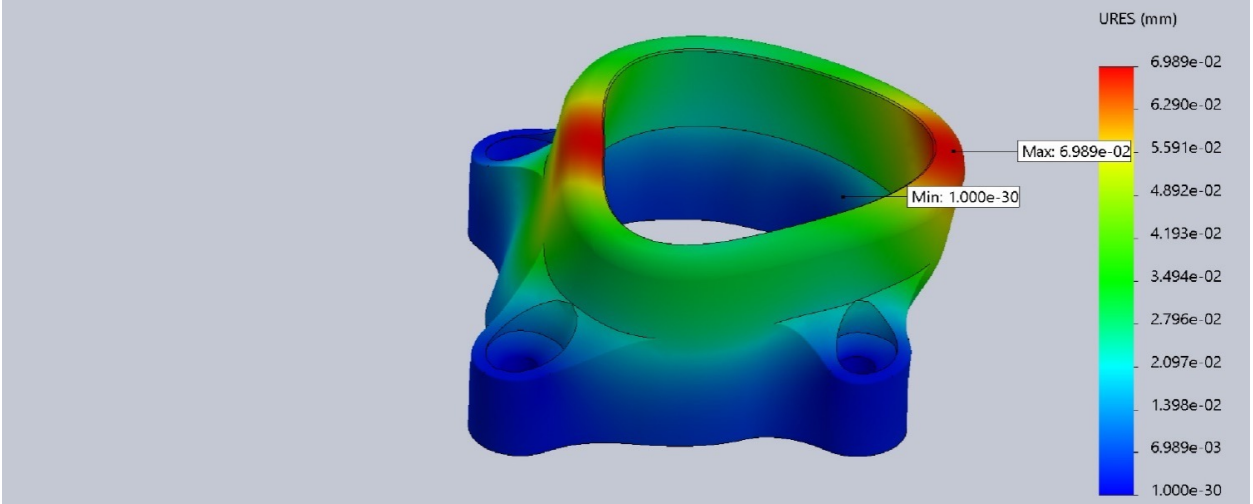


Figure 82 - Housing Attachment Bracket Opening Shearing Displacement (mm)

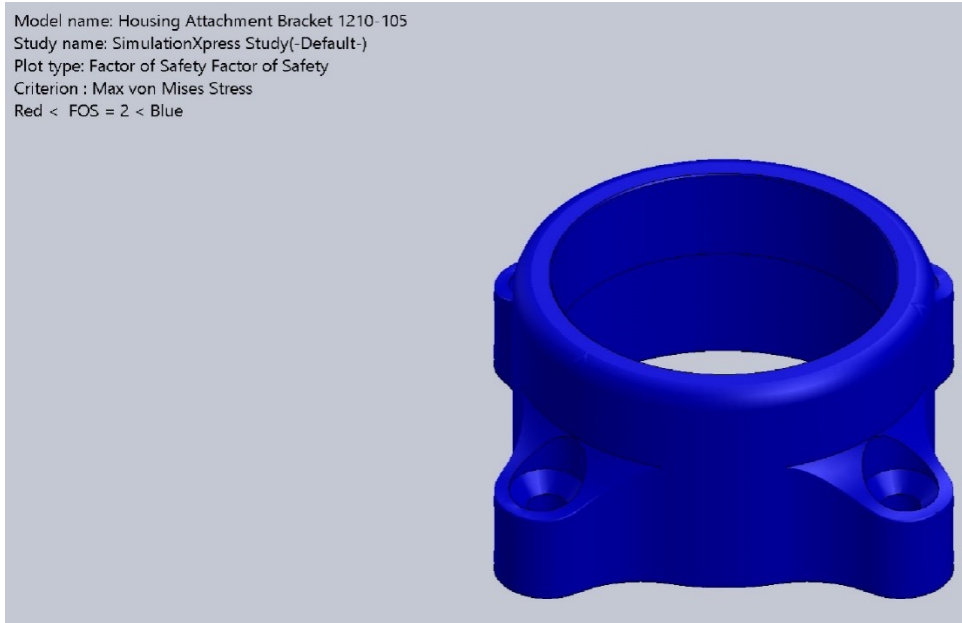


Figure 83 - Housing Attachment Bracket Opening Shearing Factor of Safety

Much like the simulation for normal forces, the housing attachment bracket was capable of withstanding the forces given in the simulation. The minimum factor of safety was 2.262, safely above the minimum value of 2. The maximum von Mises stress encountered was $3.238e^{+4}$ psi, with a maximum displacement of $6.989e^{-2}$ mm. While these results are encouraging on their own, when the ball joint is within the housing attachment bracket, the forces and displacement should be even lower since the ball joint will be able to take up some of the force in addition to the bracket.

Two simulations were performed on the bolt holes for this project. The first was a normal force simulation that would attempt to expand the bolt holes. This simulation was performed with a 15kN value for each bolt hole, with the interior faces serving as the fixed surfaces. The visualizations can be seen in Figures 84-86 below, as well as Table 17 listing the minimum and maximum values.

| | Minimum | Maximum |
|--------------------------|----------------|----------------|
| von Mises stresses (psi) | $2.190e^{-01}$ | $3.066e^{+04}$ |
| Displacement (mm) | 0 | $8.875e^{-03}$ |
| Factor of Safety | 2.389 | $3.344e^{+05}$ |

Table 17 - Housing Attachment Bracket Bolt Holes Normal Simulation

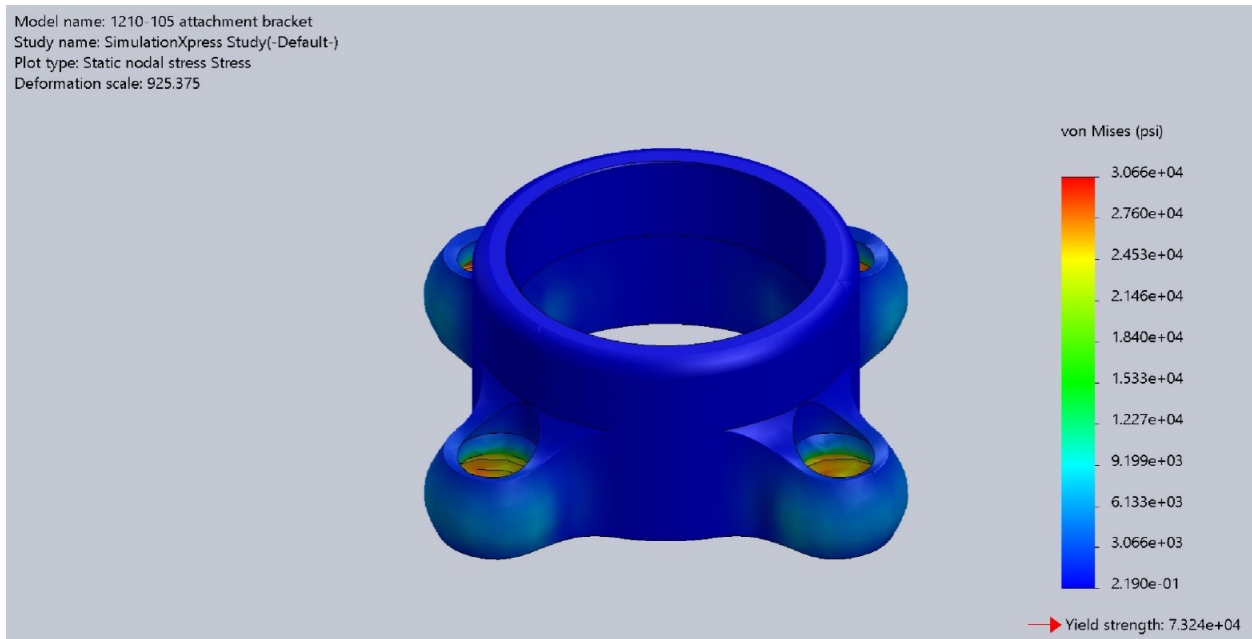


Figure 84 - Housing Attachment Bracket Bolt Hole Normal Simulation von Mises Stresses (psi)

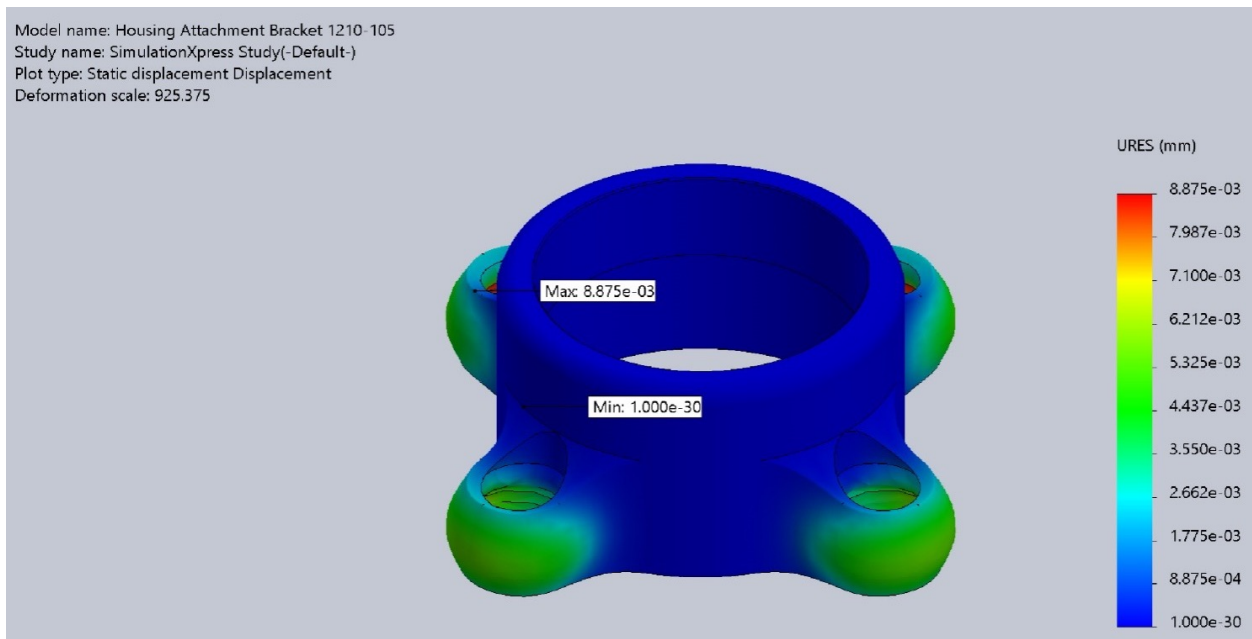


Figure 85 - Housing Attachment Bracket Bolt Hole Normal Simulation Displacement (mm)

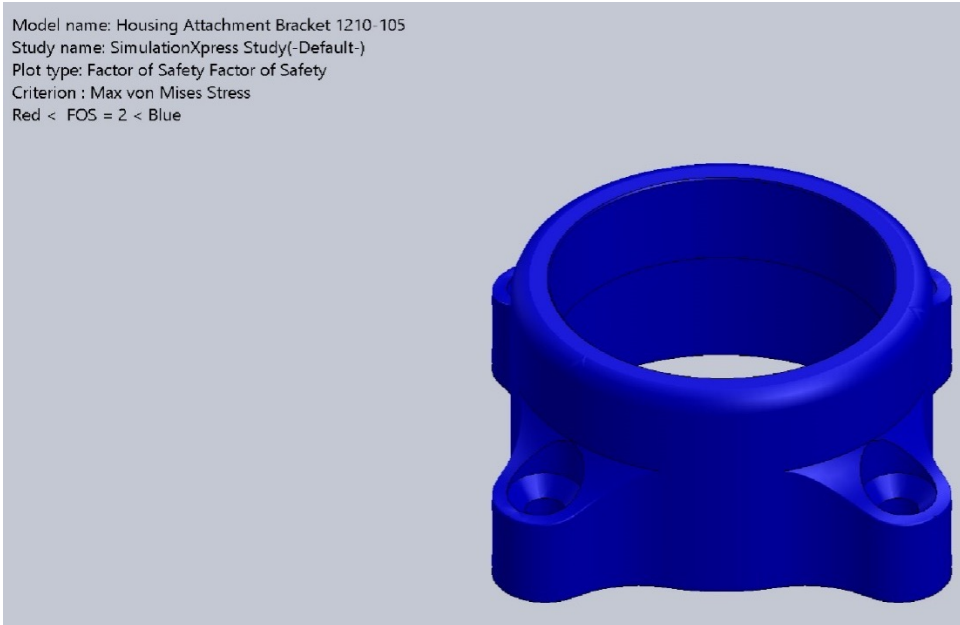


Figure 86 - Housing Attachment Bracket Bolt Hole Normal Simulation Factor of Safety

As with the upper opening, the bolt holes have been robustly designed to withstand high levels of forces. The largest displacement experienced was $3.494e^{-4}$ in, and a maximum von Mises stress of $3.066e^{+4}$ psi. The lowest factor of safety for this simulation was 2.389, indicating that it would function safely as intended.

The final simulation performed for the bolt holes was a shearing simulation. Like the upper opening, the bolt holes are likely to experience shearing forces during certain foot movements, so it is important to test to make sure the component is capable of handling these forces. This simulation tested a shearing force of 15 kN spread evenly across all bolt holes. The minimum and maximum values for the shearing simulations can be seen in Table 18, and the visualizations for the von Mises stress, displacement, and factor of safety (Figure 87Figure 89).

| | Minimum | Maximum |
|--------------------------|----------------|----------------|
| von Mises stresses (psi) | 1.024 | $1.224e^{+4}$ |
| Displacement (mm) | 0 | $8.670e^{-3}$ |
| Factor of Safety | 5.982 | $7.155e^{+4}$ |

Table 18 - Housing Attachment Bracket Bolt Holes Shearing Simulation

Model name: 1210-105 attachment bracket
Study name: SimulationXpress Study(-Default-)
Plot type: Static nodal stress Stress
Deformation scale: 1,034.4

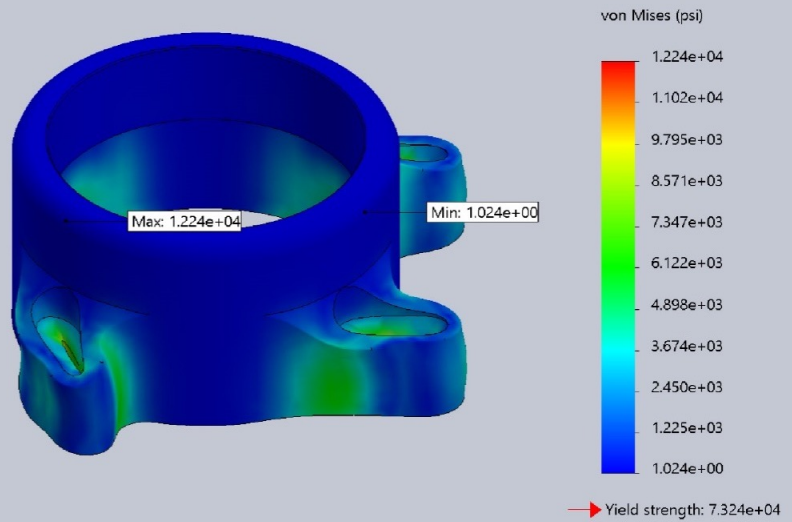


Figure 87 - Housing Attachment Bracket Bolt Hole Total Shearing von Mises Stresses (psi)

Model name: 1210-105 attachment bracket
Study name: SimulationXpress Study(-Default-)
Plot type: Static displacement Displacement
Deformation scale: 1,034.4

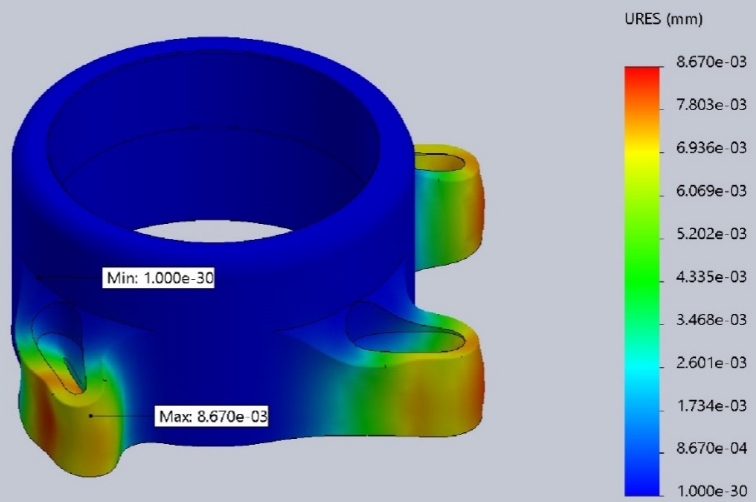


Figure 88 - Housing Attachment Bracket Bolt Hole Total Shearing Displacement (mm)

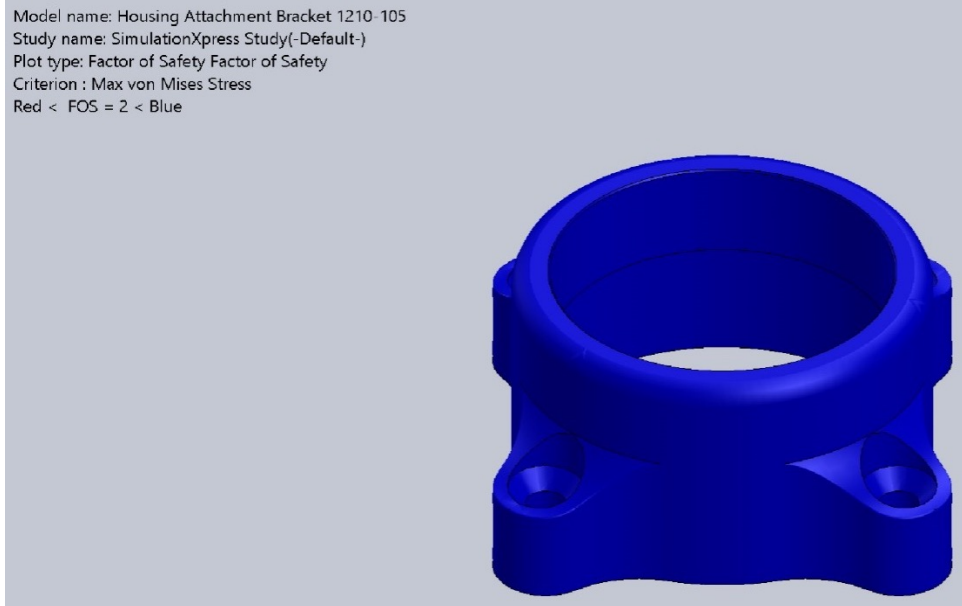


Figure 89 - Housing attachment Bracket Bolt Hole Total Shearing Factor of Safety

The shearing force simulation shows that the bolt holes are capable of withstanding substantial forces. The bolt holes moved only $8.670e^{-3}$ mm at most for a shearing force of 15 kN, while experiencing a maximum von Mises force of $1.224e^{+4}$ psi, well below the yield strength of $7.324e^{+4}$ psi. The lowest factor of safety was 5.982, which is almost three times the necessary minimum of 2.

The results of the simulations show that the housing attachment bracket is designed robustly enough to be used for this prosthetic design. The upper hole which threads to the ball joint housing should not fail in any expected real-world conditions, and the bolt holes connecting the housing attachment bracket to the upper foot plate are more than capable of withstanding the expected forces that will be encountered walking, running, and jumping.

5. CONCLUSION

5.1. Discussion

The aim of this project was to design a prosthetic foot that is more comfortable than current commercially available designs. The best method for accomplishing this was through improvements in the device's biomechanics, specifically by improving ankle mobility. It is hypothesized that increased mobility will work in tandem with an improved energy storage/return system to produce a comfortable prosthetic. A prosthetic with improved ankle mobility will allow the amputee to assume a more natural gait pattern, since the prosthetic will move more like a natural foot. In addition, by improving the energy storage/return system, the device will require less energy to operate, increasing comfort by decreasing fatigue. The prosthetic's mobility was improved through a combination of several elements.

The prosthetic's mobility was improved by combining contemporary design features with novel designs to result in a new device. A split toe feature improves inversion and eversion of the device. Carbon fiber foot plates with cambered curves and cantilevered sections are used in this design to improve the passive shock resistance in prosthetic designs. A pneumatic piston was used in this design to further improve shock resistance and return some of the energy stored during movement. In addition to these proven design features, a ball joint was incorporated into the design. Adding a ball joint to the prosthetic allows the prosthetic foot to pronate, supinate, invert, evert, adduct, and abduct at the ankle joint, vastly improving the biomechanics of the prosthetic when compared to other devices. The improved biomechanics work in conjunction with the shock absorption features and energy storage/return features, resulting in a comfortable prosthetic that moves like a natural foot. This design achieves natural foot movement without

using microprocessors or other electronics, making the design more cost-effective and resilient in harsh environments.

This prosthetic device was designed to be completely disassembled and rebuilt if needed. The intention was that a rebuildable device will be more affordable over a longer lifespan, since individual components can be replaced as necessary, rather than replacing the entire prosthetic should something be damaged. Whenever possible, the design uses standardized hardware and rebuildable components. Standardized hardware can be sourced from a multitude of locations and are generally more affordable than specialized hardware. Since they are easier to source, using standardized components also makes repairs faster and more straightforward. The ball joint and pneumatic shock used in this design are completely rebuildable. They can be serviced for longer life and can have parts replaced rather than replacing the whole component.

5.2. Limitations

As with all designs, there will be limitations that occur during the course of development. One of the main limitations was difficulty performing accurate simulations for carbon fiber components. Another limitation stemmed from difficulty in sourcing manufacturers for carbon fiber components. The final limitation was the lack of time to build and test a physical prototype.

Besides its ability to create 3D models of components, Solidworks is also capable of performing a multitude of simulations to digitally test prototype designs. While Solidworks has a large material library with pre-installed material properties, carbon fiber is not included in this collection. Carbon fiber is an anisotropic composite material with a large degree of variability in its material properties. As a result, to perform a simulation of carbon fiber in Solidworks, the various material properties must first be collected and added to the Solidworks materials library.

Once this has been done, carbon fiber must be defined as a composite material in Solidworks. This involves first determining the thickness of each carbon fiber layer, and the total number of layers in each section of the component being simulated. In addition, the orientation of each ply should be specified, as well as the overall orientation of the carbon fiber in relation to the part. Proper orientation is critical for carbon fiber, since its anisotropic structure causes its properties to change drastically with different orientations. Once the composite has been defined and oriented properly, the component simulation can continue normally. Without deep insight into the manufacturing of the carbon fiber components, it is incredibly difficult to create the component accurately in Solidworks.

Not only is carbon fiber difficult to simulate in Solidworks, but it is also difficult to manufacture in small batches. Several companies were contacted throughout the course of this project for cost estimates of the upper- and lower-foot plates. Unfortunately, none of the manufacturers replied, making it difficult to ascertain the cost and feasibility of the foot plates. Several additional companies were examined but either required minimum batch sizes or had other restrictions making them unsuitable choices for the foot plate prototypes. Carbon fiber requires specialized equipment for component creation, such as vacuum chambers and specialized ovens, making component assembly in-house a difficult prospect. Further investigation is needed to find a small-batch, custom carbon fiber component manufacturer.

The final limitation in this project was an inability to manufacture and perform physical testing of the prosthetic design prototype. While most of the components are readily available for purchase, some of the custom components require several weeks to be manufactured and delivered. And as stated earlier, a manufacturer for the upper- and lower-foot plated needs to be found to determine those components' cost. A physical prototype would provide more accurate

results than digital simulations because it would provide real-world confirmation of the simulation results performed in Solidworks. Moreover, a physical model can evaluate metrics that cannot be tested in Solidworks, such as whether the prosthetic actually offers improved comfort and improved biomechanics for an amputee using the device. Physically testing the device will evaluate its strengths and weaknesses so future designs may be refined.

5.3. Future Work

There are several areas in which further work will improve the design of this prosthetic device. One area would be to develop a better model for the forces that occur in a prosthetic foot. A better model will show the location and extent of forces acting on the prosthetic, which will in turn allow more accurate component simulations. The improved simulations will refine the components being tested, making them both as strong and as lightweight as possible. An improved model will also provide informed hardware decisions, so that the best choice can be made for each piece that goes into the prosthetic. The refined simulations, as well as the informed hardware and component selection, will result in a better prosthetic that has been functionally optimized while weighing as little as possible.

Another area of further research is the material selection for various components. As seen in Section 3.4, the stud attachment bracket and housing attachment bracket were originally intended to be made of titanium. Ultimately, they were made from 7075-T651 grade aluminum, as it provided sufficient strength while also being more affordable. Further research should be performed on each component to determine the best material choice for this application. For example, testing cyclic stress on the stud attachment bracket's arms will determine if aluminum is an appropriate material or if a different material should be used. The foot plates are another

example, as there may be a better material choice than carbon fiber for these components.

Determining the best material choice for each component will improve the overall design and will hopefully result in a more affordable device as well.

As the prosthetic's design improves, it is likely that components, and even the shape of the prosthetic will change. One component that will need further improvements is the ball joint stud attachment bracket. This bracket's arms will need to be reinforced in future versions to be able to withstand the forces experienced from moving. Larger fillets along the top and inside of the arms should improve their strength and increase the factor of safety. One change the overall prosthetic should address is the placement of the Fox Float shock. This version of the prosthetic place the shock at an angle that interferes with footwear. Future versions of the device will lower the shock, enabling the user to wear shoes and use cosmetic foot covers.

Future prosthetic designs would benefit from parallel variable damping systems, similar to the parallel systems of muscle and ligament in natural feet. As seen in Section 2.2, natural feet use parallel systems to modulate the stiffness of the foot in real time. This allows the foot to store and release energy as well as adapt to varying surfaces. Implementing multiple damping systems in a prosthetic would further improve its biomechanics and create more realistic foot motion. While it may be possible to create a passive damping system without electronics, real-time transitions may only be possible with the use of electronic systems. Regardless of the means, this type of structure should receive focus in future prosthetic development. Similarly, future versions of this design may try implementing the natural ankle's ability to lock and unlock during foot movement. This would enable further realism to the ankle mechanism and could improve ground clearance during dorsiflexion.

Finally, this design could benefit from cosmetic foot covers that would allow the user to customize their device. A prosthetic's appearance has been shown to be an important design characteristic to amputees [4]. Future research focused on this area could encourage more amputees to start and continue using a prosthetic device.

5.4. Conclusion

This project created a novel prosthetic foot design with improved biomechanics. By combining the increased energy storage and release capabilities of a pneumatic piston with the range of motion of a ball joint, the resulting prosthetic device is capable of providing improved biomechanics and ankle mobility compared with commercially available prosthetic devices. In addition, this device is made from easily obtained hardware, and can be completely broken down and rebuilt for repairs or component replacement. These factors result in a more affordable device over an extended lifetime, as components can be replaced as needed rather than replacing an entire device.

Appendix A – Component Gallery

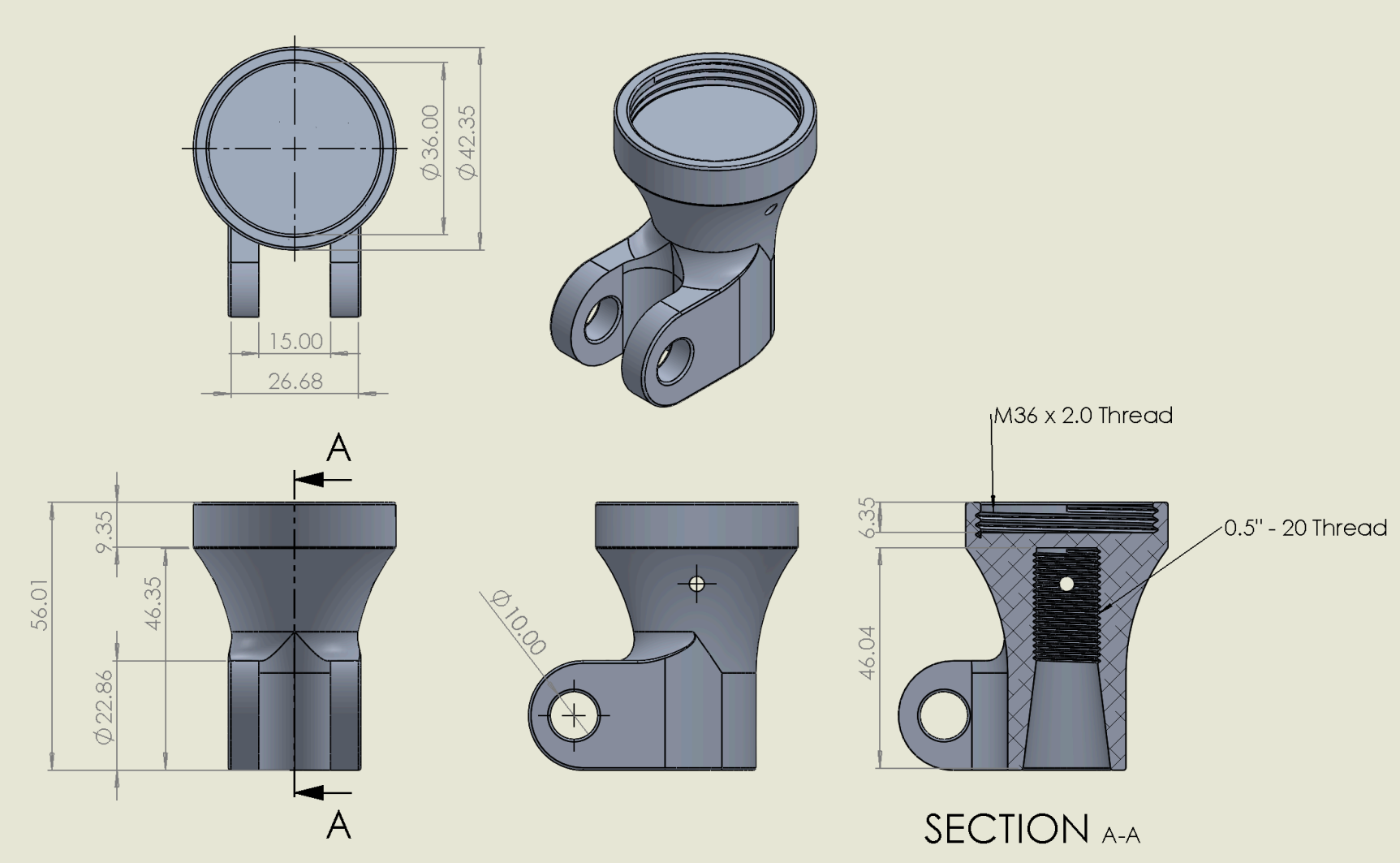


Figure 90 - Ball Joint Stud Attachment Bracket Drawing

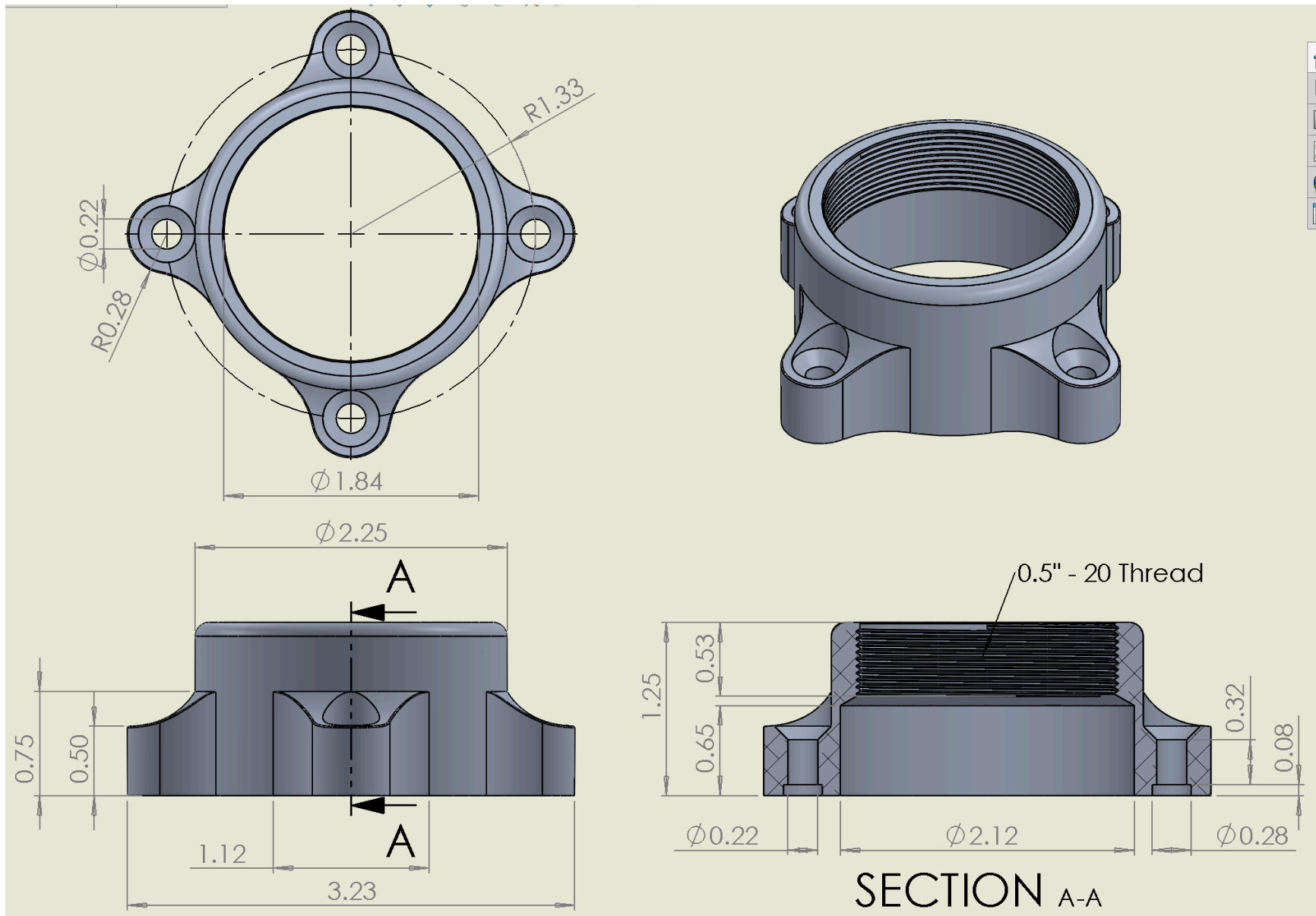


Figure 91 - Ball Joint Housing Attachment Bracket Drawing

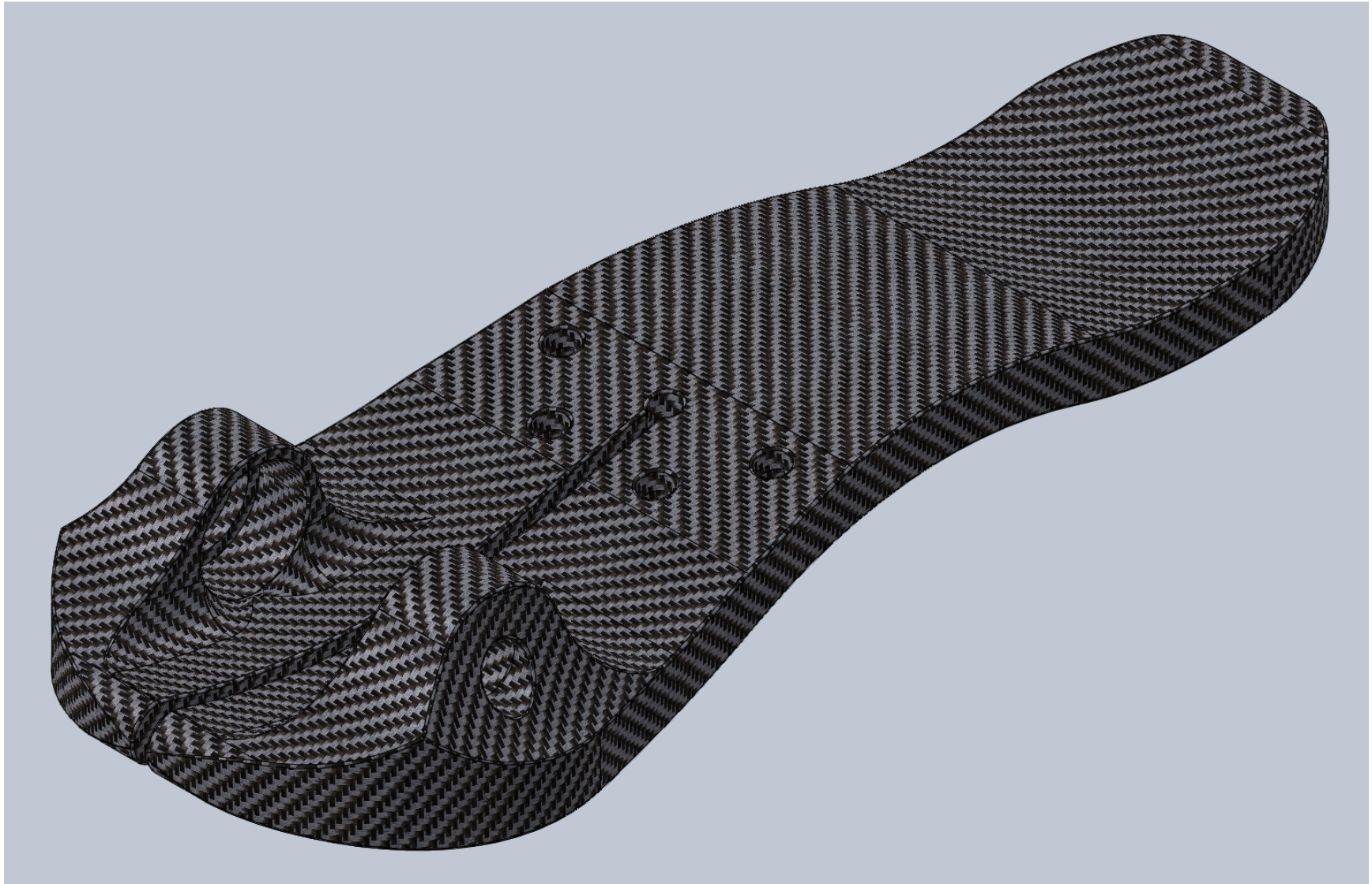


Figure 92 - Lower Foot Plate Isometric View

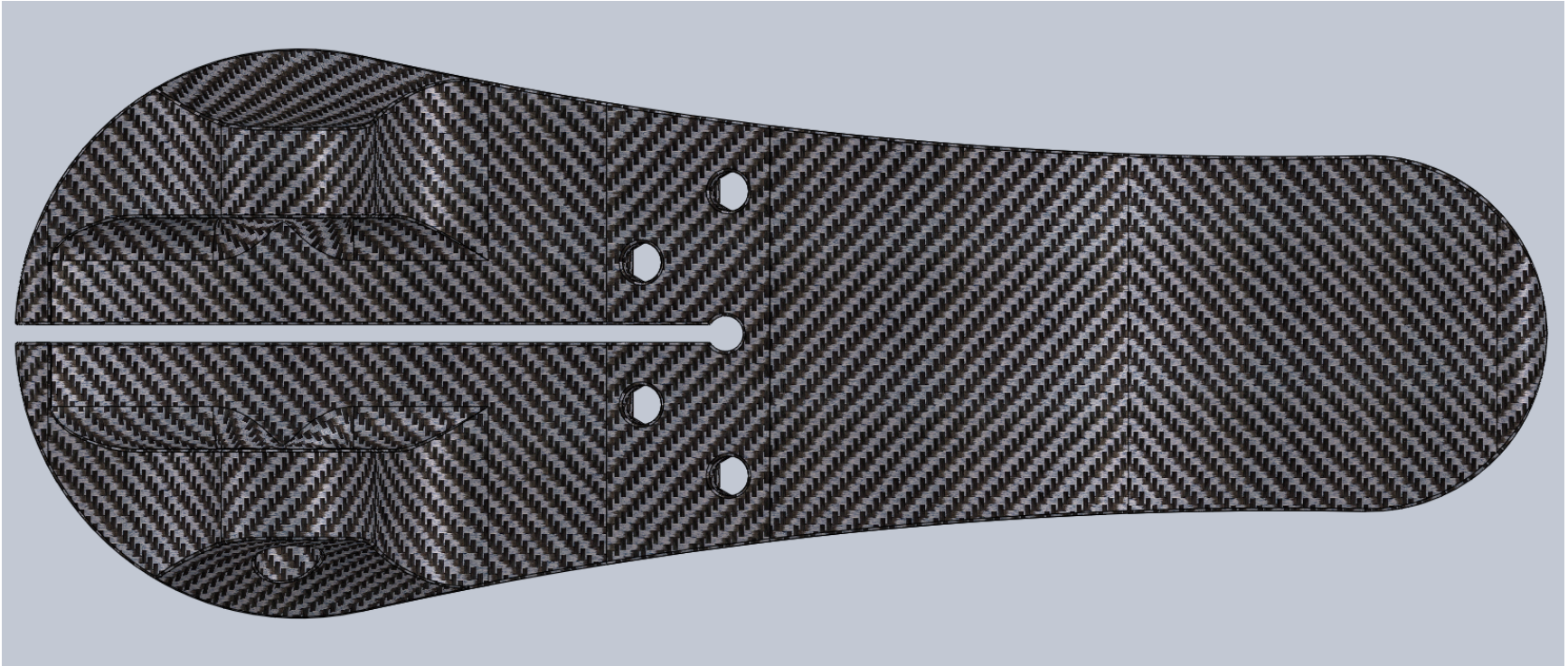


Figure 93 - Lower Foot Plate Top View

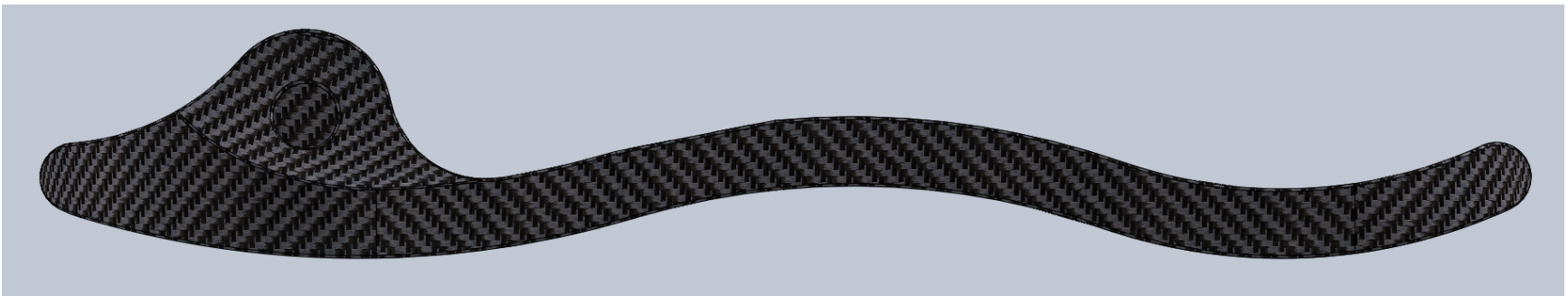


Figure 94 - Lower Foot Plate Profile View



Figure 95 - Lower Foot Plate Toe Area Detail

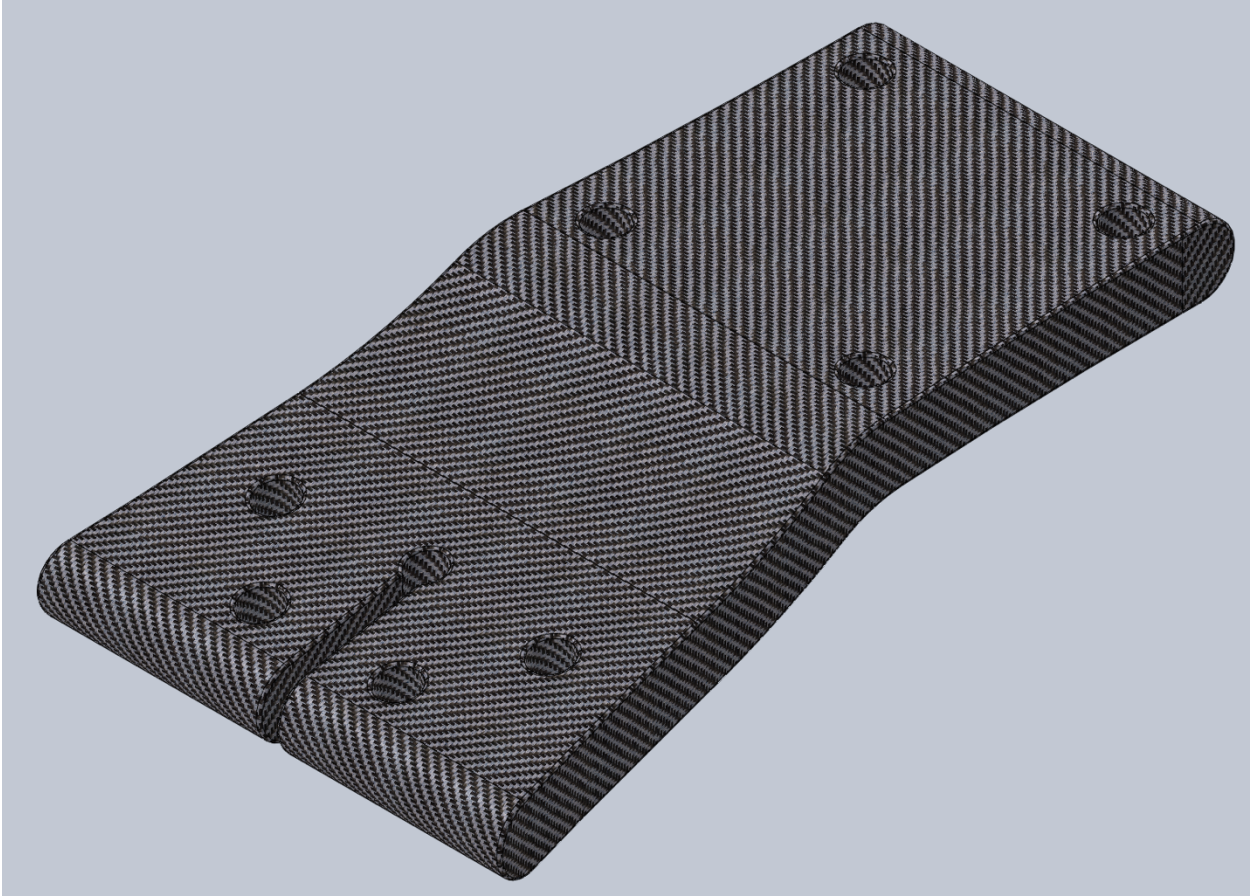


Figure 96 - Upper Foot Plate Isometric View

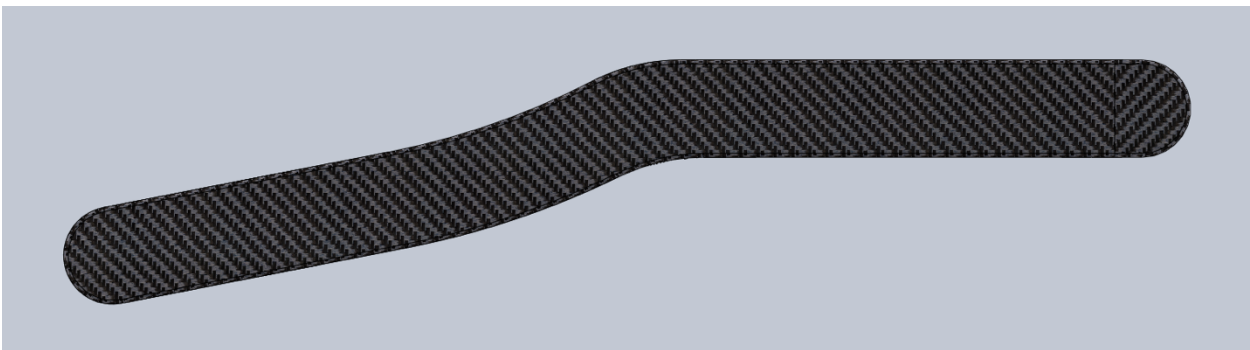


Figure 97 - Upper Foot Plate Profile View

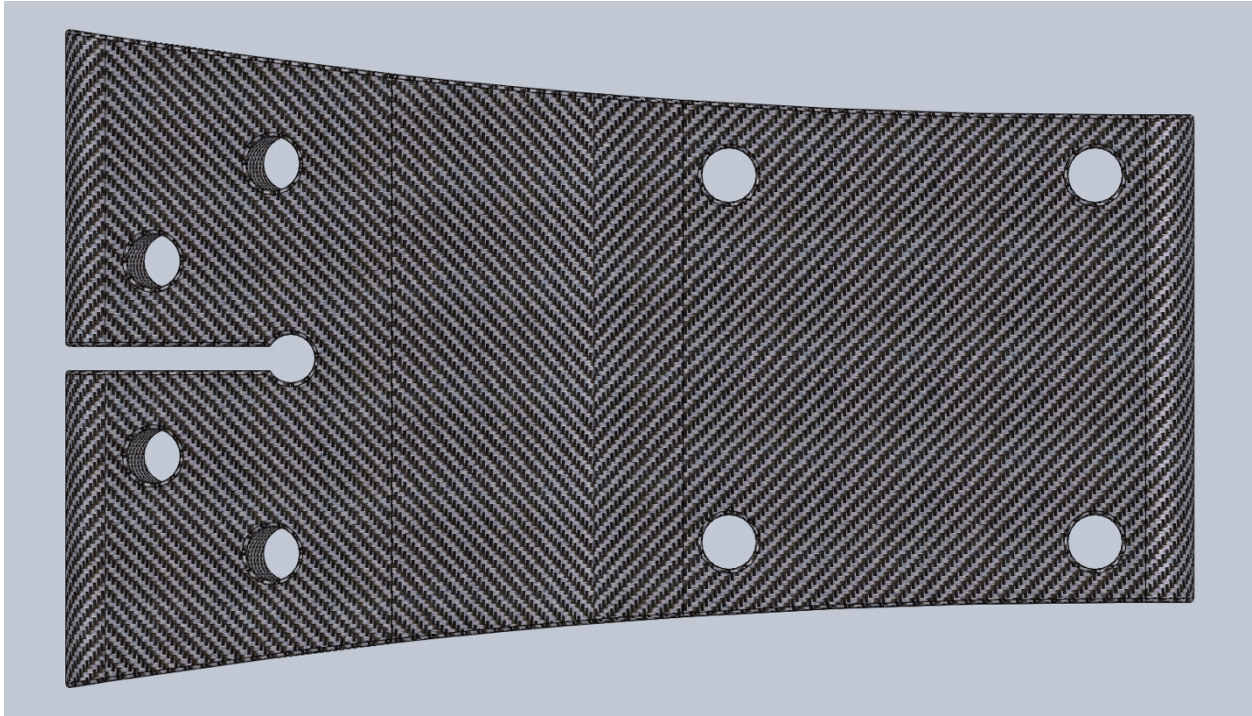


Figure 98 - Upper Foot Plate Top View (Housing Attachment Bracket Connection)

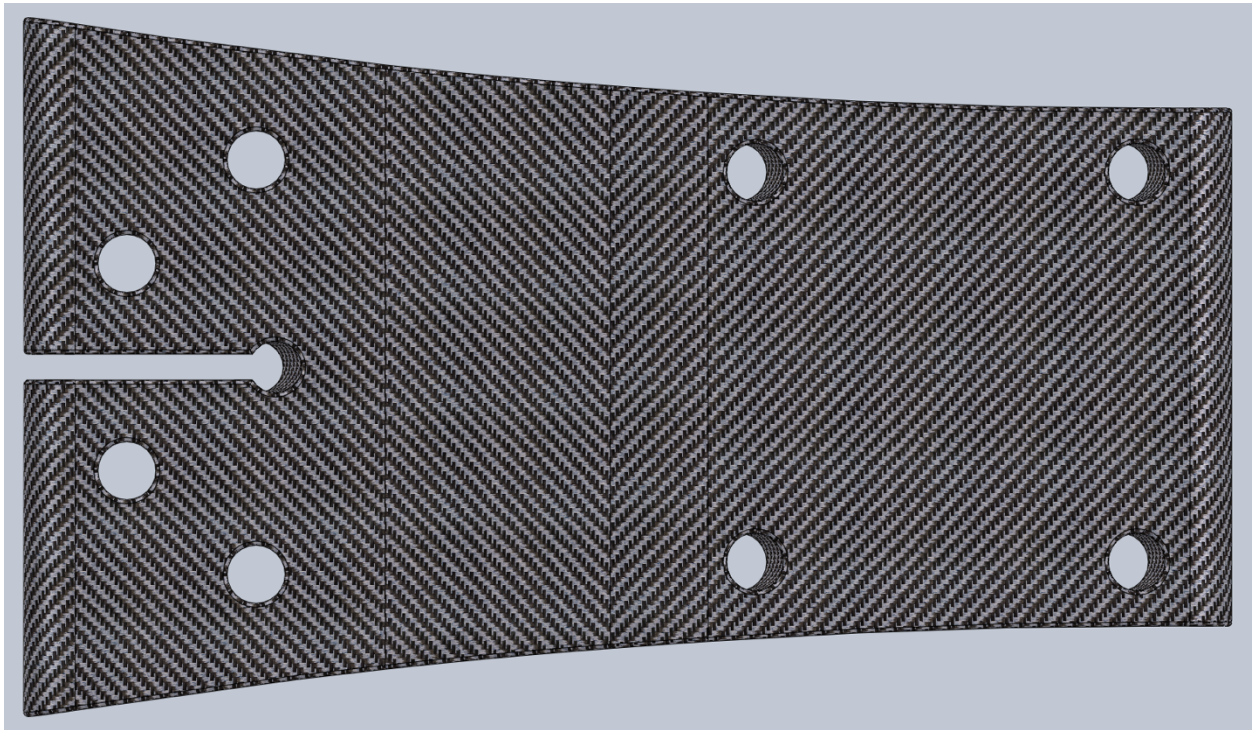


Figure 99 - Upper Foot Plate Top View (Foot Plate Connection)

REFERENCES

- [1] Ziegler-Graham, K., MacKenzie, E. J., Ephraim, P. L., Travison, T. G., and Brookmeyer, R., 2008, “Estimating the Prevalence of Limb Loss in the United States: 2005 to 2050,” *Arch. Phys. Med. Rehabil.*, **89**(3), pp. 422–429.
- [2] Owings, M. F., and Kozak, L. J., 1998, “Ambulatory and Inpatient Procedures in the United States, 1996,” *Vital Health Stat. 13.*, (139), pp. 1–119.
- [3] Amputee Coalition, 2015, “Limb Loss Statistics,” Amputee Coalit. [Online]. Available: <https://www.amputee-coalition.org/resources/limb-loss-statistics/>. [Accessed: 09-Feb-2021].
- [4] Amputee Coalition, 2011, “Patient Perspectives,” *inMotion*, **21**(5), p. 5.
- [5] Amputee Coalition of America and Limb Loss Research and Statistics Program, “People with Amputation Speak Out.”
- [6] Dr. Grant McGimpsey and Terry C. Bradford, “Limb Prosthetics Services and Devices,” p. 35.
- [7] Chan, C., and Rudins, A., 1994, “Foot Biomechanics During Walking and Running,” *Mayo Clin. Proc. Mayo Clin.*, **69**, pp. 448–61.
- [8] Hoffman, M. and MD, “Feet (Human Anatomy): Bones, Tendons, Ligaments, and More,” WebMD [Online]. Available: <https://www.webmd.com/pain-management/picture-of-the-feet>. [Accessed: 09-Feb-2021].
- [9] Zeidan, H., Suzuki, Y., Kajiwara, Y., Nakai, K., Shimoura, K., Yoshimi, S., Tatsumi, M., Nishida, Y., Bito, T., and Aoyama, T., 2019, “Comparison of the Changes in the Structure of the Transverse Arch of the Normal and Hallux Valgus Feet under Different Loading Positions,” *Appl. Syst. Innov.*, **2**(1), p. 3.

- [10] Brockett, C. L., and Chapman, G. J., 2016, "Biomechanics of the Ankle," *Orthop. Trauma*, **30**(3), pp. 232–238.
- [11] Shephard, M. K., Hoover, D. L., and Neelly, K. R., 2015, "ACL Tears: Contributing Factors and Preventive Strategies for the Home Health Care Professional—Part 2," *Home Health Care Manag. Pract.*, **27**(1), pp. 31–35.
- [12] Kelly, L. A., Farris, D. J., Cresswell, A. G., and Lichtwark, G. A., 2019, "Intrinsic Foot Muscles Contribute to Elastic Energy Storage and Return in the Human Foot," *J. Appl. Physiol.*, **126**(1), pp. 231–238.
- [13] Amputee Coalition, 2016, "Prosthetic Feet Fact Sheet," Amputee Coalit. [Online]. Available: <https://www.amputee-coalition.org/resources/prosthetic-feet/>. [Accessed: 09-Feb-2021].
- [14] Gailey, R. S., Wenger, M. A., Raya, M., Kirk, N., Erbs, K., Spyropoulos, P., and Nash, M. S., 1994, "Energy Expenditure of Trans-Tibial Amputees during Ambulation at Self-Selected Pace," *Prosthet. Orthot. Int.*, **18**(2), pp. 84–91.
- [15] Schmalz, T., Blumentritt, S., and Jarasch, R., 2002, "Energy Expenditure and Biomechanical Characteristics of Lower Limb Amputee Gait: The Influence of Prosthetic Alignment and Different Prosthetic Components," *Gait Posture*, p. 9.
- [16] Waters, R., Perry, J., Antonelli, D., and Hislop, H., 1976, "Energy Cost of Walking of Amputees: The Influence of Level of Amputation," p. 6.
- [17] Boonstra, A., Schrama, J., Fidler, V., and Eisma, W., 1995, "The Gait of Unilateral Transfemoral Amputees," *Scand. J. Rehabil. Med.*, **26**, pp. 217–23.
- [18] Klute, G. K., Kallfelz, C. F., and Czerniecki, J. M., 2001, "Mechanical Properties of Prosthetic Limbs: Adapting to the Patient," *J. Rehabil. Res. Dev.*, **38**(3), pp. 299–307.

- [19] Klute, G. K., Kantor, C., Darrouzet, C., Wild, H., Wilkinson, S., Iveljic, S., and Creasey, G., 2009, “Lower-Limb Amputee Needs Assessment Using Multistakeholder Focus- Group Approach,” *J. Rehabil. Res. Dev.*, **46**(3), p. 293.
- [20] “QA1 1210-105 K772 Style Upper Ball Joint Kit w/ Extended Length Stud,” *Speedw. Mot.* [Online]. Available: <https://www.speedwaymotors.com/QA1-1210-105-K772-Style-Upper-Ball-Joint-Kit-w-Extended-Length-Stud,84110.html>. [Accessed: 09-Feb-2021].
- [21] 2017, “Commercial Carbon Fiber | ZOLTEK.”
- [22] “TF Tuned Mount Kit 12.7mm M10 - TF Tuned 12.7mm (Fox/RockShox/Inline) Mount Kits - TF Tuned” [Online]. Available: <https://www.tftuned.com/tf-tuned-mount-kit-127mm-m10/p2938>. [Accessed: 27-Mar-2021].
- [23] “Explore FLOAT DPS Bike Shocks | FOX” [Online]. Available: <http://www.ridefox.com/family.php?m=bike&family=float>. [Accessed: 25-Feb-2021].
- [24] Fox Factory, Inc., “SHOCK- 2021 FLOAT DPS and DPX2 | Bike Help Center | FOX” [Online]. Available: <https://www.ridefox.com/fox17/help.php?m=bike&id=1079#usingthevolairsleeve>. [Accessed: 26-Feb-2021].
- [25] FOX, 2015, *FOX DPS Shock Technology Explained – FOX Factory, Inc.*
- [26] “M36 Threaded Male Adapter with Center Hole - View Options - Male Components - Adult Components - M36” [Online]. Available: http://www.bulldogtools.com/prosthetic/rotating-pyramid-insert-hole-titanium_p_5479.html?osCsid=1e3dbf010b0becb3b0f812d0548c8327. [Accessed: 02-Mar-2021].